December 2017

Land Use Land Cover Change Effects on Southern Great Plains Precipitation

Alexandra Caruthers
University of Nebraska-Lincoln, alexandra.caruthers@huskers.unl.edu

LAND USE LAND COVER CHANGE EFFECTS ON SOUTHERN GREAT PLAINS PRECIPITATION

By:

Alexandra L. Caruthers

A THESIS

Presented to the Faculty of

The Graduate College at the University of Nebraska

In Partial Fulfillment of Requirements

For the Degree of Master of Science

Major: Earth and Atmospheric Sciences

Under the Supervision of Professor Matthew Van Den Broeke

Lincoln, Nebraska

December 2017

LAND USE LAND COVER CHANGE EFFECTS ON SOUTHERN GREAT PLAINS PRECIPITATION

Alexandra L. Caruthers, M.S.

University of Nebraska, 2017

Advisor: Matthew Van Den Broeke

Great Plains land use has changed substantially over the last 160 years, altering the properties of the land through increased settlement and advances in irrigation. Changing the interface between the land and atmosphere has implications for the atmospheric boundary layer, the regional circulation, the local surface energy budget and resulting precipitation patterns. Land use land cover (LULC) changes are an important topic for this region due to its heavy dependence on agriculture. This study investigates differences in Southern Great Plains precipitation patterns between four LULC scenarios: the pre-settlement, 1920's, Dust Bowl and present day eras. Using the Weather Research and Forecasting (WRF) model coupled to the Community Land Model (CLM), simulations for each LULC scenario were run for a 13-year period (1990-2002), as this period encompasses a wide variety of remote forcing conditions. It is hypothesized that the impact of the conversion of native vegetation to cropland will alter the regional circulation of the Southern Great Plains through changes in the surface energy budget. Crops transpire more than native vegetation, such as grassland, which will result in higher surface latent heat fluxes, and higher surface dewpoints, in the modern day than in the earlier LULC scenarios.

The increase in the surface latent heat flux will decrease the surface sensible heat flux, and 2m air temperatures will be cooler in the modern day, ultimately resulting in an altered regional circulation. It is hypothesized that the shift in the regional circulation will have an impact on the moisture flux and moisture transport from the Gulf of Mexico. The greater surface latent heat flux, along with the shift the regional circulation will result in greater precipitation in the modern day than in the pre-settlement, 1920's and Dust Bowl scenarios.

Acknowledgements

I would like to thank my advisor, Dr. Matthew Van Den Broeke, for his guidance, encouragement, and patience throughout my graduate research and coursework. I would also like to thank my committee members, Dr. Oglesby and Dr. Rowe for their assistance and insight, as well as fellow graduate student Abraham Torres, and Cindy Hays and Dr. Hu for their knowledge and help with this project. This work was made possible with the support of my peers, especially Alexander Carne, Adrianne Engel, Wolfgang Hanft and Alexander Krull. Finally, my parents, sister and friends back home provided me with the encouragement and love when I needed it most. This work was financially supported through the University of Nebraska-Lincoln Department of Earth and Atmospheric Sciences and the National Science Foundation (Grant # AGS-1355916). Computing resources were provided by the National Center for Atmospheric Research's Computational and Information Systems Laboratory (CISL) and the University of Nebraska's Holland Computing Center.

Table of Contents

List of Figures

Chapter 1. Introduction

Anthropogenic land use land cover (LULC) changes can impact the global climate through deforestation, degradation (grassland, cropland and other vegetation changed to sparsely vegetated and bare soil) from overgrazing and overuse, expansion of agriculture and the inclusion of irrigation, and urbanization. Changing the interface between the land and atmosphere has implications on the local surface energy budget, atmospheric boundary layer (ABL), regional circulation and precipitation patterns. The Southern Great Plains (SGP) is an ideal location to study the effects of LULC changes because it has undergone dramatic LULC changes over the last 160 years. The westward expansion of civilization has resulted in the conversion of native land cover types into widespread agricultural and urban areas. In the present day, the land utilized for agriculture now includes modern irrigation techniques, which were implemented in the mid-twentieth century. Urban areas have increased to accommodate the growing population.

The Southern Great Plains' strong dependence on agriculture also makes it an ideal study area for LULC impacts, as catastrophic droughts in this region have a substantial negative impact on the economy. For example, the drought of 2012 caused approximately $30 billion (U.S. dollars) loss of revenue (Smith et al. 2016). Droughts of this magnitude that affect the SGP are often linked to large-scale climatic forcings, such as the El Niño Southern Oscillation (ENSO) and the Atlantic Multidecadal Oscillation (AMO). Drier (wetter) conditions are common during negative (positive) phases of ENSO, and past research has found that these anomalous conditions are enhanced when phases of ENSO and of the Pacific Decadal Oscillation (PDO) are in phase (Hu and Huang 2009). During a negative phase of ENSO, or La Niña condition, drier than

average conditions are more common for the Southern Great Plains because of a blocking high pressure over the eastern Pacific Ocean due to colder than average sea surface temperatures. The regional circulation of the SGP shifts and results in anomalously dry southwesterly winds from the Mexican Plateau (Hu and Feng 2012), and these anomalously dry conditions associated with a La Niña event are more prevalent in the winter. In addition, cool sea surface temperatures (SSTs) indicative of a La Niña phase are also attributed to a weaker low-level jet (LLJ), which serves as a crucial moisture source for the SGP by transporting maritime tropical air northward from the Gulf of Mexico (Weaver et al. 2009).

The AMO includes periodic phases of warm and cool SSTs in the north Atlantic Ocean. It has been concluded that the warm phase of the AMO impacts precipitation over the SGP (Hu et al. 2011). A statistical reconstruction of twentieth century droughts found that the warm phase of the AMO was the dominant factor in the Dust Bowl drought in the mid-1930s (Nigam et al. 2011). In a warm phase of the AMO, the North American subtropical high pressure weakens and shifts northeastward. This leads to an anomalous three-cell circulation driven by thermal lows over land, resulting in anomalously westerly winds over the SGP, disrupting southerly flow from the Gulf of Mexico (Hu et al. 2011). Since the Southern Great Plains is susceptible to remote forcing that leads to well-documented and catastrophic droughts, it is crucial to understand the impacts of local forcings, such as LULC changes, on the local and regional climates that may also promote drought conditions.

Surface characteristics altered by changing the LULC include albedo, surface roughness, leaf area index, canopy conductance, root depth, and soil properties such as

texture and structure. Changing the surface albedo changes the reflectance of the surface, and therefore alters the amount of net radiation received. For example, darker surfaces such as water, wet soil and forests have lower surface albedos and subsequently absorb much the incoming solar radiation. Conversely, surfaces such as snow and dry soil have characteristically high surface albedos, so these surfaces reflect much of the incoming solar radiation (Bonan 2016).

The effects of LULC changes are most pronounced in the ABL due to changes in the surface energy budget. The structure of the ABL is dependent on surface energy fluxes, due to the partitioning of latent and sensible heat fluxes. The surface energy budget represents the exchange of energy from the land to the atmosphere, and is comprised of four components:

$$R_n = H + LE + G$$

where R_n is the net radiation at the surface, H is the sensible heat flux, LE is the latent heat flux, and G is the flux into subsurface layers or ground heat flux.

The upward sensible heat flux results from the difference in temperature between the ground and the adjacent air above:

$$H = -C_p(\theta_a - T_S)g_{ah}$$

where C_p is the specific heat of moist air at constant pressure, θ_a is the potential temperature of the air, T_S is the temperature at the surface and g_w is a conductance term dependent on atmospheric turbulence and surface characteristics (equation adapted from Bonan 2016). Heat is transferred by direct thermal conduction. Generally, the sensible heat flux is positive (upward from the surface to the air) during the day, as the surface is

warmer than the air above. Overnight, radiational cooling results in a negative (downward) sensible heat flux, directed from the air to the surface.

The upward latent heat flux accounts for the transfer of energy as water changes state, primarily through evaporation at the surface and condensation in the atmosphere. For a saturated surface, the latent heat flux can be expressed in the following equation:

$$LE = -\frac{C_p}{\gamma}(e_a - e_*[T_S])g_w$$

where C_p is the specific heat of moist air at constant pressure, γ is the psychometric constant (which depends on the heat capacity, atmospheric pressure and latent heat of vaporization), e_a is the vapor pressure of air, the term $e_*[T_S]$ is the saturation vapor pressure at a surface temperature of T_S and g_w is a conductance term dependent on atmospheric turbulence and surface characteristics (equation adapted from Bonan 2016). Thus, the main driver in the latent heat flux is the difference between the vapor pressure of the air and the saturation vapor pressure of air at the surface temperature. Generally, over wet surfaces such as bodies of water (lakes, ocean), moist soils and vegetation, heat is transferred upward as liquid water at the surface evaporates and thus the latent heat flux is generally positive (towards the atmosphere). However, it is not always positive, as in the case of dew at the surface, where heat is transferred downward as liquid water condenses at the surface.

Finally, the downward ground heat flux represents the transfer of energy into the subsurface layers:

$$G = \frac{\kappa(T_s - T_g)}{\Delta z}$$

where κ is the thermal conductivity, T_s and T_g are the temperatures of the surface and ground (respectively) and Δz is the depth. This flux is driven primarily by conduction, and largely reflects the seasonal cycle. When the soil is cooler than the surface, a positive (from surface to subsurface layers) ground heat flux is produced. A negative ground heat flux results when the subsurface layers are warmer than the surface.

The surface sensible and latent heat fluxes are related through the Bowen ratio and the evaporative fraction:

$$B = \frac{H}{LE}$$

where B represents the Bowen ratio, and

$$EF = \frac{LE}{H + LE}$$

where EF represents the evaporative fraction.

A Bowen ratio greater than one indicates the energy at the surface is primarily being used to heat the surface. Conversely, a Bowen ratio less than one indicates that more energy is being used for evaporation at the surface. The evaporative fraction is a similar measure that isolates the impact of surface properties (soil moisture and vegetation) in the partitioning of the surface energy budget. An evaporative fraction near one indicates that the latent heat flux usage at the surface is greater than that of the sensible heat flux (Gentine et al. 2011).

Past research has quantified the impact of LULC changes on the surface energy budget for a range of locations and time periods. One component of the 2002 International H2O Project (IHOP_2002) and the 1997 Cooperative Atmosphere Surface Exchange Study (CASES-97) was to examine the influence of LULC changes on the

sensible and latent heat fluxes. The International H2O Project was a multiagency field campaign that collected data using ground instrumentation and aircraft observations to improve the knowledge of the distribution of water vapor and its implications for convection. Nine National Center for Atmospheric Research (NCAR) Integrated Surface Flux Facility Portable Automated Mesonets were included in the campaign. The observations of LeMone et al. (2007) utilized data from the flux towers and revealed that the fluxes were sensitive to the underlying vegetation; the sensible heat flux was maximized over land with sparse vegetation with a minimum over green vegetation while the opposite was true for the latent heat flux (LeMone et al. 2007).

One idealized case studied the impacts of a LULC change from forest cover to grassland on the global scale. This change increased the surface albedo globally, with a global decrease in the average temperature. There are a few counteracting mechanisms that resulted in a temperature change. The increase in surface albedo resulted in less absorbed net radiation at the surface, which therefore decreased the temperature. However, deforestation decreased the latent heat flux, so more energy was available to heat the surface through the surface sensible heat flux. While the two mechanisms worked against each other, ultimately the decrease in net radiation had a greater influence on the global climate (Davin and de Noblet-Ducorudre 2010).

A recent study (Chen and Dirmeyer 2017) examined the influence of anthropogenic LULC changes over the last 2000 years on precipitation in North America and linked the results to changes in the surface energy balance. They focused on the years AD 850, 1850 (pre-industrial) and present (circa 2000). From 850 to 1850, the sensible heat flux decreased over much of the eastern United States while the surface

albedo increased, coinciding with a LULC change from forest to cropland as a response to European colonization. The authors attribute the decrease in the surface sensible heat flux to the aerodynamic differences between forests and cropland; crops are aerodynamically smoother than forests and therefore transfer heat less effectively. Subsequently, the latent heat flux increased as a result of this LULC change, as crops transpire more readily than forests. Both the changes in the sensible heat flux and the latent heat flux were significant at the 95% confidence interval. From 1850 to 2000, the sensible heat flux decreased over the Great Plains while the latent heat flux increased, which were again significant at the 95% confidence interval. The surface albedo slightly decreased. The change in LULC associated with these differences was a conversion of native grassland to cropland. The authors attributed the LULC changes from 1850 to 2000 as the cause for the increase in precipitation, resulting from the altered partitioning of latent and sensible heat fluxes (Chen and Dirmeyer 2017).

Land use changes in other regions have also been studied. Over the last 300 years, between 42-68% of the global land surface has experienced human alteration (Hurtt et al. 2016). For example, eastern China has undergone a range of LULC changes, including farmland expansion, changes in the grassland regions through overgrazing and eventual restoration, deforestation, afforestation (introducing forests into region with no history of tree cover), reforestation and an increase in urbanization. These changes were examined through model simulations (Yan et al. 2014) of four land use conditions circa 1989, 1995, 2000 and 2005, each chosen because they represented a large LULC change from the previous time period. With the baseline of the 1989 scenario, Yan et al. (2014) found that the average sensible and latent heat fluxes varied slightly in the 1995 and 2000

scenarios, but were much different in the 2005 scenario compared to the 1989 LULC scenario. Between the 1989 and 2005 scenarios, the sensible heat flux increased at the expense of the latent heat flux. This change was attributed to the conversion of wetlands and woodlands to cropland, accounting for 0.9% of the study area (eastern China), which provided a substantial decrease in the local evapotranspiration. The most significant changes in the surface energy budget results from the 1.21% of the study area that underwent a LULC change from cropland to evergreen needleleaf forest. This conversion led to a 19.39% decrease in H, a 7.44% increase in LE and an overall increase in net radiation of 2.7% over the region where the change occurred (Yan et al. 2014).

a. Land Use Land Cover Changes

i. Deforestation

Some of the earliest studies of LULC change focused on deforestation in the Amazon Basin. More than half of the rainforest in the Amazon Basin was cleared through deforestation, and extensive research has converged on the conclusion that tropical deforestation results in a locally warmer and drier climate. An early study used a Global Climate Model (GCM) to simulate two scenarios, one as a control with conditions modeling land use of the mid 1980's and the other with increased deforestation. It was found that deforestation resulted a warming of 1-3°C in the Amazon Basin. This was coupled with a decrease in precipitation, in conjunction with lower values of specific humidity (Nobre et al. 1991).

Notable deforestation has also occurred in Australia, where the native forests have been replaced by grassland and cropland. Narisma and Pitman (2003) used a mesoscale model to simulate 200 years of LULC changes in Australia. This study was unique as the

model resolution was 50 km, a higher resolution than other global models. Since the impacts of LULC changes can occur on the mesoscale, the use of finer resolution allowed for some of these interactions to be realized by the model. Land surface vegetation data were obtained from the Atlas of Australian Resources on Vegetation by Australian Surveying and Land Information Group (AUSLIG) for the period of 1788-1988. They focused their analysis on the southwest and southeast where appreciable LULC change occurred. Both of these regions underwent a change from trees to grassland. This deforestation resulted in a warming of about 1°C, likely due to the increased partitioning to sensible heating, as trees hold more moisture than grassland (Narisma and Pitman 2003). With less moisture occurring with grassland, less energy would be partitioned to the latent heat flux and an increased sensible heat flux and surface temperature would result.

ii. Overgrazing

Charney et al. (1975) examined potential feedbacks caused by overgrazing in the African Sahel. Overgrazing decreased the plant cover, which increased the surface albedo due to the exposed barren soil, with characteristically has a higher surface albedo. A general circulation model was used to calculate differences in precipitation based on two surface albedo conditions, one representing the natural plant cover (lower albedo) and the other representing the barren soil (high albedo). The simulation with the higher albedo, representing overgrazing, resulted in less precipitation than the simulation with the lower albedo (without overgrazing). Their results suggested the potential for a positive feedback; overgrazing decreased the plant cover which lowered the surface

albedo and resulted in less precipitation. This, in turn, would increase the extent of the barren soil and subsequently lower precipitation (Charney et al. 1975).

A more recent example of land degradation from overgrazing is found in the semiarid climate along the United States – Mexico border. On the Mexican side of the border, the grass is considerably shorter due to overgrazing, leaving 28% more bare soil. Thus, with the increase in exposed soil, the surface albedo is higher than on the U.S. side. The higher surface albedo on the U.S. side has decreased the temperature relative to the Mexican side of the border, resulting in a difference in summertime temperatures of about 4°C. Seasonally, precipitation exacerbates the temperature difference. The vegetation on the U.S. border has remained unchanged (and therefore is more vegetated than the Mexican side), which results in a larger partitioning to the latent heat flux, reducing the sensible heat flux and thus the temperature. Meanwhile, with less vegetation on the Mexican side of the border, there is less partitioning to the latent heat flux (Balling 1989; Bonan 2016).

iii. Agriculture and Irrigation

Land use land cover changes frequently are the result of an increasing demand for agricultural use. Matching the demand is accomplished through altering the land to create a more suitable environment for agriculture. The former was briefly discussed in Section ii, and the latter is primarily accomplished by irrigation. While irrigation techniques have improved crop yield and enhanced agriculture from an economic standpoint, its impact on the climate cannot be ignored. During dry conditions when irrigation is needed to sustain agriculture, irrigation alters the soil moisture, resulting in greater moisture content compared to natural vegetation without irrigation. The increase

in moisture increases the latent heat flux, and subsequently alters the partitioning of energy in the surface energy budget. All else equal, the increase in soil moisture from irrigation allows for greater evaporation and thus an increase in low-level moisture, which increases the latent heat flux at the expense of the surface sensible heat flux. As a result, cooler temperatures are expected in the presence of irrigation (Bonan 2016). Therefore, the impacts of irrigation on the climate are only evident during the growing season when precipitation alone is not enough for agriculture. It should be noted that the effects of irrigation will not be investigated in this study.

Past work utilized climate models to simulate the effects of land use change on the climate of the eastern and central United States (Oleson et al. 2004, Mueller et al. 2017). These simulations revealed that, during the summer, the conversion of grasslands to croplands in the Great Plains has led to an overall cooling. It is noted that the magnitude of the cooling is sensitive to the land use and biophysical data used. The main driver is the increase in surface albedo, which decreased the net radiation. In addition, increased evapotranspiration associated with cropland increases the relative humidity.

The climate impacts from the conversion of natural wetlands to agriculture in South Florida were studied by Marshall et al. (2004). Hard freezes in northern Florida drove the citrus production into southern Florida to prevent future occurrences of catastrophic freezes. Areas of natural wetland were drained in the late 20th century and converted to cropland for citrus agriculture. The purpose of this study was to determine if this LULC change had an impact on future freezes. The authors used three catastrophic freeze events, and imposed reanalysis data from these events on two model simulations, one with natural LULC conditions and one with current LULC conditions accounting for the

southward shift of citrus cropland. This study found that areas that shifted from natural land cover to agricultural land were colder during the catastrophic freeze events. While the agriculture land still had relatively high soil moisture content, it was still less than that of the natural wetlands. Thus, the natural land cover also had a greater moisture flux during the nighttime hours that prevented below-freezing, and this moisture flux was reduced over agriculture land allowing for temperatures to drop to below-freezing and result in freeze events. The results suggest that despite the southward shift in the citrus production, an attempt to remove the possibility of catastrophic freezes, the crops may still be susceptible to hard freezes (Marshall et al. 2004). Feedbacks such as this demonstrate the importance of studying the impacts of LULC changes, as the consequences may not coincide with the desired results.

b. Purpose of Research

The Southern Great Plains has experienced substantial and regionally-varying LULC changes. Portions of the Southern Great Plains have undergone deforestation and have been converted from native vegetation to cropland with the inclusion of irrigation. The LULC change of greatest magnitude spatially in this region is the expansion of cropland. The United States Geological Survey Land Cover Trends study estimated 88% of land in the Great Plains is now dominated by agriculture and grassland/shrubland, with each contributing about 44% (Drummond and Auch 2015). This is a large increase from the late nineteenth century, when agriculture was about 5% of the land use land cover usage in the Great Plains (Gutmann et al. 2005).

In the Southern Great Plains, many LULC changes can be attributed to agricultural expansion. In addition, the westward expansion of settlement has resulted in urbanization. The impacts of these LULC changes in the Southern Great Plains are of interest because of the region's dependence on agriculture. Understanding the impacts of past LULC changes is critical since land use continues to change. The purpose of this study is to investigate the changes of LULC conditions on Southern Great Plains precipitation patterns.

It is hypothesized that the widespread conversion of native grassland to cropland has resulted in a cooling of 2m air temperature during the growing season, as concluded in previous research. The overall cooler temperatures have altered the regional circulation, with higher surface pressure over the region with cooler temperatures. Subsequently, the surface winds have been altered and it is predicted that the change in winds will change the moisture transport from the Gulf of Mexico to the Southern Great Plains. With stronger positive meridional winds along the west side of the higher surface pressure, over the region that is now cropland, the meridional moisture flux will also be stronger. This will allow for greater precipitation in the modern day, compared to the pre-settlement, 1920s and Dust Bowl scenarios. This hypothesis will be discussed in the following sections. Section 2 explains the land use land cover datasets used and the model configuration. Section 3 presents the results and discusses their implications. Section 4 summarizes the important conclusions of this research.

Chapter 2. Data and Methods

a. Land Use Land Cover Scenarios

Four LULC scenarios were chosen for this study: pre-settlement, 1920's, Dust Bowl and modern day. The pre-settlement scenario describes the natural Southern Great Plains vegetation prior to extensive human settlement and cropland development. The 1920's scenario was chosen due to the substantial westward expansion of cropland. The Dust Bowl altered the LULC of a substantial portion of the domain, creating large areas of barren and sparsely vegetated land. This is a valuable scenario, as the effects of barren soil can be studied in quasi-isolation. The final scenario, the present day, was used as the control and was compared to the other three scenarios. Each scenario's LULC conditions are described below.

i. Pre-settlement

The pre-settlement land use conditions were based on the Level IV ecoregion data from the United States Environmental Protection Agency (EPA) (Omernik and Griffith 2008). The data were obtained as a shapefile, and ArcGIS was used to extract the values into a table. The EPA data were compared to the 24 default WRF land use conditions from the United States Geological Society (USGS), and the EPA data were mapped to a functional WRF land cover category. The resulting grid of land use categories served as the land use condition for the WRF pre-settlement simulation.

In this scenario, about half of the domain is covered in grassland (Figure 2.2a). This land use extends from the northwestern corner of Iowa and includes nearly all of Nebraska and Kansas, the western half of Oklahoma, parts of Texas and into the eastern portions of New Mexico, Colorado and Wyoming. The remaining part of Iowa,

northwestern Missouri, far eastern Kansas, the eastern half of Oklahoma, and most of Illinois is classified as savanna. Southeastern Missouri, all of Arkansas, northern Louisiana, western Illinois, Tennessee and Mississippi and a portion of central Texas are classified as either deciduous broadleaf forest or a mix of forest types, including deciduous and evergreen forests. In central and far west Texas, there is a region of mixed shrubland/grassland and barren or sparsely vegetated land, respectively. Finally, the far western portion of the domain, including the western half of New Mexico, Colorado and Wyoming, is also covered in shrubland, barren or sparsely vegetated land, or a mixed shrubland and grassland. The Rocky Mountains region is dominated by evergreen needle leaf forest, with small areas of shrubland and grassland intermixed.

ii. 1920's

USGS reconstructed historical biophysical land cover data (Steyaert and Knox 2008) were used for the western half of the domain, and the Population and Environment in the U.S. Great Plains dataset was used for the eastern half of the domain (Gutmann et al. 2005). Both datasets were based on agriculture census data by county, where the acreage dedicated to particular land use in each county was used as a proxy for the land use conditions. Using this data, if the ratio of cropland to native land (from the pre-settlement data) was greater than half, then the dominant land use condition for that county was categorized as dry cropland. Both datasets were compared to the natural land cover conditions from the pre-settlement scenario, which acted as the default, and the changes were made accordingly. These conditions were used in the 1920's simulation.

In the 1920's scenario, there is a clear division between the land used for agriculture and that remaining as native vegetation. Eastern Nebraska, Kansas,

Oklahoma, Texas, all of Iowa and Illinois (or the portions that are included in the domain), northern Missouri, and parts of Arkansas, Tennessee, Mississippi and Louisiana are classified as dryland cropland and pasture (Figure 2.2b). The shift to dryland cropland and pasture in portions of Missouri south through Louisiana was at the expense of the mixed forests evident in the pre-settlement era. Western Nebraska, Kansas, Oklahoma and Texas and eastern Wyoming, Colorado and New Mexico remained grassland. Southern Missouri, parts of Arkansas, Louisiana, Texas and Mississippi were classified as either deciduous broadleaf forest or mixed forest. The Dallas-Fort Worth, Oklahoma City, and St. Louis metropolitan areas are denoted as urban land use, also a change from the pre-settlement condition. Finally, the far western portion of the domain, including the Rocky Mountains, remained similar to the pre-settlement condition.

iii. Dust Bowl

Prolonged drought in the early 1930's resulted in areas of barren soil or sparsely vegetated land in parts of the Southern Great Plains. The 1920's land use scenario served as the base condition, and was manipulated based on known soil erosion conditions from the Dust Bowl era (Figure 2.1). Portions of the LULC were altered to bare soil or sparse vegetation based on the extent of wind erosion. On a county scale, the severity of the wind erosion was estimated and used to alter the LULC to bare soil. In the regions characterized by severe wind erosion, 80% of the area was changed to bare soil. Moderate wind erosion was assumed to result in 60% bare soil, and counties with the least severe wind erosion were set to 20% bare soil. Starting from the 1920's scenario, only the region impacted by the Dust Bowl was altered for this scenario. Western Kansas, eastern Colorado and the panhandles of Texas and Oklahoma underwent the

greatest alteration of LULC conditions. Native grassland and newly altered cropland in this region changed to barren soil or sparely vegetated land as a result of the drought (Figure 2.2c).

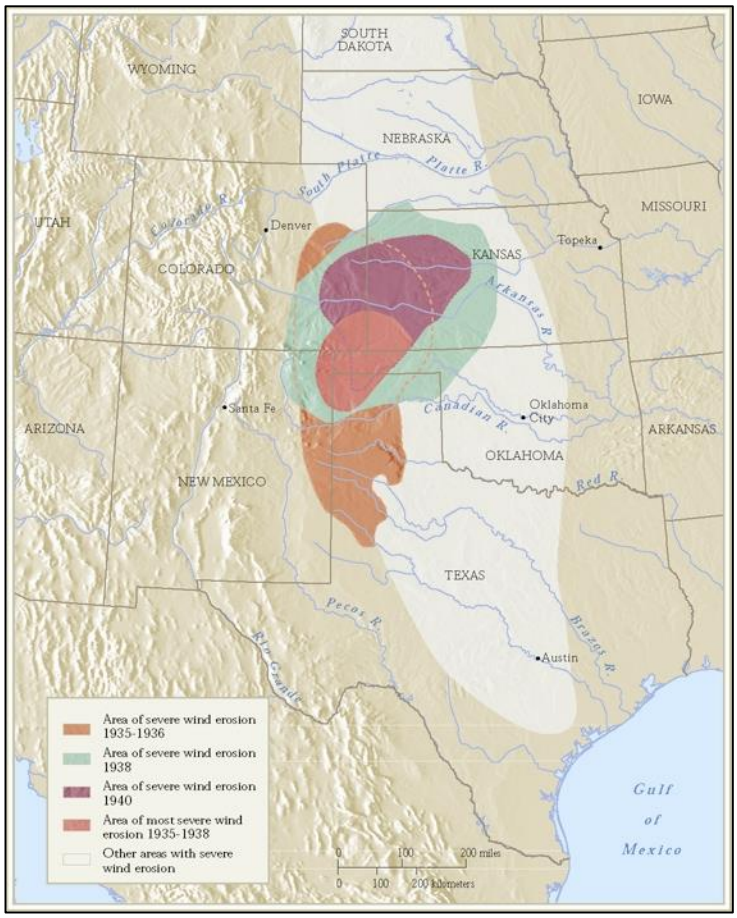

Figure 2.1. Areas of severe wind erosion during the Dust Bowl, 1935-1940. (Image courtesy of Dr. Chuck Boening, Shelton State Community College)

iv. Present Day

Data for this LULC scenario were obtained from the National Land Cover Database 2011, from the Multi-Resolution Land Characteristics Consortium (Homer et al. 2015). It should be noted that some of the changes of the LULC are not a consequence of the land use itself changing, but a result of the increase in spatial resolution in the

National Land Cover Database 2011 compared to the datasets used for the previous land use conditions. However, it was assimilated to a common grid spacing of 4 km to be consistent with the prior LULC scenarios. In a process similar to that used to generate the pre-settlement conditions, the 2011 data were compared to the 24 default WRF land use conditions from USGS and were mapped to a functional land condition to create the present day land use conditions.

The expansion of urbanization is most evident in the present day LULC condition (Figure 2.2d). A continued westward expansion of cropland is visible, now extending to the foothills of the Rocky Mountains and across the Texas Panhandle. Cropland now covers much of the eastern portion of the domain. Notable in this scenario is a reversal in the LULC conditions; some of the land which earlier changed from the native vegetation to dry cropland/pasture in Kansas and Oklahoma is now covered by grassland or savanna and a mixed forest once again. Finally, in western Wyoming, Colorado, Texas and most of New Mexico there is now predominantly shrubland and savanna. The Rocky Mountains are classified as a combination of forests, with a greater area of grassland and shrubland intermixed than in the natural vegetation scenario.

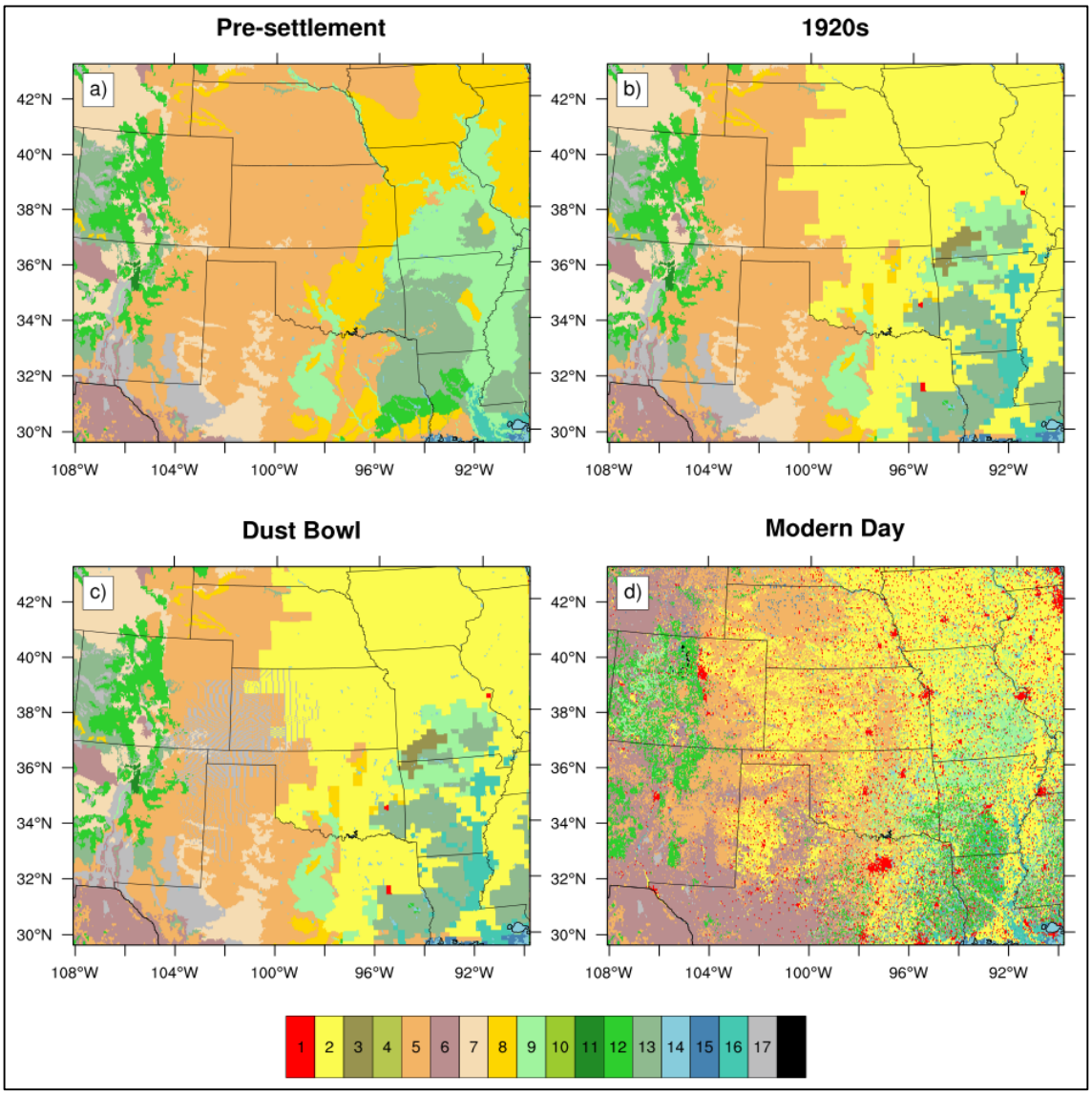

Figure 2.2. Land use land cover change for the pre-settlement (a), 1920's (b), Dust Bowl (c), and present day (d) time periods. The land use classifications are shown below.

1. Urban and Built-Up Land	10. Deciduous Needleleaf Forest
2. Cropland and Pasture	11. Evergreen Broadleaf Forest
3 Cropland/Grassland Mosaic	12. Evergreen Needleleaf Forest
4. Cropland/Woodland Mosaic	13. Mixed Forest
5. Grassland	14. Water Bodies
6. Shrubland	15. Herbaceous Wetland
7. Mixed Shrubland/Grassland	16. Woodland Wetland
8. Savanna	17. Barren or Sparsely Vegetated
9. Deciduous Broadleaf Forest	

b. Model Configuration

The Weather Research and Forecasting Model, version 3.6 (WRFv3.6; Skamarock et al. 2008), was the primary tool used in this study. North American Regional Reanalysis (NARR) data were used to provide initial and boundary conditions for the model simulations (Mesinger et al. 2006). The WRF was initialized using a nested domain, with a 12 km outer domain and a 4 km inner domain (Figure 2.3). The model parameterizations are shown in Table 1. With the exception of the land surface option, which was tested specifically for this project, all of the parameterization choices were determined based on similar studies utilizing WRF for land use studies (Lee and Berbery 2012, Cheng et al. 2013, Bagley et al. 2014).

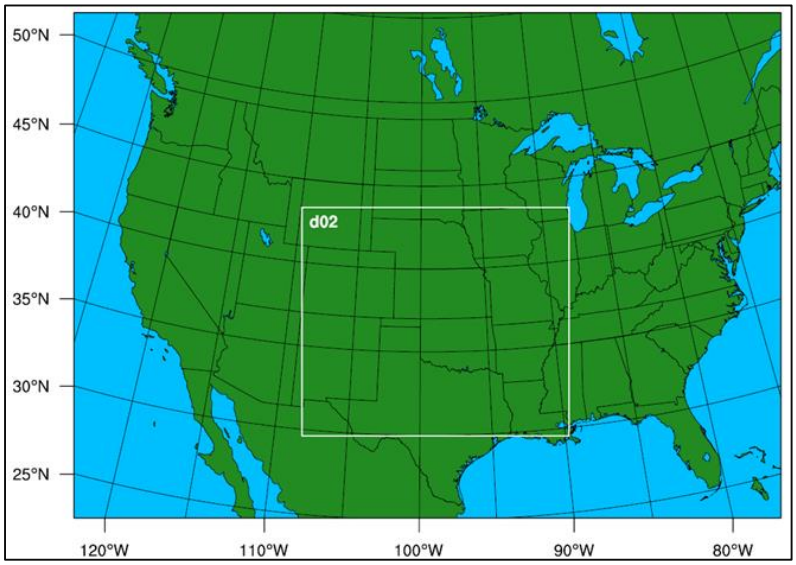

Figure 2.3. Domain for WRF simulations. Outer box represents the 12 km outer domain, with a 4 km nested domain indicated as d02.

Table 2.1. Parameterization schemes used in WRFv3.6 simulations.

Cumulus Parameterization	Kain-Fritsch Scheme	(Kain 2004)
Planetary Boundary Layer	Yonsei University Scheme	(Hong et al. 2006)
Microphysics	WRF single moment 5-class	(Hong et al. 2004)
Land Surface Option	Community Land Model Version 4	(Oleson et al. 2010)
Radiation	Dudhia Shortwave Scheme	(Dudhia 1989)
Surface Layer	MM5 Similarity Scheme	(Zhang and Anthes 1982)

The land surface model was chosen based on the results of Van Den Broeke et al. (2017), in which three land surface models, the Community Land Model version 4.0 (CLMv4; Oleson et al. 2010), Noah-MP (Niu et al. 2011) and the Bucket Model (Manebe 1969), were coupled to the WRF and the validity of their results (precipitation and

temperature) were compared to reanalysis data to determine the best land surface model for this study. The Bucket Model had the largest biases in temperature and monthly precipitation, likely due to its simplistic design—the land surface and underlying soil levels are represented by a bucket that is filled by precipitation and snowmelt, and emptied by evaporation and drainage. When the bucket is filled past its field capacity, it overflows as runoff. CLMv4 and NOAH-MP have multiple soil levels, so these models are able to resolve temperature and moisture profiles below the ground level. This was likely the reason for the smaller biases with the two more complex models. However, it should be noted that the CLMv4 does include more soil levels than Noah-MP. This, combined with its ability to allow for more vegetation types per grid cell than NOAH-MP, made this land surface model the most suitable option for this study (Van Den Broeke et al. 2017).

The CLMv4 is the land component of the Community Earth System Model developed at NCAR. The land surface is composed of five sub-grid land cover types: glacier, wetland, vegetated land, lakes and urban regions. There is a subgrid level for the plant functional type, with 16 possibilities based on leaf and stem optical properties such as canopy height, leaf area index (LAI) and stem area index. The CLMv4 also includes a dynamic vegetation option, the ability to simulate transient LULC changes, which has made it increasingly suited for research dealing with LULC changes (Lawrence et al. 2011). For the purpose of this study, dynamic vegetation was not used since little prior work has been performed to validate the realism of this approach. Instead, static vegetation based on each of the four LULC scenarios was used, which still allows for seasonal LAI changes.

The WRF was run for a thirteen-year period (1990-2002) for each LULC condition. This time period was chosen because it encompasses a wide range of oceanic sea surface temperature variability, specifically both warm and cool phases of ENSO and the AMO, which has implications for Southern Great Plains precipitation patterns (Hu and Feng 2012, Weaver et al. 2009, Hu et al. 2011). From this thirteen-year period, the latter eight years were used for analysis. Previous research concluded that soil moisture can take about 5.5 years to spin-up to an equilibrium state, since it is largely controlled by temperature and precipitation (Cosgrove et al. 2003). Therefore, the first five years of the thirteen-year period were discarded to allow for model spin-up. Analysis focused on the months of May-August, as these months best highlighted the changes in warm season precipitation.

c. Model Validation

The work of Van Den Broeke et al. (2017) demonstrated the validity of the model set-up, to ensure that WRF produced realistic simulations over the Southern Great Plains domain. WRFv3.6 was coupled with the CLMv4 and the results were compared to data from the Parameterization Relationships on Independent Slopes Model (PRISM; PRISM Climate Group 2015) and Atmospheric Radiation Measurement (ARM) and AmeriFlux observations. Overall, the model was warmer than observations and this warm bias increased throughout the summer months. Precipitation biases were attributed to the spatial and temporal variability of precipitation events, as there was no consistent bias through the summer months. Past work has identified a warm bias in the CLMv4 (Lu and Kueppers 2012). Due to this limitation, the results should not be interpreted based on the magnitude of the data but on the trends in the comparisons.

Chapter 3. Results and Analysis

Means were computed for each month in the eight-year dataset (1995-2002), yielding 32 monthly means for each scenario. The comparisons were done with respect to the modern day scenario to examine differences in the regional climate as a result of changing LULC. Therefore, positive differences indicate an increase in the modern day scenario, and negative differences indicate a decrease in the modern day scenario. In addition, the significance of the differences was computed using the standard deviation of the differences of the mean:

$$\sigma_{m_1-m_2} = \sqrt{\frac{\sigma_1}{n} + \frac{\sigma_2}{n}}$$

where σ_1, σ_2 are the standard deviations of the respective monthly means, and n is the number of samples. Herein, σ_1 and σ_2 represent the standard deviation of the different scenarios, and the number of samples, n, is eight, for the eight years in the dataset. This assumes that the results follow a normal distribution, and they meet this requirement (not shown). The standard deviation will be shown in each figure, and values two standard deviations from the mean will be contoured. Values two standard deviations from the mean represent values that are statistically significant at the 95% confidence interval. In the figures, they will be displayed as a solid line (for positive 2σ), and as a dashed line (for negative 2σ).

The results will illustrate differences in the surface energy budget (surface albedo, surface sensible and latent heat fluxes), the low-level temperature and moisture profiles and the regional circulation to diagnose changes in boundary layer characteristics and moisture transport that lead to differences in precipitation. The following sections will discuss the atmospheric differences between the modern day and pre-settlement (a),

1920's (b) and Dust Bowl (c) scenarios as a result of the LULC changes.

a. Modern Day versus Pre-settlement

i. Surface Energy Budget

Surface albedo of the modern day was higher in the eastern portion of the domain (from the Mississippi River to the eastern edge of the domain) and lower in the southwest (far West Texas and southern New Mexico). In May and June, there were higher surface albedos over the Rocky Mountains that was statistically significant. This difference can be attributed to deforestation in this region from the pre-settlement scenario, where evergreen forests were the dominant LULC. In the modern day, this region is covered by grassland and barren soil, as well as the native evergreen forests (Figure 3.1). Since the higher surface albedos were only evident in May and June, this change may be representative of snow cover. Generally, snow does not remain on trees for very long, so the albedo of the forest is lower than other surfaces where snow cover is more prevalent, such as the grassland and barren soil present in the modern day scenario.

Over far West Texas, the surface albedo of the modern day scenario was lower compared to that of the pre-settlement scenario. This region underwent a LULC change from barren or sparsely vegetated soil to a shrubland/grassland mix. This change in surface albedo was also statistically significant. This result indicates that the shrubland/grassland mix has a lower surface albedo than that of the barren soil in this region (Figure 3.1). The soil prevalent in this area is primarily brown soil that is light when dry and darker when saturated (Natural Resources Conservation Service, United States Department of Agriculture). Since this area does not receive much rain

climatologically, the albedo is likely higher on average to reflect the dry soil. A dry and light brown soil will have a greater surface albedo than shrubland, and thus lower surface albedo resulted.

Generally, the regions with higher (lower) surface albedos in the modern day align with regions of lower (higher) surface sensible heat flux. Surfaces with higher (lower) albedo reflect more (less) energy than they absorb, so this result makes sense. For example, in May and June, the sensible heat flux was lower over the same area where the surface albedo was higher in the modern day. Similarly, in far West Texas where the surface albedo was lower, the sensible heat flux was higher (Figures 3.1, 3.2).

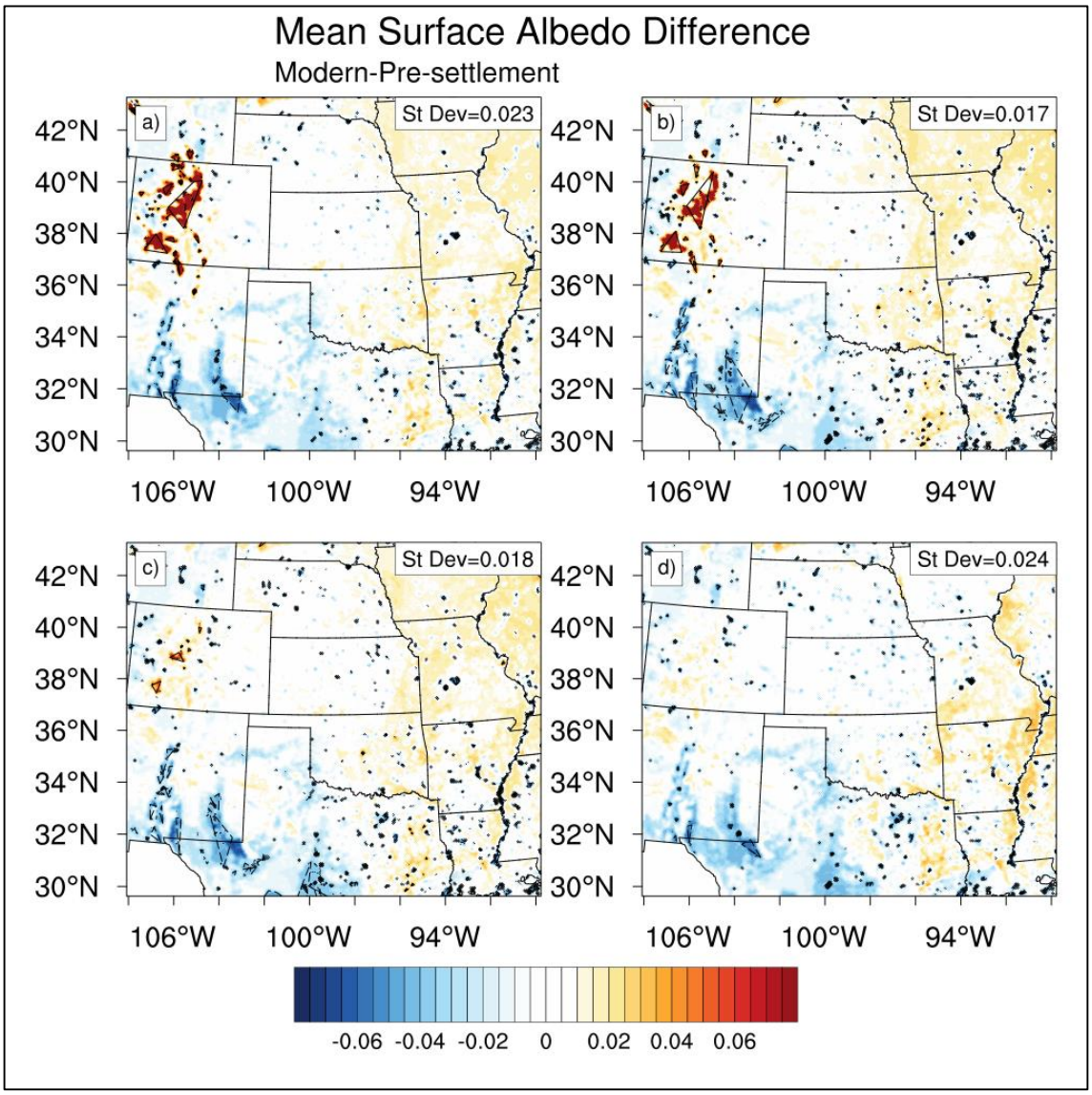

Figure 3.1. Mean May (a), June (b) July (c) and August (d) surface albedo differences (modern day minus pre-settlement). $\pm 2\sigma$ contoured in black; solid line for $+2\sigma$ and dashed for -2σ.

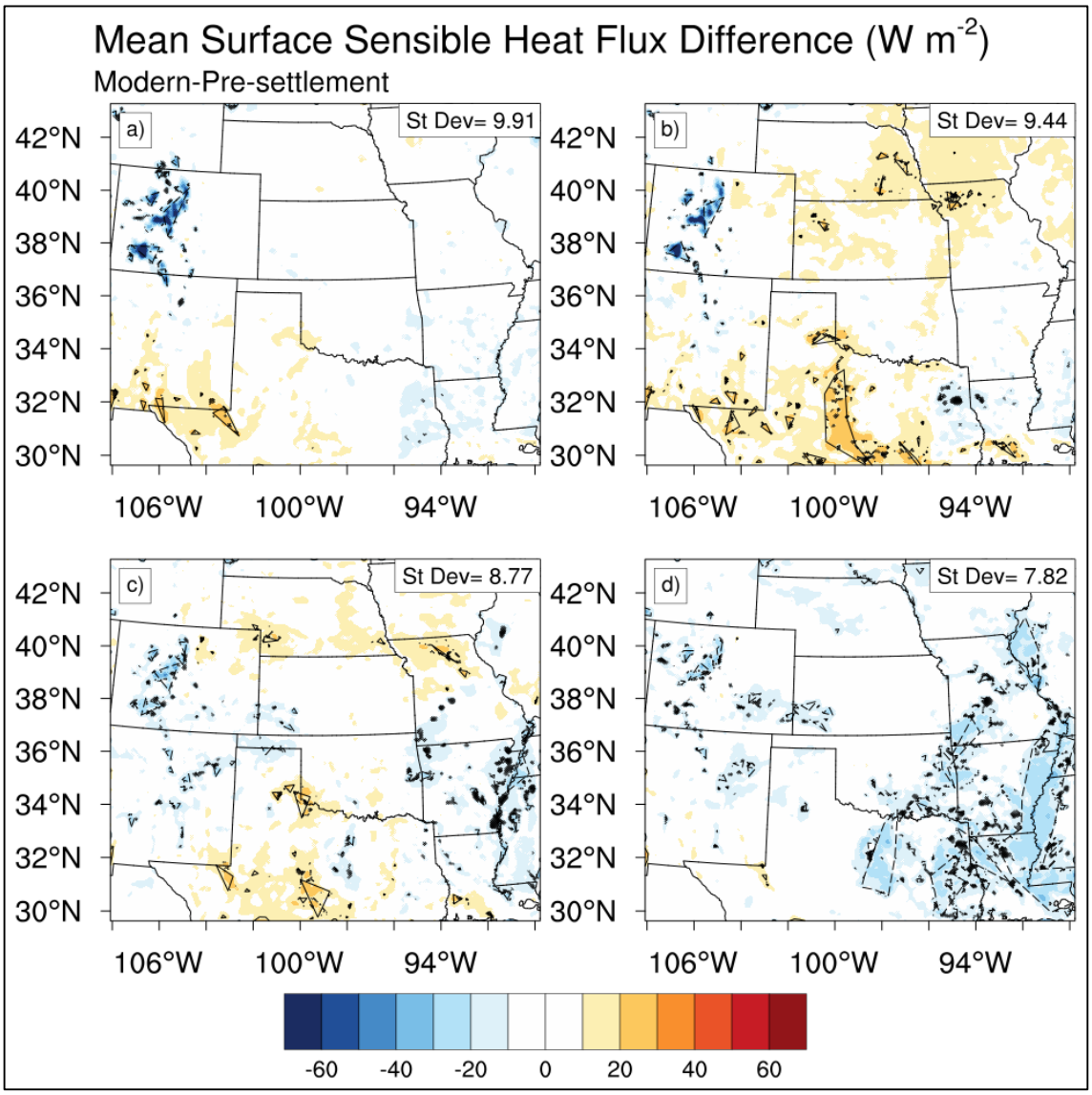

Figure 3.2. Mean May (a), June (b) July (c) and August (d) surface sensible heat flux differences (modern day minus pre-settlement).
$\pm 2\sigma$ contoured in black; solid line for $+2\sigma$ and dashed for -2σ.

Based on the mean surface sensible heat flux of the modern day scenario (Figure 3.3), the higher surface albedos did not cause the average sensible heat flux to switch signs but rather decreased the magnitude of the positive flux. This relationship is not valid for the entire domain; in July, the surface albedo over most of Iowa was higher in

the modern day, as was the sensible heat flux. However, these differences were not statistically significant.

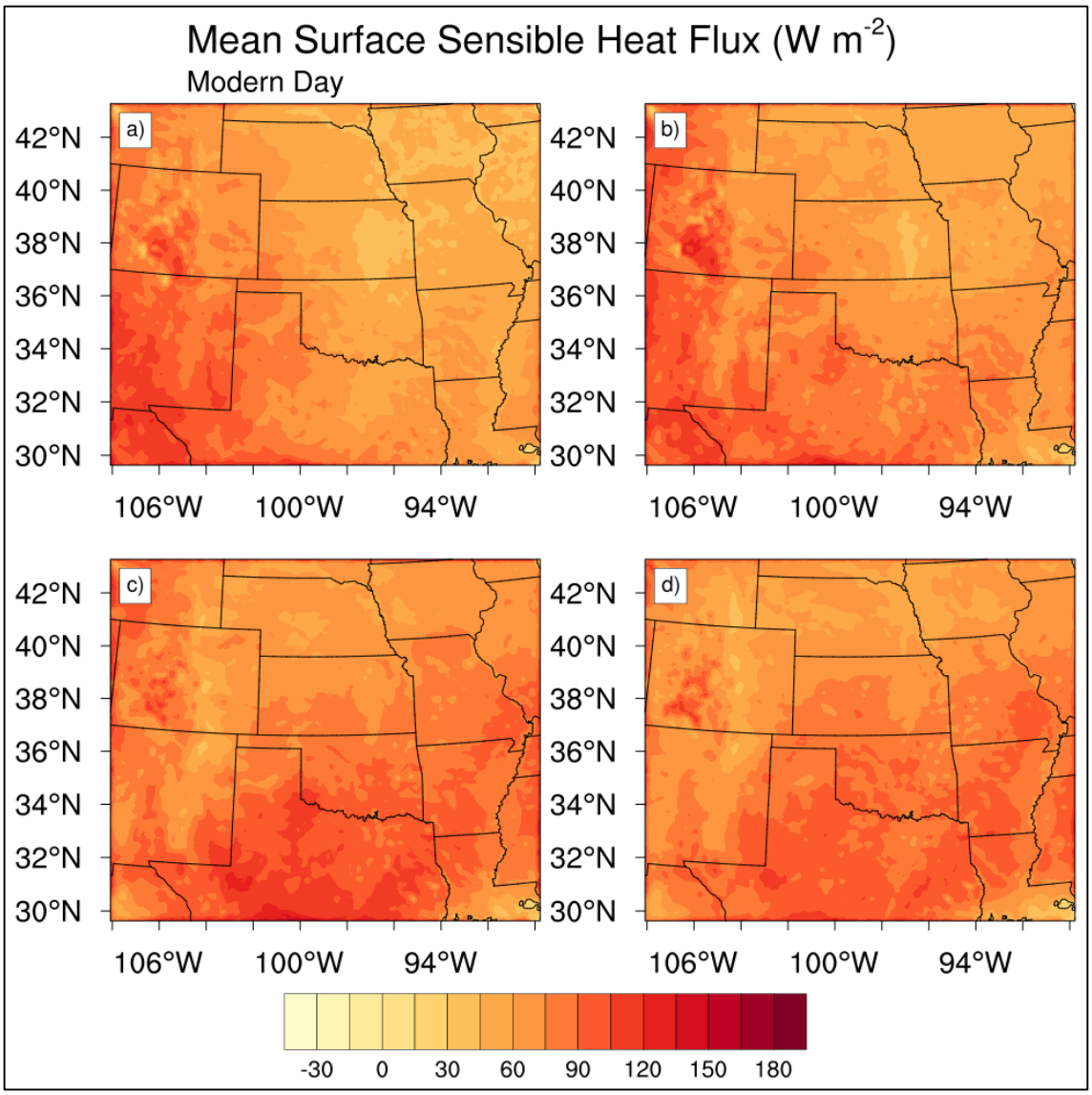

Figure 3.3. Mean May (a), June (b) July (c) and August (d) surface sensible heat flux for the modern day scenario.

The differences in the surface latent heat flux can be related to the changes in surface albedo as well as soil moisture. Higher soil moisture content in the modern day is associated with higher surface latent heat fluxes. Therefore, the differences found in the

latent heat flux were anticipated to mirror the differences in soil moisture. Similar to the differences in soil moisture, the results were most significant in August, where significantly higher surface latent heat fluxes covered nearly the entire domain (Figures 3.4, 3.5).

In both June and July, significantly lower surface latent heat fluxes were found over northern Missouri and southern Iowa, which does not support the aforementioned relationship between the surface latent heat flux and soil moisture, or the relationship between surface albedo and surface sensible heat differences. The surface albedo in this region was higher in the modern day, and counterintuitively, the surface sensible heat flux was as well. This result does not have an intuitive explanation.

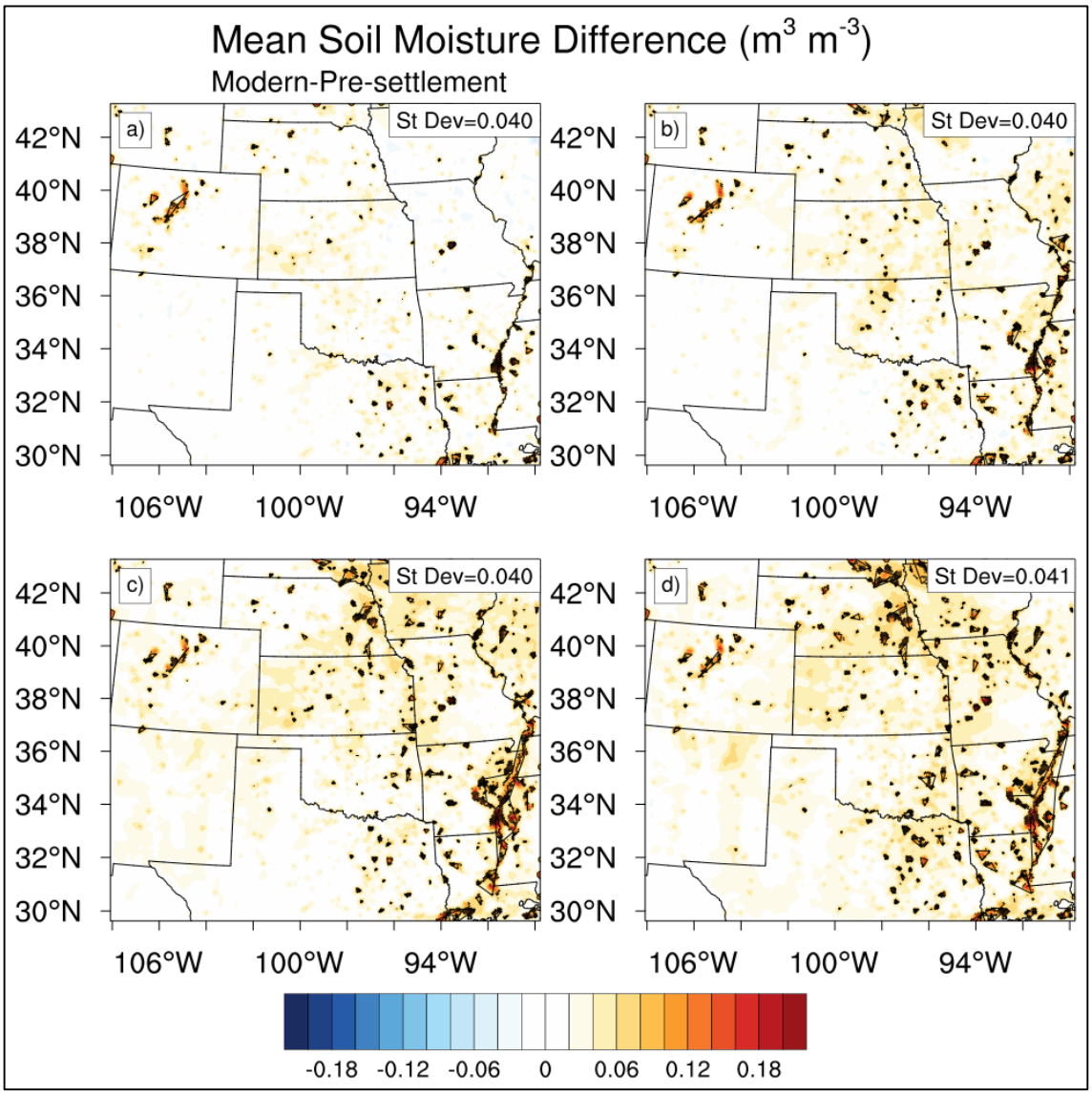

Figure 3.4. Mean May (a), June (b) July (c) and August (d) soil moisture differences, from the top soil level centered at 7cm (modern day minus pre-settlement). $\pm 2\sigma$ contoured in black; solid line for $+2\sigma$ and dashed for -2σ.

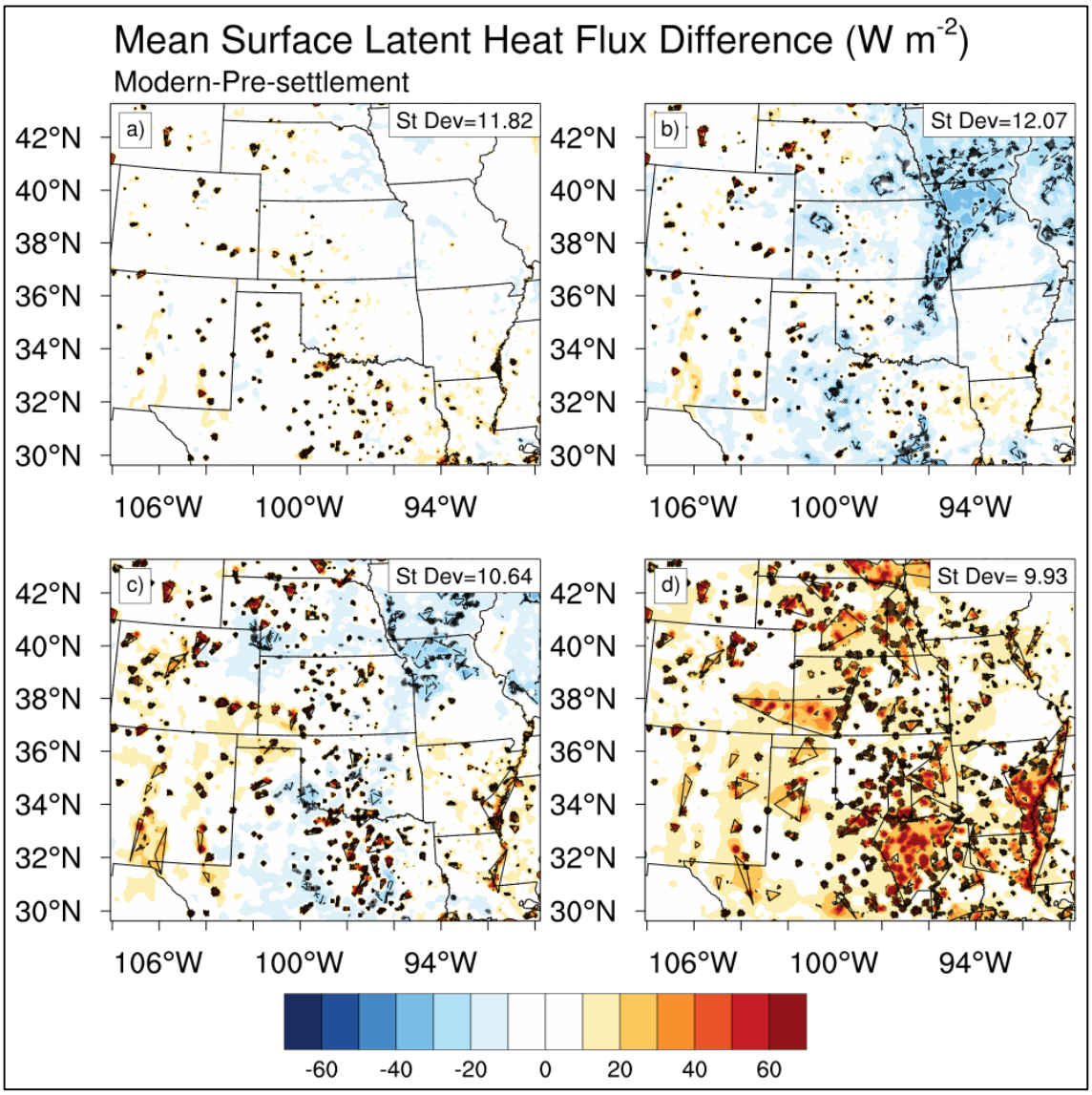

Figure 3.5. As in Figure 3.2 but for surface latent heat flux differences.

ii. Temperature and Dewpoint

The differences in surface albedo are not well aligned with the differences in 2m air temperature. It was anticipated that regions with a lower surface albedo in the modern day should have a higher mean 2m air temperature. However, this is not necessarily the case. This suggests that the differences in surface albedo are not the only factors leading to the differences between the regional climates of each LULC scenario. For example,

the region in far West Texas with significantly lower surface albedos in the modern day did not show higher 2m air temperatures. Instead, no change in 2m air temperature was found for this region (Figures 3.1, 3.6).

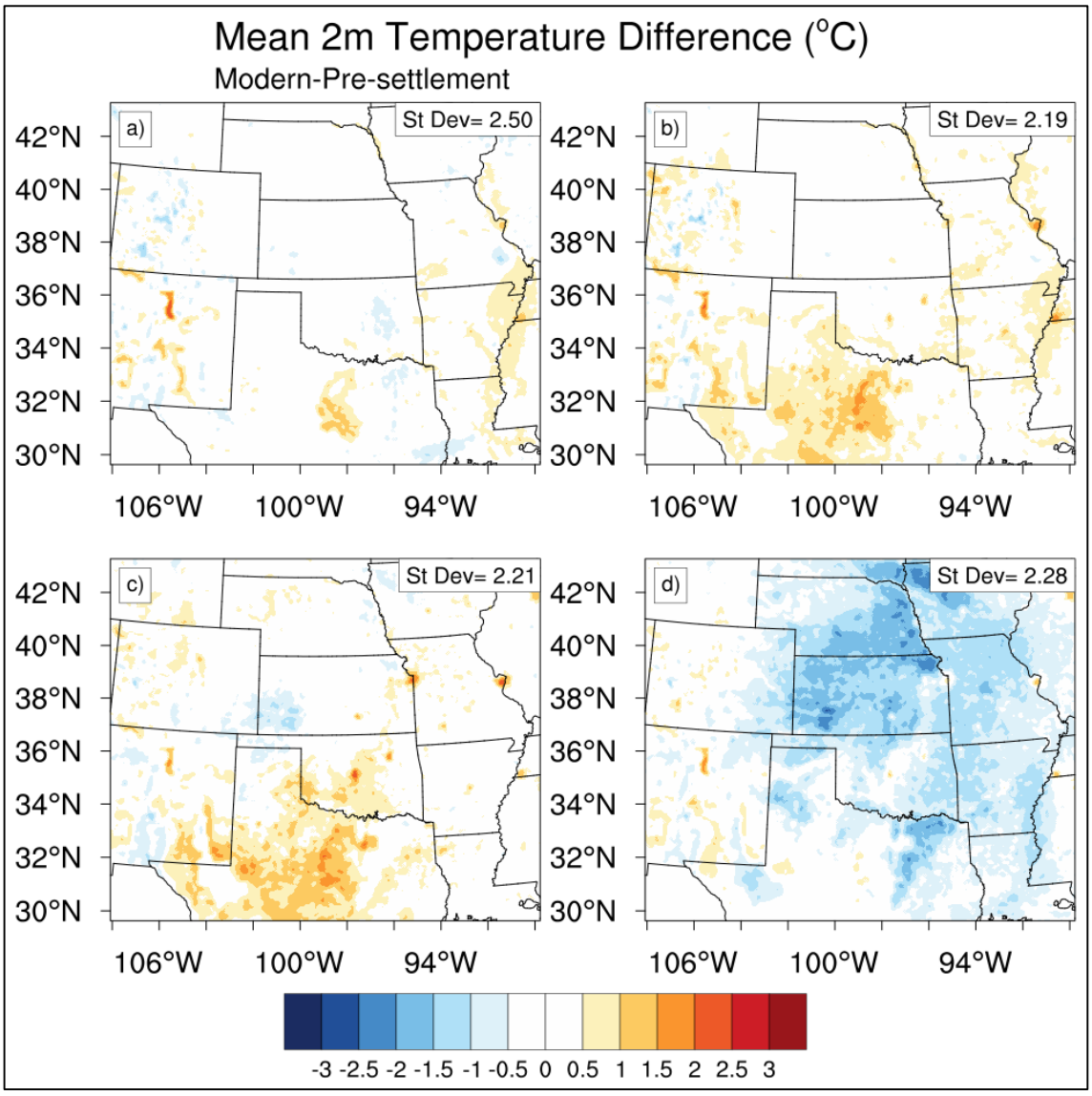

Figure 3.6. Mean May (a), June (b) July (c) and August (d) 2m air temperature differences (modern day minus pre-settlement).

In June and July, there was a broad area of higher temperatures centered in central Texas. This region underwent a land use change from native vegetation of grassland/shrubland and deciduous broadleaf forest to a mosaic composed of grassland, cropland and sparsely vegetated land. However, this region's LULC did not result in a large difference in surface albedo. This LULC change explains the higher temperatures, as the modern day vegetation is able to use the net radiation to warm the surface, whereas the native vegetation (specifically broadleaf forest) holds more moisture and therefore some of the net radiation would be utilized as latent heat. It should be noted that this warming result disappears in August. As seen in Figure 3.7, the climatological maximum in 2m air temperature occurred over the domain in August. This result suggests that the changing land use did not cause the overall summertime maximum temperature to increase, but instead caused the region to reach its maximum temperature earlier in the season (Figure 3.6).

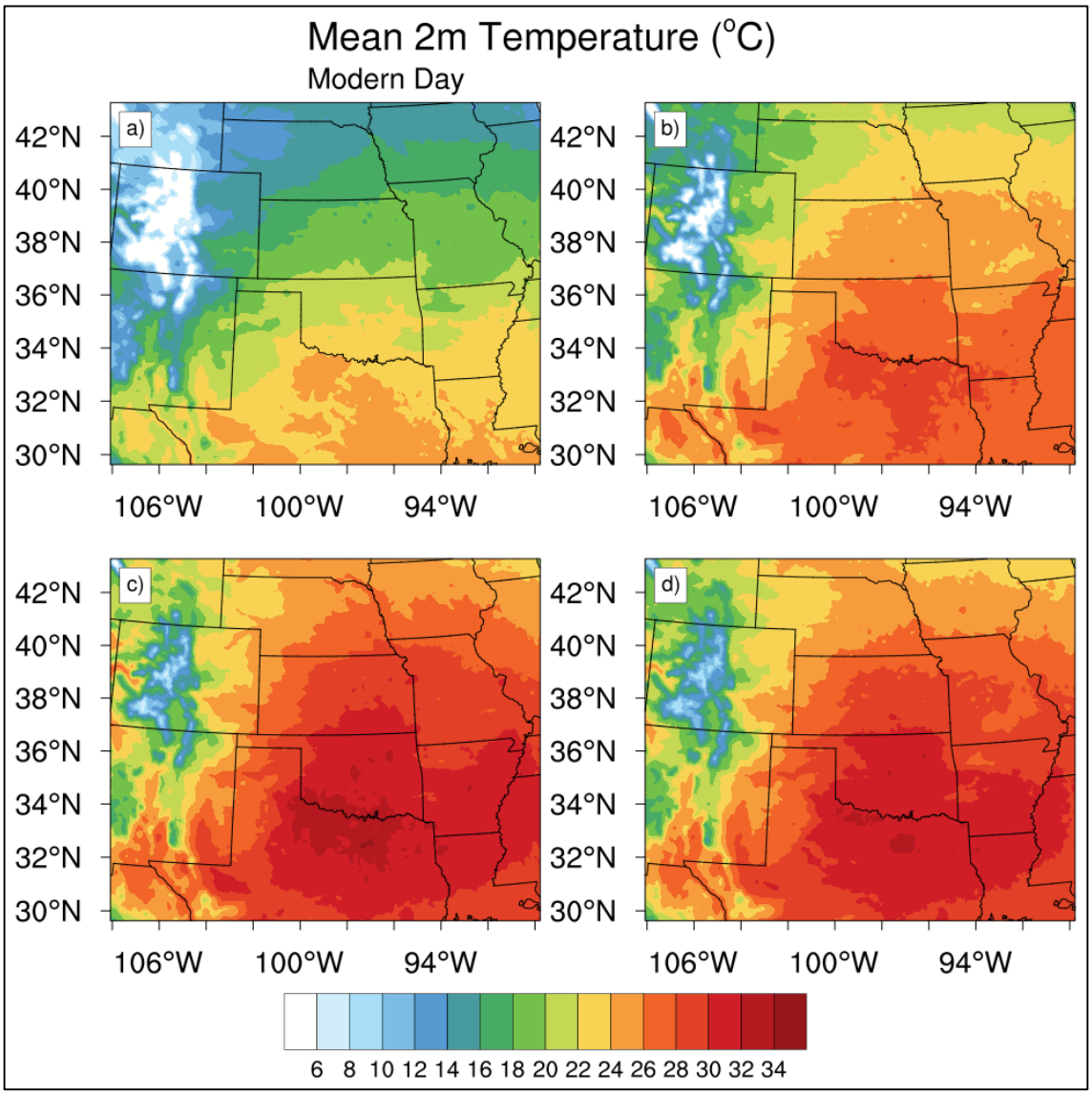

Figure 3.7. Mean May (a), June (b) July (c) and August (d) 2m air temperature for the modern day scenario.

A few cities are distinguishable, such as Dallas-Fort Worth, St. Louis, Kansas City, and Oklahoma City, due to their urban heat island, with higher temperatures in the modern day than in the pre-settlement LULC scenario (Figure 3.6). In August, lower temperatures were found in much of Nebraska, Kansas, Oklahoma, Iowa, and Missouri in the modern day compared to the pre-settlement scenario. This broad area changed from

the native vegetation of grassland, savanna, deciduous broadleaf forests (Missouri only) to a mix of cropland and pasture and grassland, without large differences in the surface albedo. However, there were much higher surface latent heat fluxes. This region also displayed the most dramatic results in the dewpoint differences, where higher dewpoints in the modern day resulted over a broad area. The magnitude of the difference ranges from 1-3ºC, with largest differences over regions where the dominant land use is cropland. These results suggest that, during the climatologically warmest and driest month, cropland, pasture and grassland are relatively cooler than the native vegetation but have higher dewpoints. The higher surface latent heat fluxes indicate that there was more evaporation associated with the modern day vegetation than in that of the pre-settlement, and the higher evaporative fraction supports this (Figure 3.8). Increased evaporation resulted in an overall cooling of the surface, since evaporation requires energy from the atmosphere to complete the phase change. The increase in 2m dewpoint also supports this, as the dewpoint increases with the increased water vapor in the atmosphere. The temperature differences are not significant, but the dewpoint differences above 3ºC do hold significance (Figure 3.9).

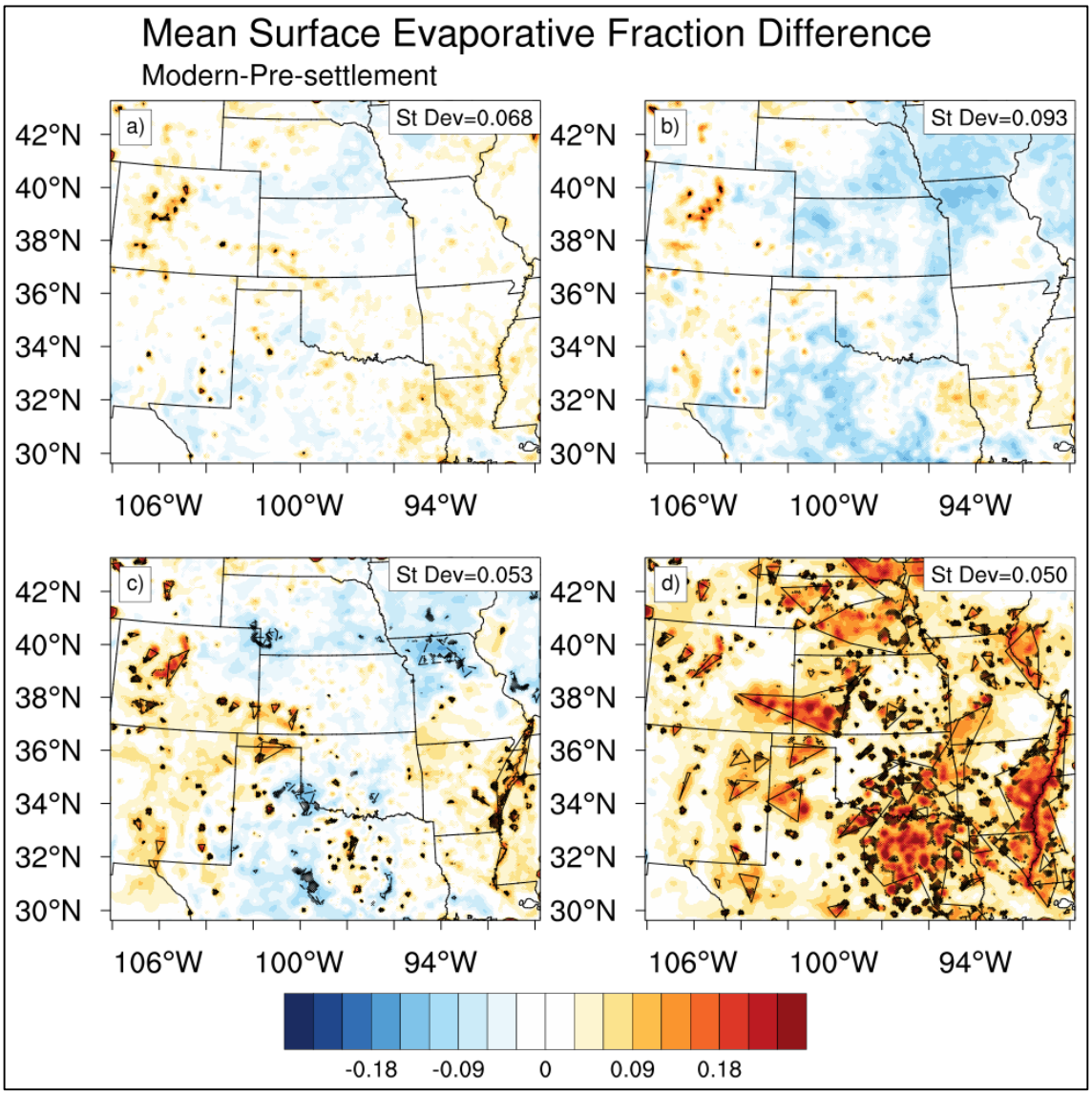

Figure 3.8. Mean May (a), June (b) July (c) and August (d) evaporative fraction differences (modern day minus pre-settlement).
$\pm 2\sigma$ contoured in black; solid line for $+2\sigma$ and dashed for -2σ.

Far West Texas and southern New Mexico exhibited lower dewpoints through the summer months with respect to the modern day scenario (Figure 3.9). The magnitude of the difference decreased from 3ºC to 1ºC through the summer, but even in August the difference is notable. This area coincides with a LULC change from barren soil or

sparsely vegetated land in the pre-settlement era to a mixed shrubland/grassland in the modern day that also resulted in lower surface albedo in the modern day. This result is peculiar; both LULC types inheritably have a relatively low moisture content, but higher surface dewpoints with barren soil was not anticipated. Furthermore, as mentioned above, there were not dramatic differences in temperature in this region which would suggest the ability to increase the moisture content with higher temperatures. This may be a result of an altered regional circulation, which will be addressed in a further section.

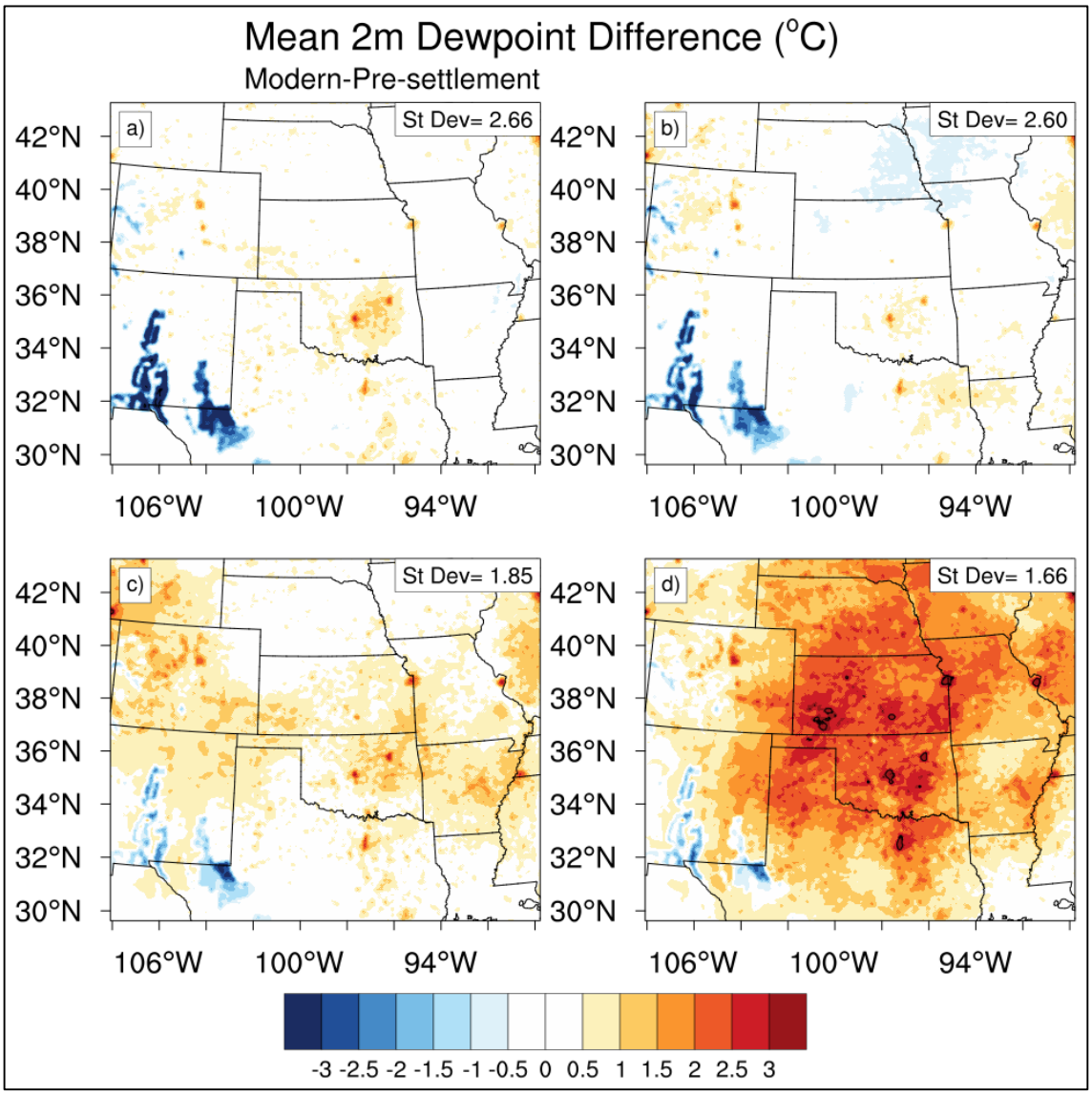

Figure 3.9. Mean May (a), June (b) July (c) and August (d) 2m dewpoint differences (modern day minus pre-settlement). $\pm 2\sigma$ contoured in black; solid line for $+2\sigma$ and dashed for -2σ.

iii. Regional Circulation

The changing LULC between the modern and pre-settlement scenarios only resulted in subtle differences in mean sea level pressure, with the most substantial differences occurring in August. The mean surface pressure over parts of Kansas and

Missouri was 0.6-0.8hPa higher in the modern day in August. An area of lower pressure in the modern day was also present in June, July and August in Texas and New Mexico. Both differences were fairly small and not significant. The higher surface pressure differences in August suggest higher pressure over this region in the modern day. These differences are indicative of a slight change in the regional circulation from the pre-settlement to the modern day as a result of the LULC changes. The differences in the 10m winds, both in the U and V direction, also indicate a slight change in the regional circulation (Figure 3.10).

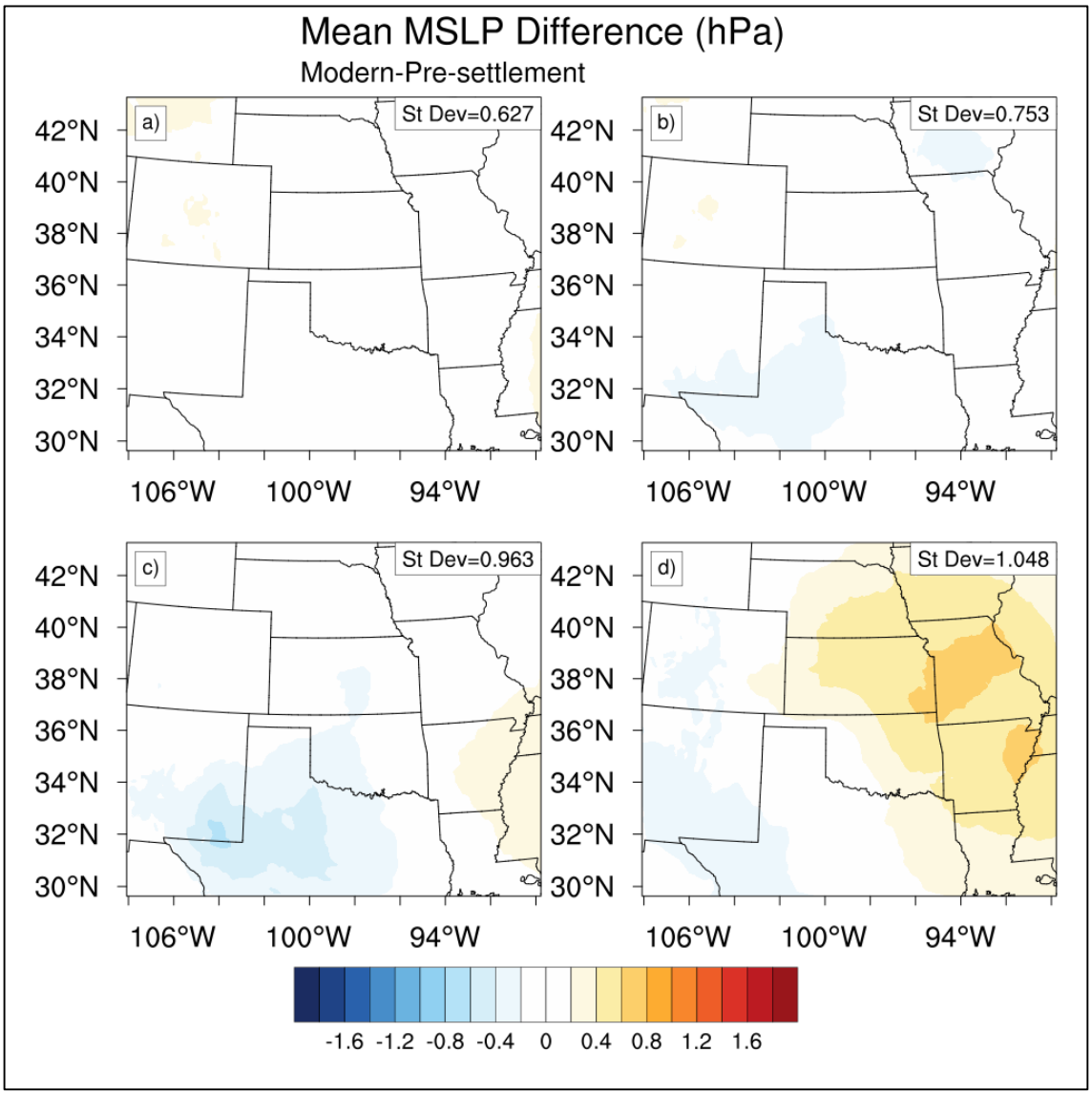

Figure 3.10. Mean May (a), June (b) July (c) and August (d) mean sea level pressure differences (modern day minus pre-settlement).

There are a few ways to interpret the differences in the wind field. For instance, a positive difference in the zonal wind could indicate either stronger westerly winds or a weaker easterly winds, and similar for the meridional winds. For this reason, these results will be compared to the results of the modern day scenario to correctly interpret

the differences. Differences in the U-component of the wind (hereafter referred to as U-wind, and the V-wind for the V-component of the wind) were on the order of tenths of meters per second. There were small areas of significantly stronger positive U-winds in the Rocky Mountains region and in central New Mexico in May and June (Figure 3.11a-b). In July and August, an area of stronger positive U-winds was evident in far southwest Texas (Figure 3.11c-d). Since this region exhibited a negative average U-wind in the modern day scenario, this suggests that the flow in the negative U-direction has weakened in the modern day due to the LULC changes (Figure 3.12c-d). In June, parts of north central Texas and south central Oklahoma exhibited negative U-winds. This area became broader in July and August. In August, the stronger negative U-winds were greatest over Oklahoma, but also extended through most of the domain. The average U-wind in the modern day scenario over this region was weakly negative, indicating that the LULC change resulted in stronger negative U-winds (Figure 3.12). These results support the suggestion that the change in LULC changed the regional circulation from the pre-settlement to the modern day, as stronger negative U-winds indicate enhanced easterly winds, which would be found along the southern extent of high pressure.

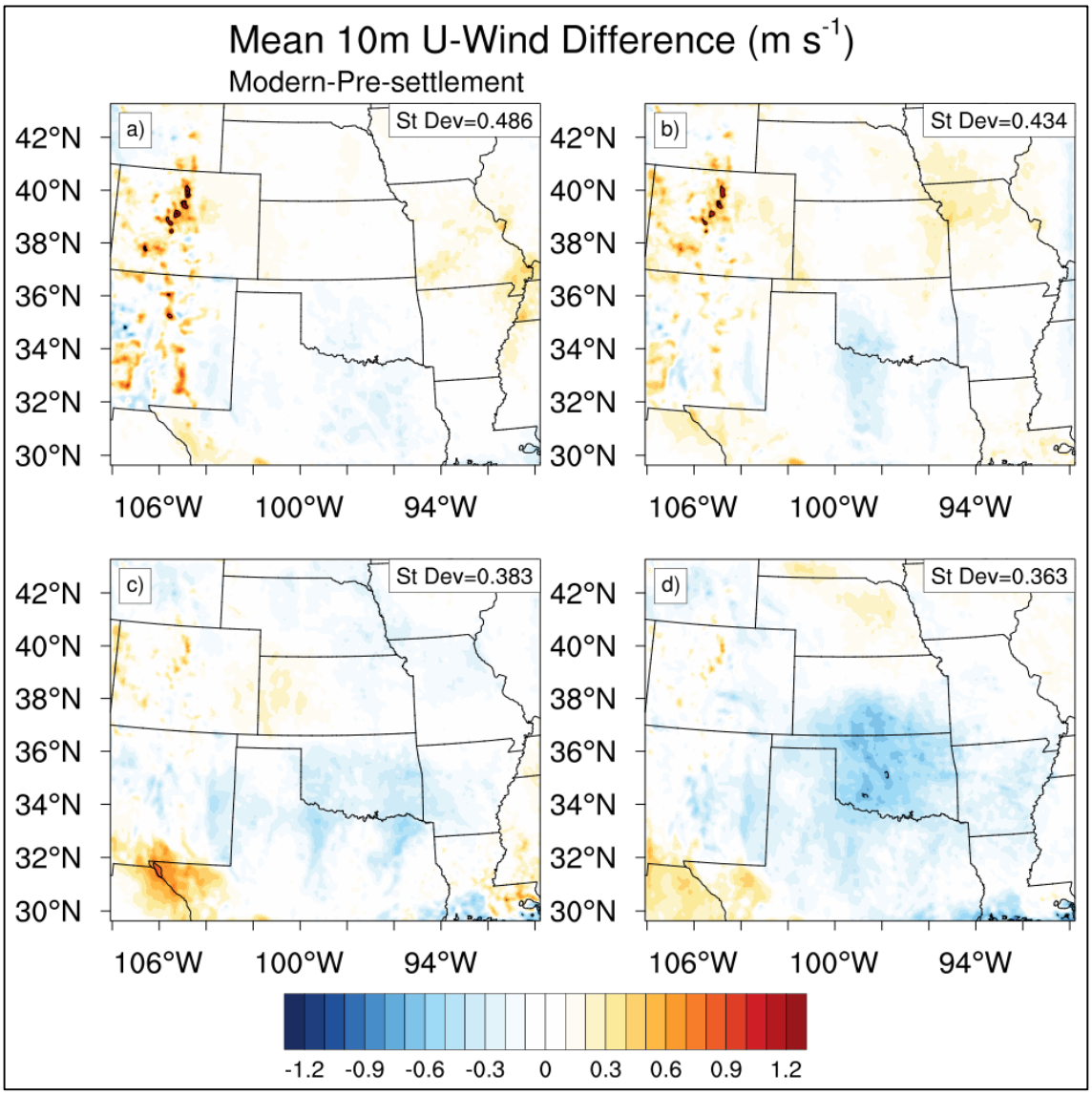

Figure 3.11. Mean May (a), June (b), July (c) and August (d) 10m U-wind differences (modern day minus pre-settlement). $\pm 2\sigma$ contoured in black; solid line for $+2\sigma$ and dashed for -2σ.

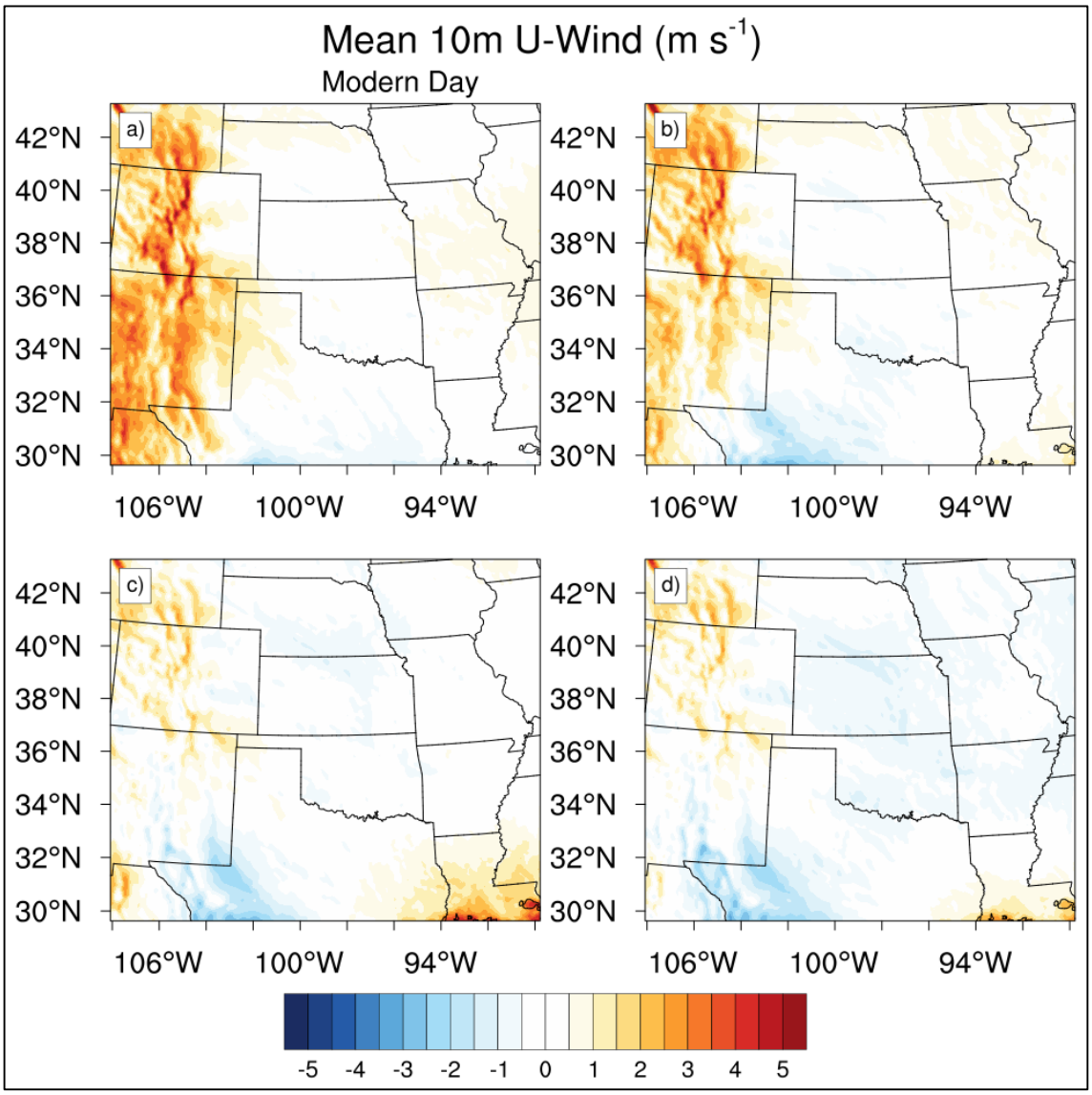

Figure 3.12. Mean May (a), June (b) July (c) and August (d) 10 U-winds for the modern day scenario.

The most noteworthy difference in the meridional winds was located over central Texas and Oklahoma, where there were stronger positive V-winds in the modern day (Figure 3.13). The average V-winds of the modern day were generally all positive, so the LULC change resulted in stronger positive V-winds (Figure 3.14) The difference in V-wind was significant in May, June and July. Stronger positive V-winds were also found

over much of the eastern portion of the domain. The stronger positive V-winds are indicative of enhanced southerly winds, which could increase moisture transport from the Gulf of Mexico. This is supported by the differences in the mean vertically integrated meridional moisture flux (hereby referred to as moisture flux), as a greater moisture flux generally coincided with the regions of stronger positive V-winds. The differences in the V-winds also indicate a regional circulation change, due to location of the stronger positive V-winds in correspondence with the higher surface pressure in August.

Finally, over far West Texas, stronger negative V-winds occurred in the modern day scenario, indicating a weaker positive V-wind, as the average V-wind for this region in the modern day was positive (Figures 3.13, 3.14). As mentioned above, this region transitioned from a barren soil/sparsely vegetated land to shrubland between the pre-settlement and modern day scenarios. Lower 2m dewpoints were found in the present day, which was not anticipated (Figure 3.9). One cause for the lower dewpoints may be the shift in the regional circulation, as negative V-winds resulted in this region in the modern day. This would suppress the moisture flow from the Gulf of Mexico and result in less moisture and thus a lower 2m dewpoint. This holds true at the surface, however the differences in mean vertically integrated meridional moisture flux does not support this. The mean vertically integrated meridional moisture flux was greater in this region in the modern day than in the pre-settlement scenario in June and July, which indicates increased moisture transport and should result in higher 2m dewpoints (Figure 3.15). In August, the moisture flux over the region was slightly lower in the modern day, but the differences in 2m dewpoint were lowest in this month.

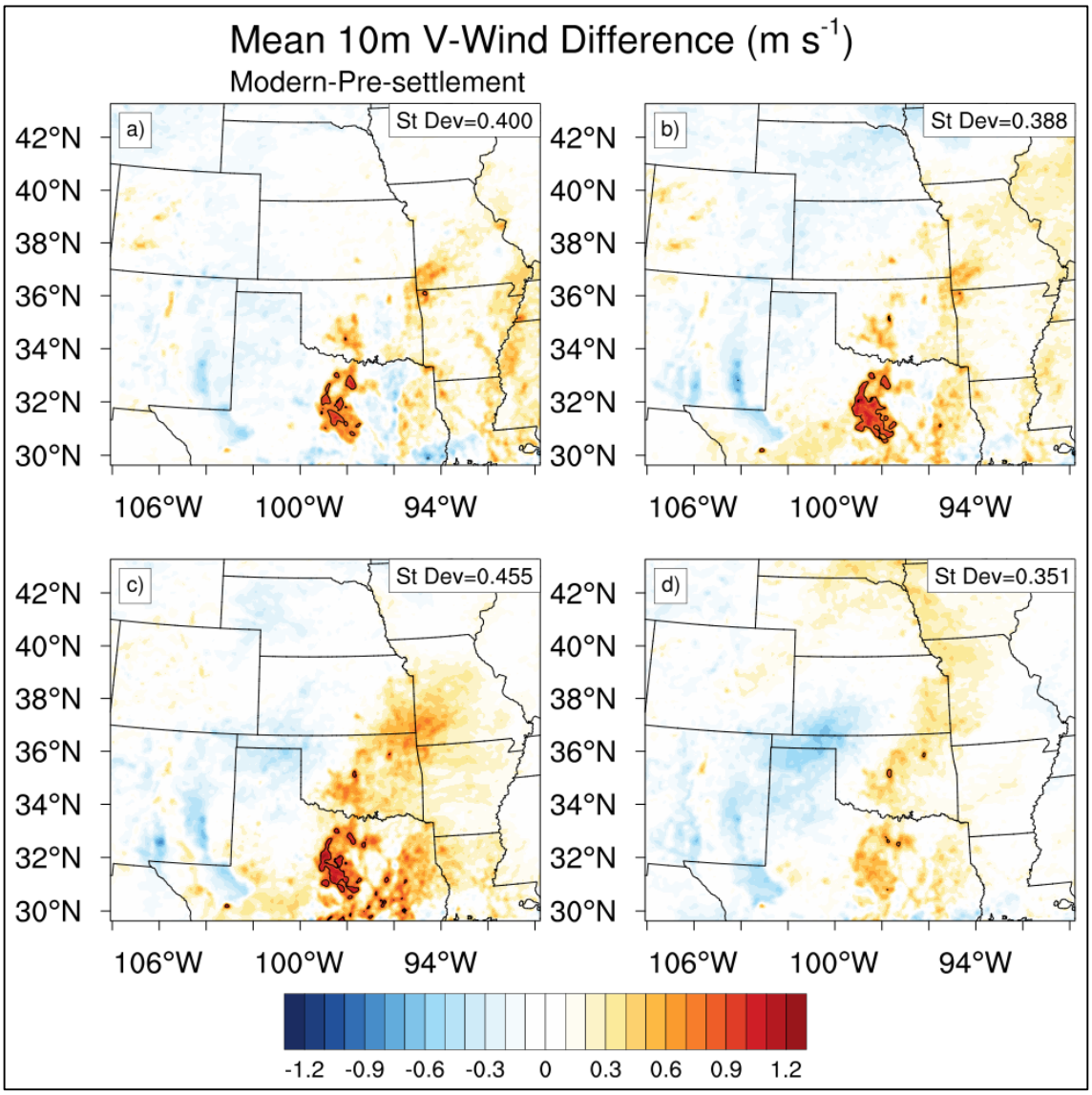

Figure 3.13. As in Figure 3.11 but for 10m V-wind differences.

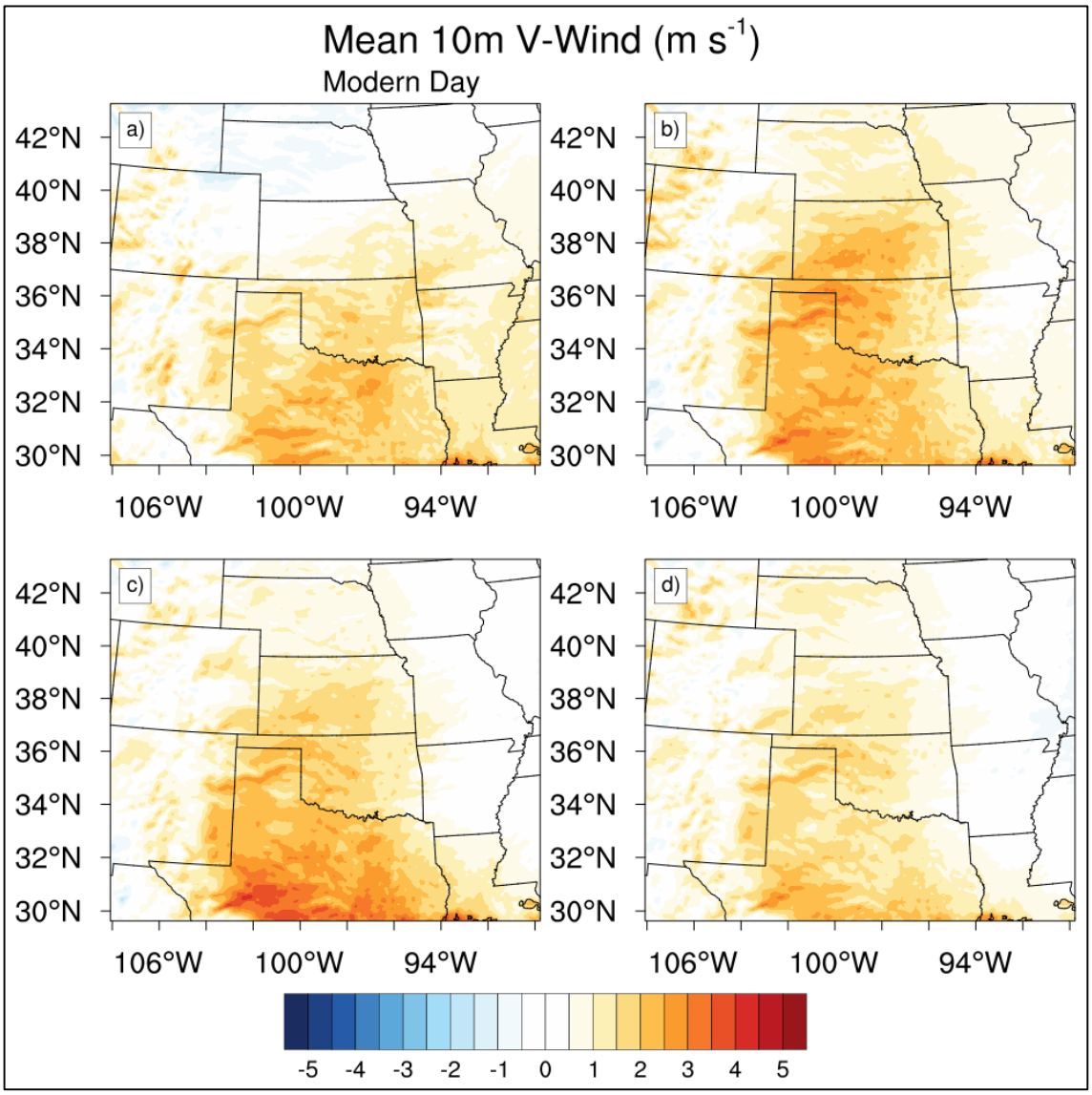

Figure 3.14. As in Figure 3.12 but for 10m V-wind.

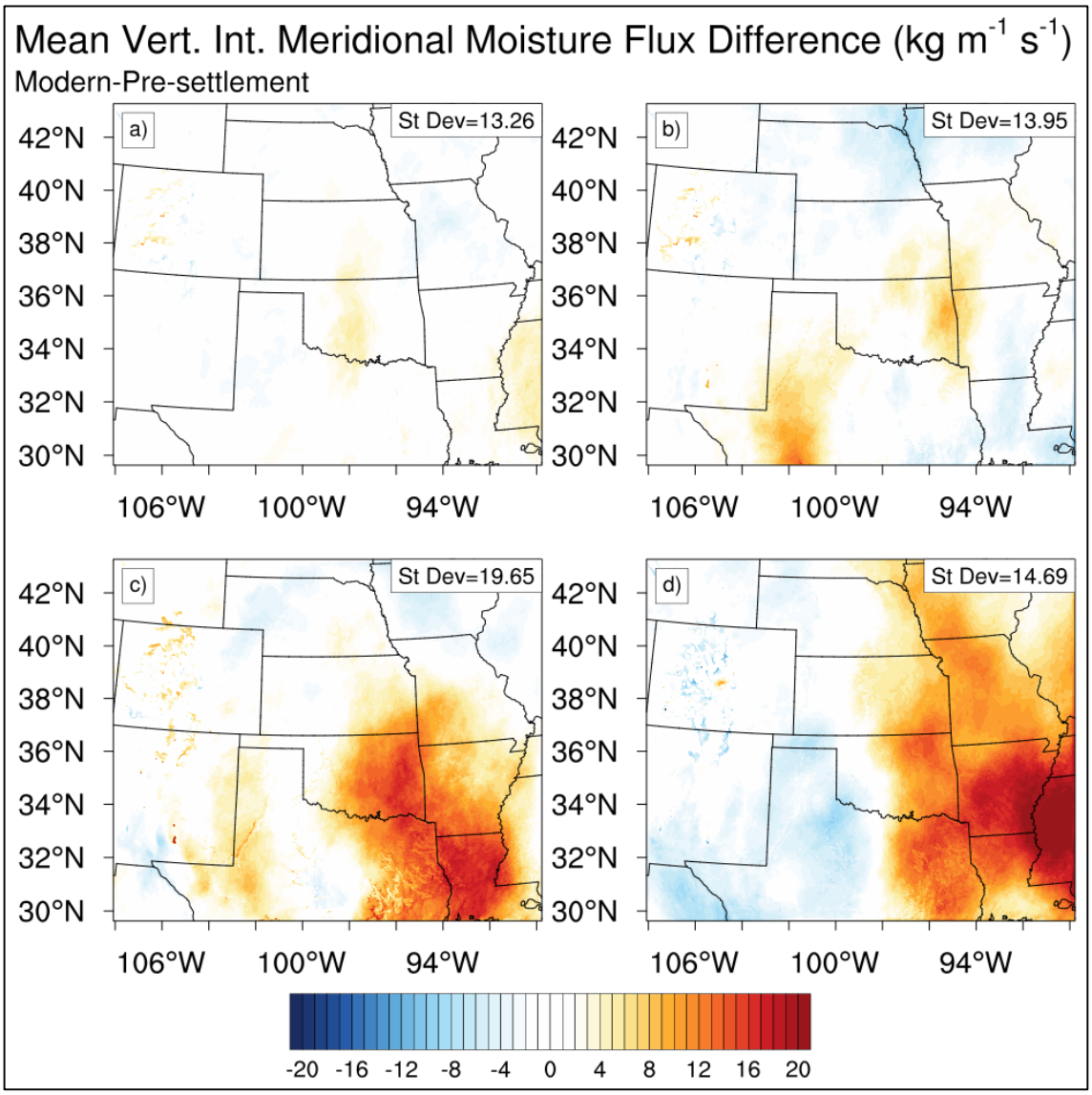

Figure 3.15. Mean May (a), June (b), July (c) and August (d) vertically integrated (1000hPa – 700hPa) meridional moisture flux differences (modern day minus pre-settlement).

iv. Precipitation

The spatial extent and magnitude of the precipitation differences increases through the summer months. In May and June, small regions of positive precipitation

differences were evident over the eastern half of the domain (Figure 3.16a-b). In June, a significant positive precipitation difference was also evident in Mississippi and Louisiana (Figure 3.16b). In July, there is a large area of greater precipitation over western New Mexico (Figure 3.16c). More precipitation with respect to the modern day LULC scenario was found in much of the domain in August. The greatest difference in precipitation was over southern Oklahoma and northern Texas, where significantly more precipitation occurred in the modern day. A broad area of smaller increases is also modern in Nebraska, Kansas, Iowa and Missouri (Figure 3.16d). The areas of greatest differences in June-August were also statistically significant.

The largest area of precipitation differences generally coincides with the differences in the moisture flux. Most of the greater precipitation differences were evident over the eastern portion of the domain, aligning with greater moisture flux differences. This suggests that the altered regional circulation and associated differences in moisture flux resulted in greater precipitation. While the greater moisture flux differences over New Mexico are weaker than over the eastern portion of the domain in July, the relationship between a greater moisture flux and greater precipitation is still evident (Figures 3.15, 3.16). It is important to note that the only differences between the each of the scenarios is the LULC. Therefore, the changes in precipitation are an implication of these changes.

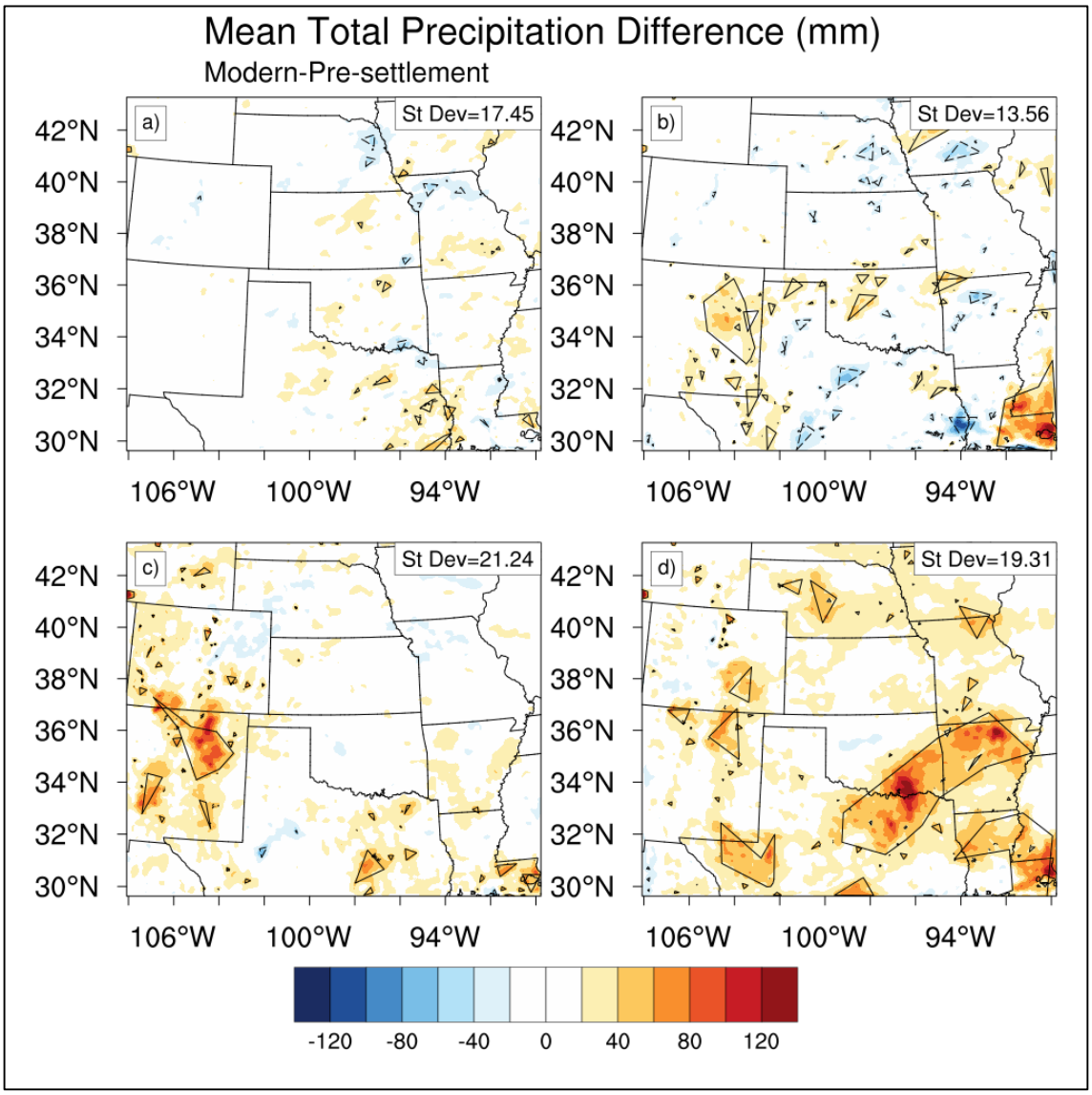

Figure 3.16. Total May (a), June (b), July (c) and August (d) total precipitation differences (modern day minus pre-settlement).

$\pm 2\sigma$ contoured in black; solid line for $+2\sigma$ and dashed for -2σ.

b. Modern Day versus 1920s

i. Surface Energy Budget

Overall, surface albedo was lower in the modern day compared to the 1920s. Only one region of significantly higher surface albedo exists; in May and June the Rocky Mountains had a significant increase in surface albedo. This region was unchanged from the pre-settlement to the 1920s scenario, so the LULC change that caused this change in albedo is the same as in the previous section. This region underwent a change from evergreen needleleaf forests to a mix of evergreen needleleaf forests, grassland and sparse vegetation due to deforestation. The presence of snow cover is likely the cause for the higher surface albedo in the modern day. This result diminishes throughout the warm season because of snow melt (Figure 3.17).

Regions with higher (lower) surface albedo in the modern day generally also had a lower (higher) surface sensible heat flux. For example, the higher surface albedo over the Rocky Mountains was matched with a significantly lower surface sensible heat flux. The opposite is true for the lower surface albedo in far West Texas. However, the significantly lower surface sensible heat flux evident over Kansas and Oklahoma in June and over Texas in August do not fit that relationship, as the surface albedo in this region was lower in the modern day. The region over Kansas and Oklahoma underwent a LULC change from cropland in the 1920s back to grassland in the modern day. While the lower albedos were evident in each month, the significantly lower surface sensible heat flux was only evident in June, and a difference is nonexistent in the other months. Texas underwent a LULC change from cropland in the 1920s to a mix of cropland and urban and developed land in the modern day, so a significant difference in the surface sensible

heat flux was not anticipated (Figures 3.17, 3.18).

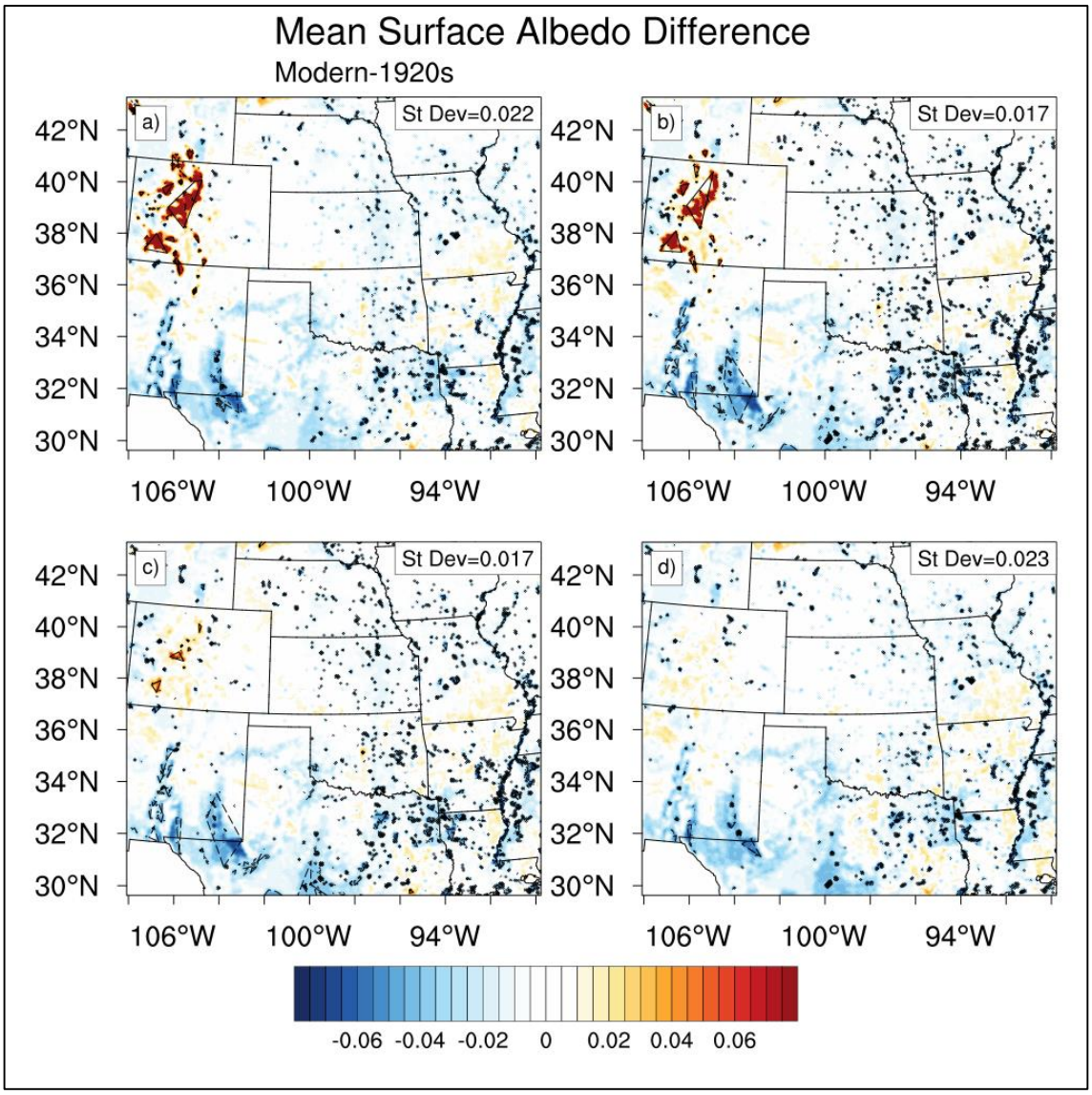

Figure 3.17. Mean May (a), June (b) July (c) and August (d) surface albedo differences (modern day minus 1920s). $\pm 2\sigma$ contoured in black; solid line for $+2\sigma$ and dashed for -2σ.

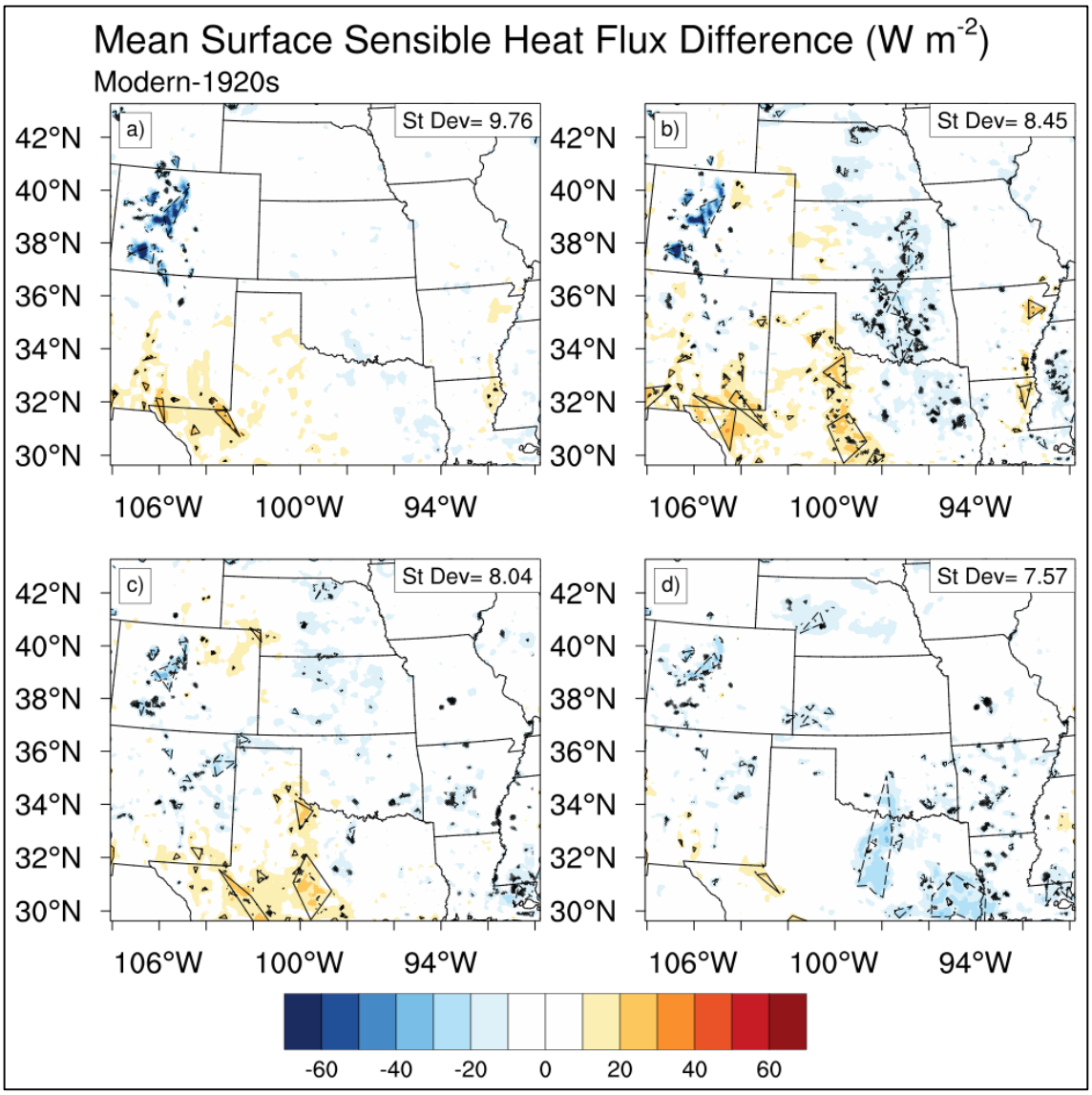

Figure 3.18. Mean May (a), June (b) July (c) and August (d) surface sensible heat flux differences (modern day minus 1920s). $\pm 2\sigma$ contoured in black; solid line for $+2\sigma$ and dashed for -2σ.

Overall, the spatial extent of significantly higher surface latent heat fluxes with respect to the modern day was greatest in August, as well as the greater soil moisture content within the top layer. While August had the greatest significantly higher surface latent heat fluxes (both spatially and in magnitude), they were present in each warm

season month (Figure 3.19, 3.20).

In each month except August, eastern Arkansas and northeastern Louisiana had a significantly lower surface latent heat flux. Both regions underwent a LULC change from wooded wetlands to cropland, so the lower surface latent heat reflects the decrease in moisture held by the wooded wetlands compared to the cropland (Figure 3.20).

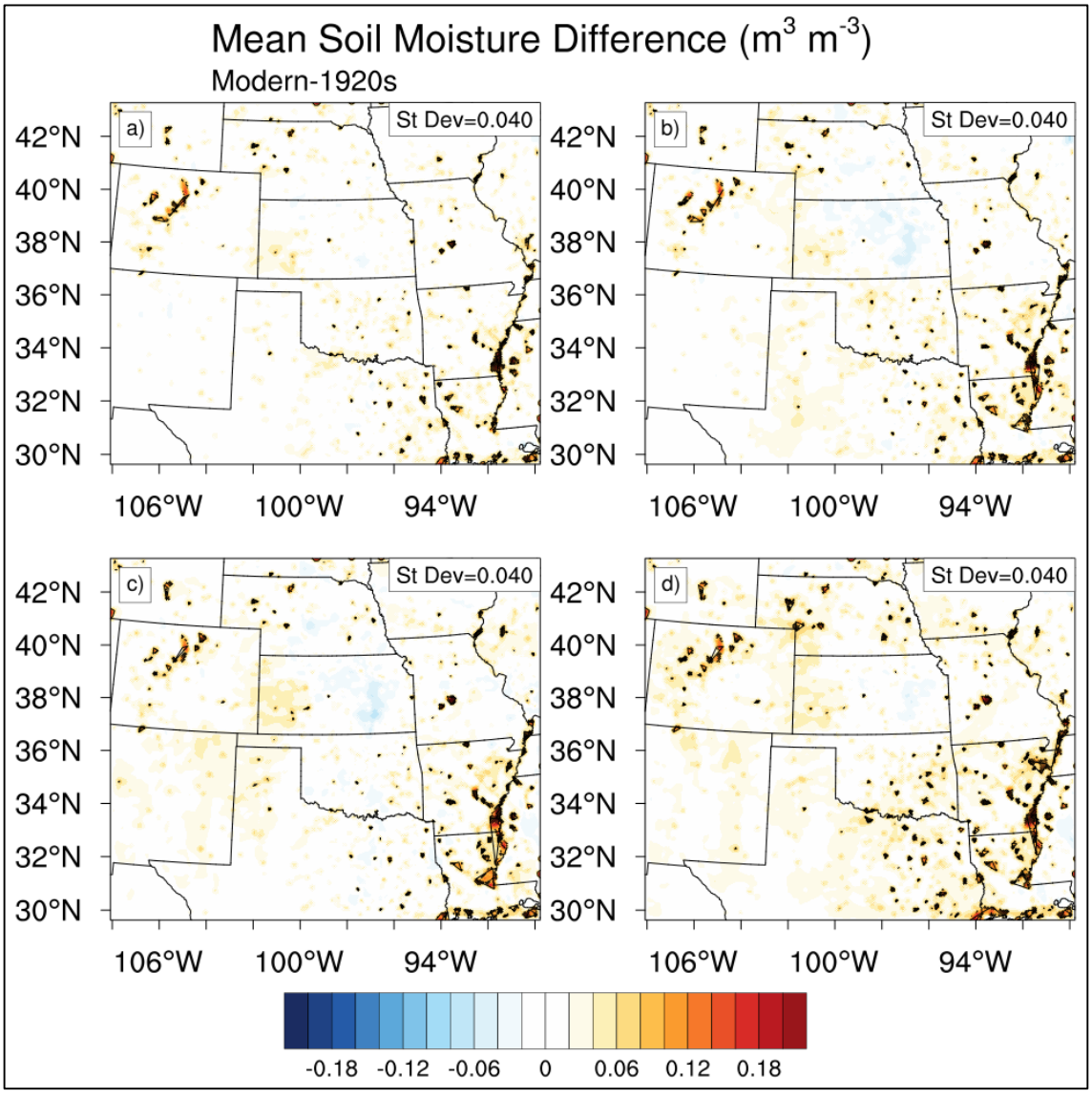

Figure 3.19. Mean May (a), June (b) July (c) and August (d) top level soil moisture differences, centered at 7 cm (modern day minus 1920s). $\pm 2\sigma$ contoured in black; solid line for $+2\sigma$ and dashed for -2σ.

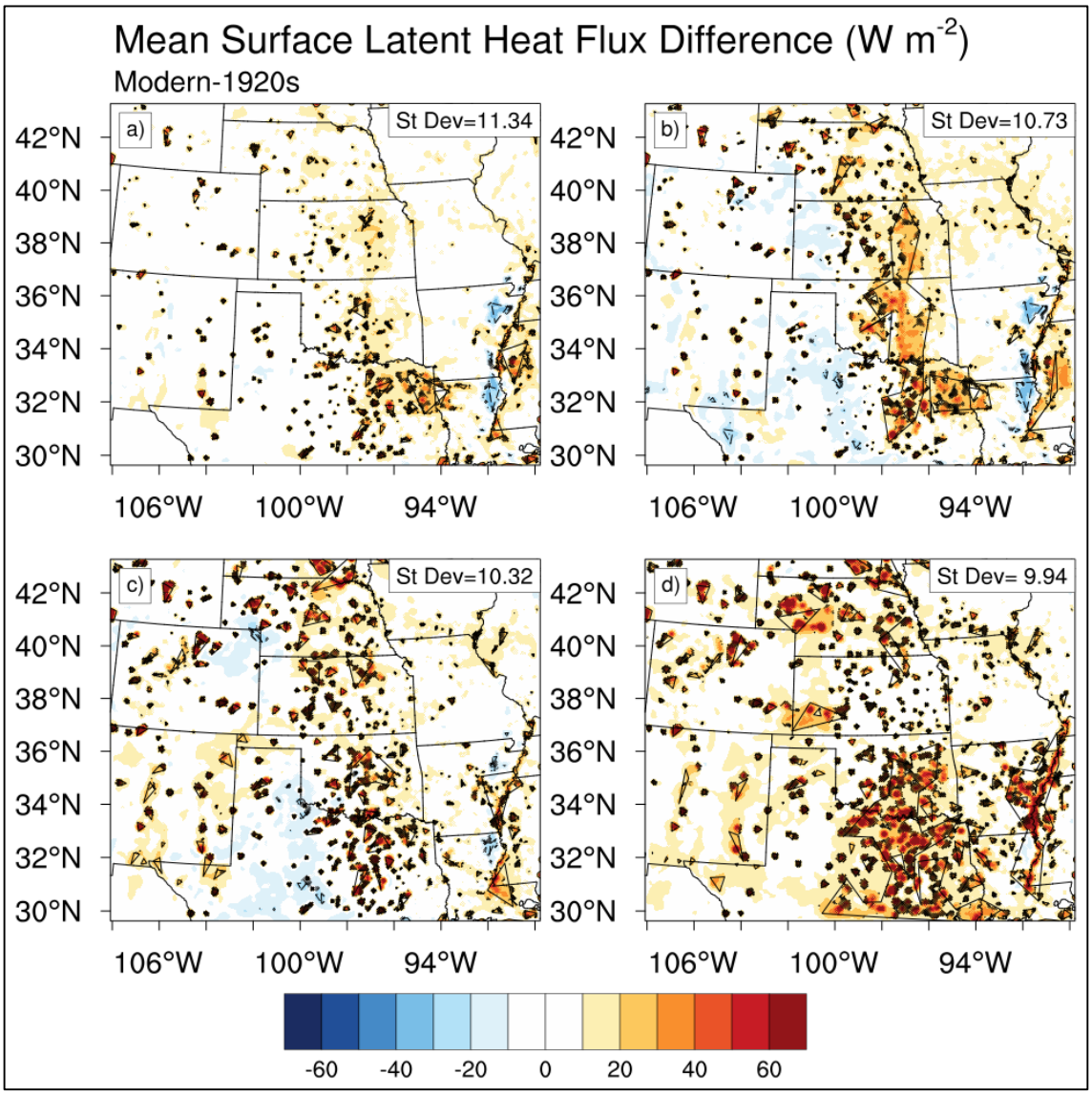

Figure 3.20. As in Figure 3.18 but for surface latent heat flux differences.

ii. Temperature and Dewpoint

An area of substantially lower dewpoint in portions of New Mexico and west Texas was evident in each warm-season month. The lower dewpoints were greatest in May and decrease through the season, but were still evident in August (Figure 3.21). As noted in the previous section, this result was not intuitive since this region did not

undergo a change from its natural vegetation of barren or sparsely vegetated land, and there was not a notable difference in temperature to support the increase of moisture content with the native vegetation compared to the modern day shrubland. This means that the change was not a direct result of the partitioning of latent and sensible heat.

Higher dewpoints were also found in May and June, and the spatial extent increases through the summer reaching a maximum in August. Higher dewpoints, though only a small area of which was significant, covered nearly the entire domain in August. The reason for this difference is similar to the previous section, comparing modern day and pre-settlement dewpoint differences. The 1920s vegetation of cropland was changed to mix of cropland, pasture and grassland. Again, the results suggest that during the climatologically warmest and driest month, modern day vegetation was relatively cooler than native vegetation but had higher dewpoints, and that there was more evaporation associated with the modern day vegetation that the cropland of the 1920s (Figure 3.22). In addition, the higher surface latent heat fluxes and higher dewpoints suggest that there was increased evaporation in the modern day (Figures 3.20, 3.21).

The changes in temperature in May and June were largely sporadic and small in magnitude, and confined to the southern portion of the domain (Figure 3.23a-b). July was the only month that had higher 2m temperatures in the modern day, in most of Texas and southern Oklahoma. This region's LULC was unaltered from its native vegetation of grassland and deciduous forests between the pre-settlement and 1920's. In a similar manner to the modern day compared to the pre-settlement, the warming in this region is a result of the partitioning the net radiation, as less energy was necessary for latent heat in the modern day as a result to the 1920's. The warming trend disappeared in August

because the entire region experiences the warming temperatures at this time, and the LULC change did not cause the summertime maximum temperature to increase (Figure 3.23c).

In both July and August, urban areas are evident due to the urban heat island effect. In August, western Kansas, Oklahoma and the Texas panhandle, 2m air temperatures were lower in the modern day compared to the 1920s. The magnitude of the change was about 1°C. This region underwent a LULC change from grassland in the 1920's to a grassland and cropland mix in the modern day (Figure 3.23).

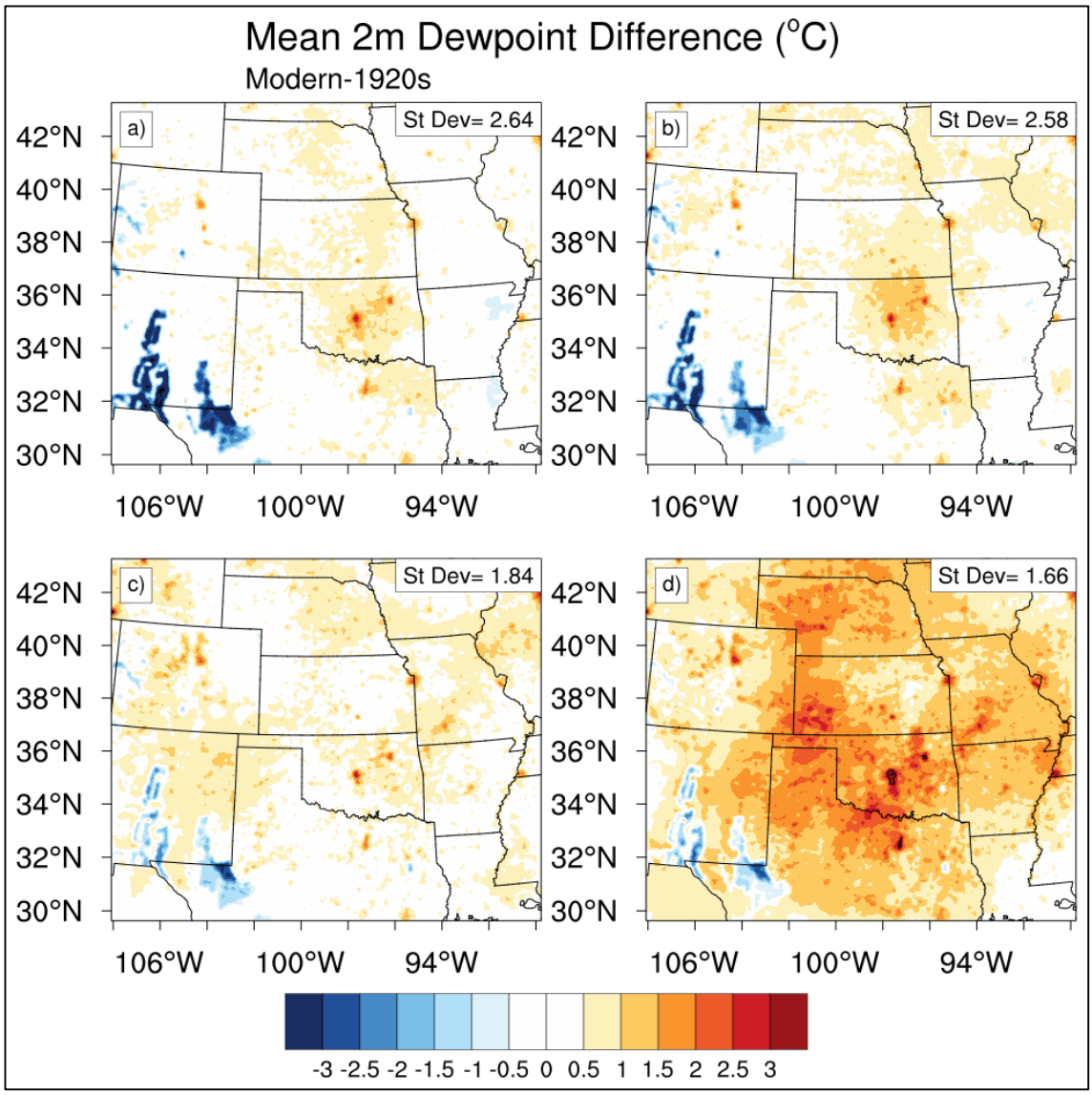

Figure 3.21. Mean May (a), June (b), July (c), and August (d) 2m dewpoint differences (modern day minus 1920's). $\pm 2\sigma$ contoured in black; solid line for $+2\sigma$ and dashed for -2σ

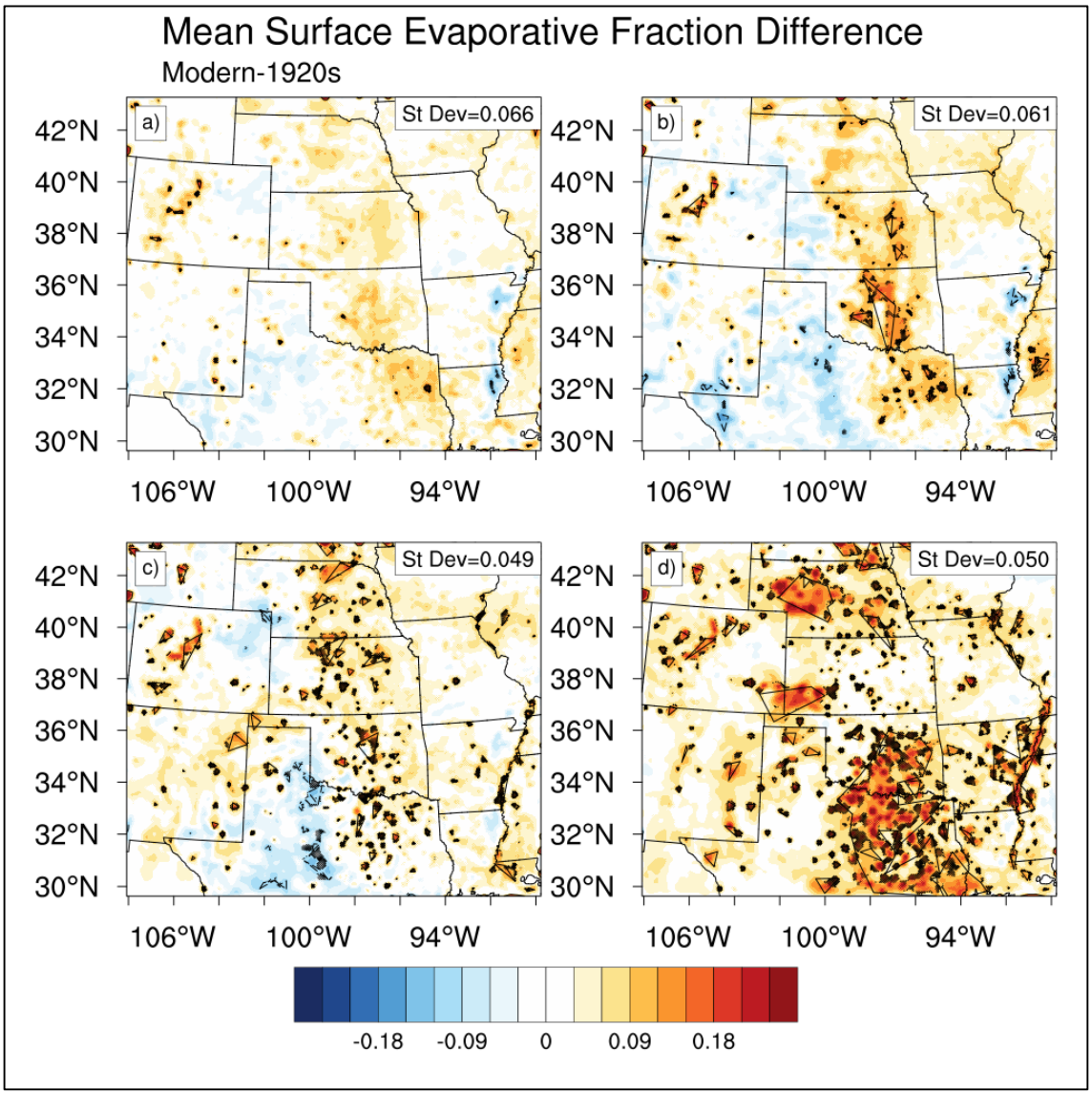

Figure 3.22. Mean May (a), June (b) July (c) and August (d) surface evaporative fraction differences (modern day minus 1920s). $\pm 2\sigma$ contoured in black; solid line for $+2\sigma$ and dashed for -2σ.

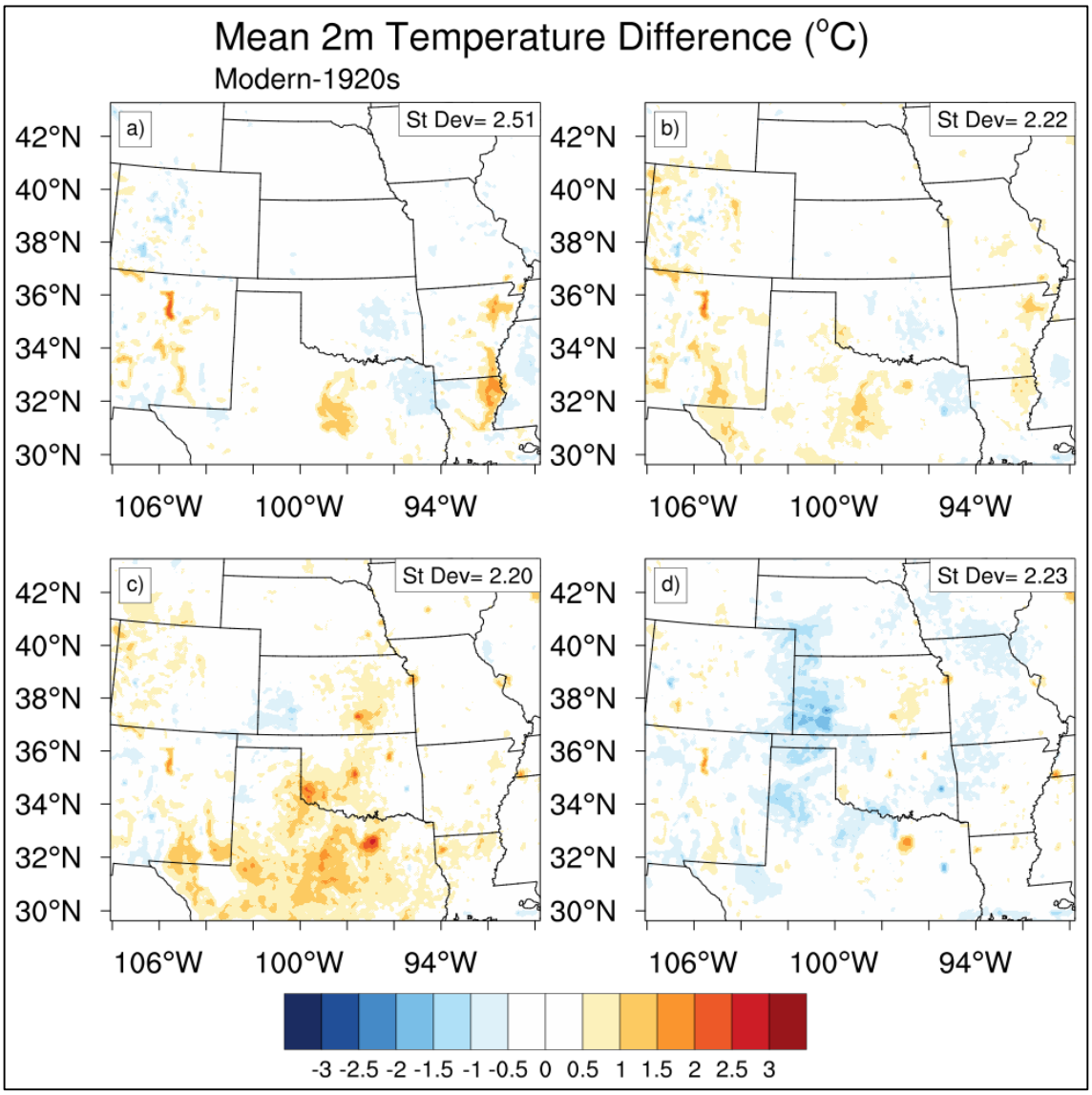

Figure 3.23. As in Figure 3.21 but for 2m air temperature differences.

iii. Regional Circulation

May and July exhibited no substantial change in the mean sea level pressure (Figure 3.24a, c). In June and August, an area of higher pressure covered eastern Kansas, Oklahoma and Texas and extended eastward into southern Missouri and Illinois and Arkansas, Louisiana and Mississippi (Figure 3.24b, 3.24d). Finally, in each month there was a small and weak area of lower pressure in New Mexico and west Texas. None of

the differences in mean sea level pressure were significant. However, this still suggests a change in the regional circulation.

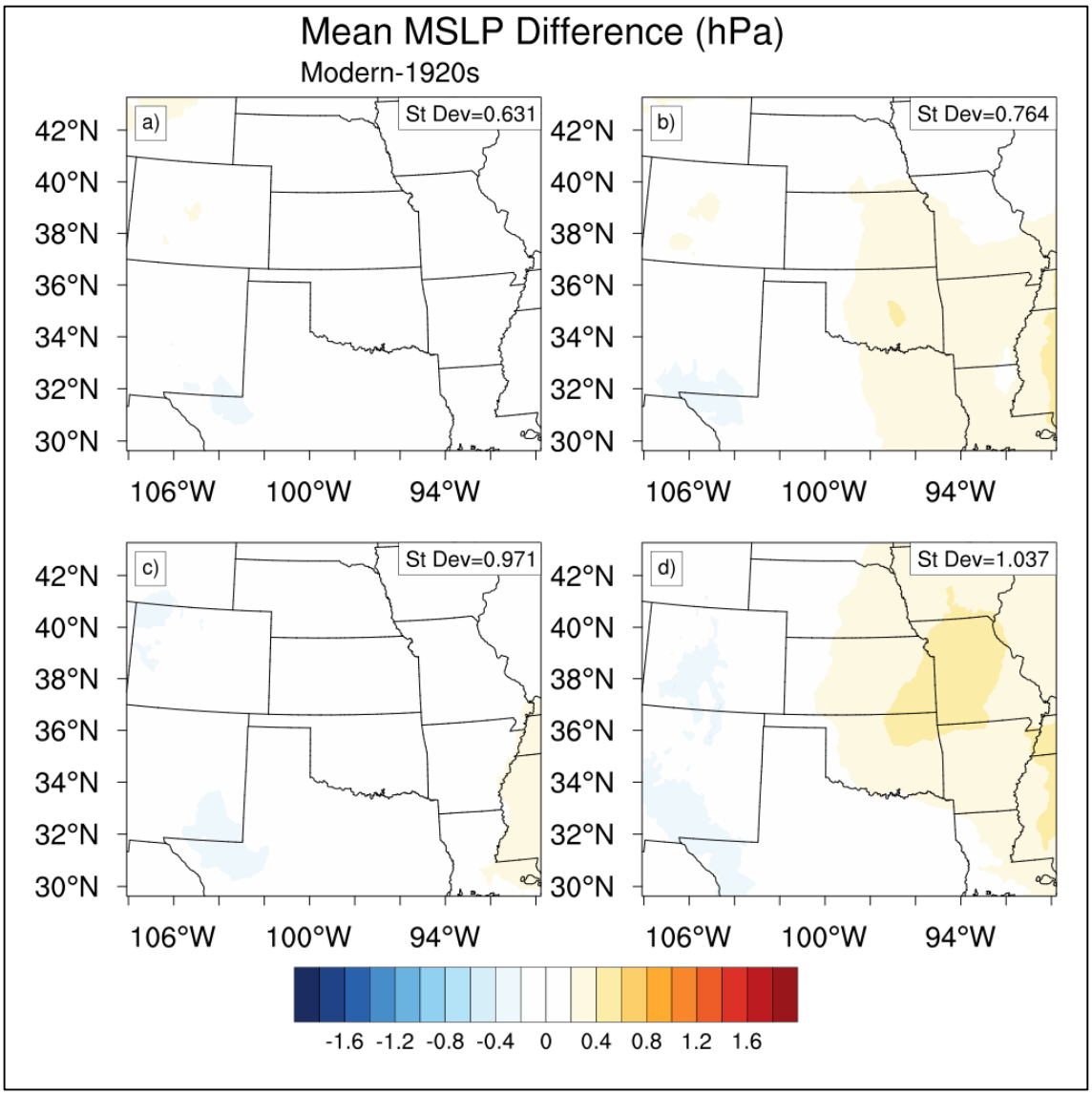

Figure 3.24. Mean May (a), June (b), July (c) and August (d) mean sea level pressure differences (modern day minus 1920's).

Stronger negative U-winds occurred in Texas and Oklahoma throughout the warm-season months (Figure 3.25), suggesting the LULC change resulted in stronger negative U-winds in this region for the modern day scenario (Figure 3.12). Over the

Rocky Mountains, stronger positive U-winds were present, although this result dissipated throughout the summer. The average U-wind in the modern day scenario was positive, indicating that the LULC change resulted in stronger positive U-winds (Figure 3.12). The stronger negative U-winds coincide with the higher surface pressure mentioned above.

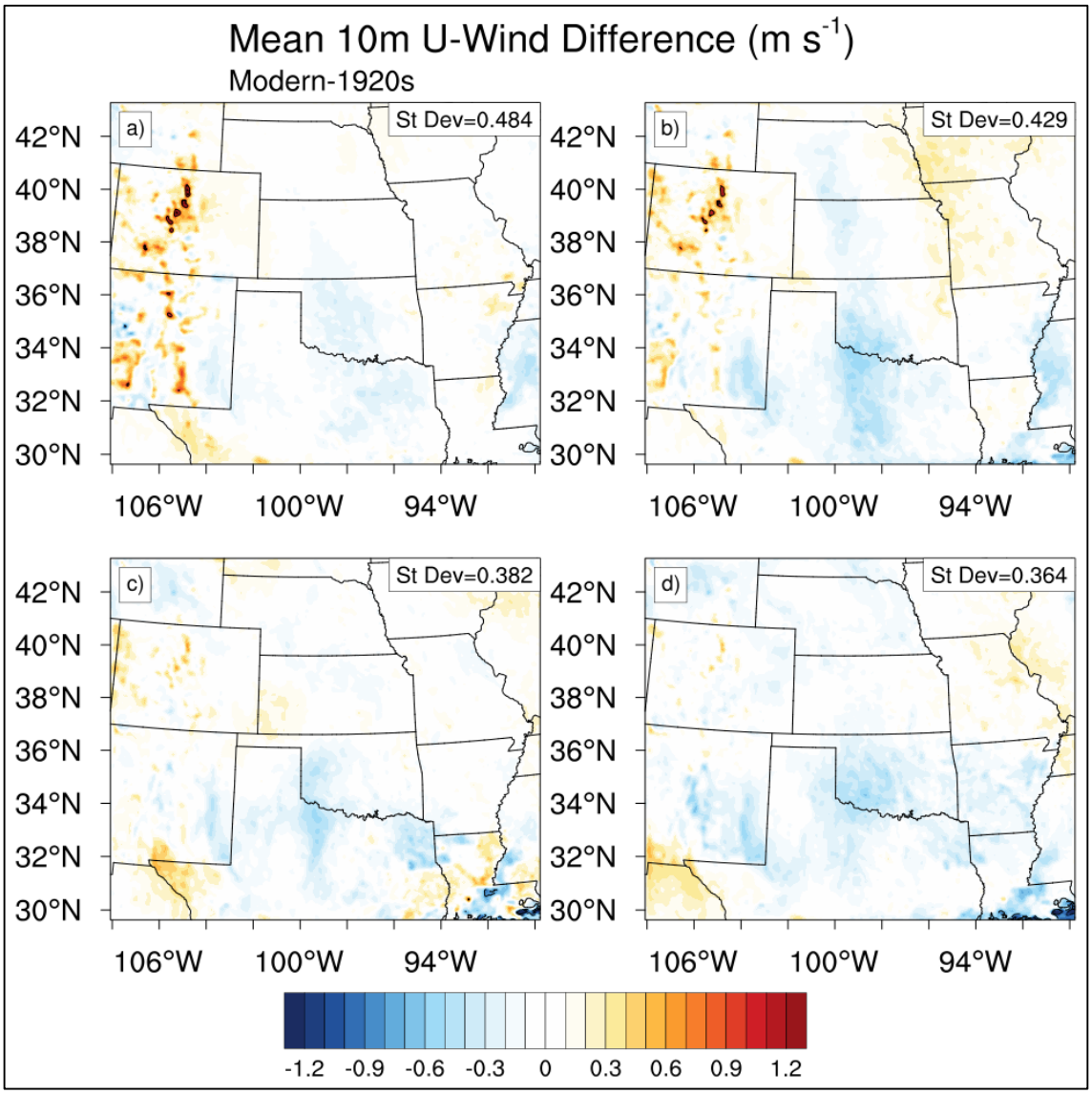

Figure 3.25. Mean May (a), June (b), July (c) and August (d) 10m U-wind differences (modern day minus 1920's). $\pm 2\sigma$ contoured in black; solid line for $+2\sigma$ and dashed for -2σ.

Stronger positive V-winds were evident through the warm season in central Texas with modern land use, with a range in magnitude of 0.5 to 1 m s^{-1}. In May and June, there was a couplet of wind differences over central Texas; stronger negative V-winds were located to the east of the region of stronger positive V-winds winds evident in central Texas (Figure 3.26a-b). This region dissipated through the summer, and was minimal in August. Other areas of stronger positive V-winds winds occurred with modern land use; in June the aforementioned area in central Texas extends into central Kansas and in August it extends through eastern Nebraska, although the magnitude lessens through the summer (Figure 3.26). Since the mean V-winds in the modern day scenario were predominately positive, the LULC changes resulted in stronger positive V-winds (Figure 3.14). Again, the area of stronger positive V-winds is an important factor when considering moisture transport and this region generally coincides with areas of increased moisture flux in the modern day, suggesting an increase in moisture transport from the Gulf of Mexico.

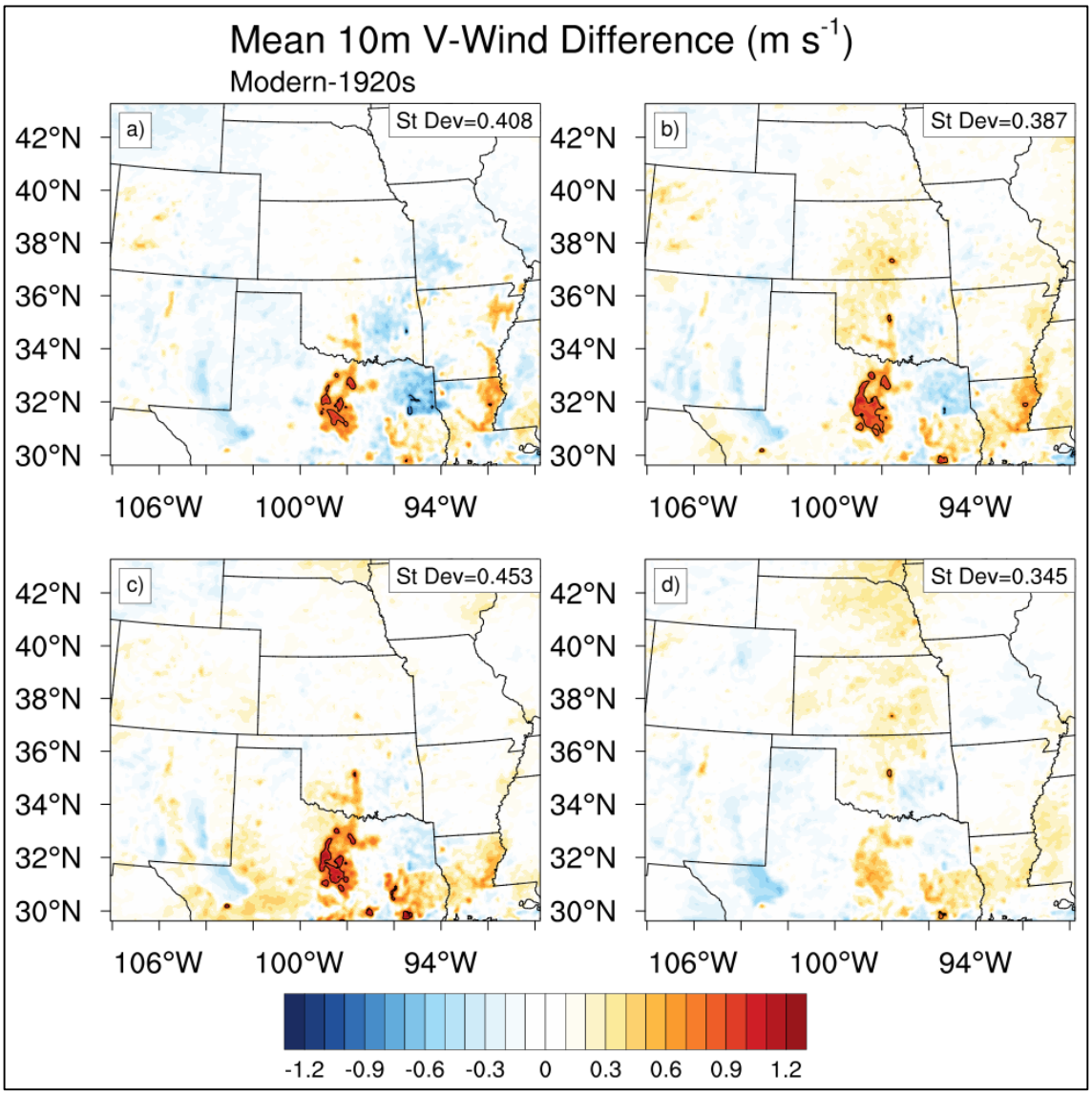

Figure 3.26. As in Figure 3.25 but for 10m V-wind differences.

The differences in the surface winds are also related to the changes in surface pressure. The stronger positive V-winds winds that extend from central Texas through Nebraska and the stronger positive U-wind coincide with the higher surface pressure in the modern day scenario.

iv. Precipitation

The overall precipitation increased in the modern day compared to the 1920's. Similar to the previous section, in May and June there were small regions of greater precipitation, and also a large region over Louisiana and Texas in June. In July, there is an area of significantly lower precipitation in southeastern Texas, as well as an area of greater precipitation in northern New Mexico. Finally, in August there are two areas of significantly lower precipitation: one in eastern Kansas/western Missouri and the other in Mississippi and Louisiana. The greatest areas of significantly higher precipitation in May, June, July and August are in eastern Texas, Louisiana, New Mexico, and Texas, Oklahoma and Arkansas, respectively (Figure 3.27).

The regions of greater precipitation in the modern day scenario are very well aligned with the regions of greater moisture flux, suggesting that the cause of the precipitation difference were a result of the altered regional circulation allowing for a greater transport of moisture from the Gulf of Mexico (Figures 3.27, 3.28).

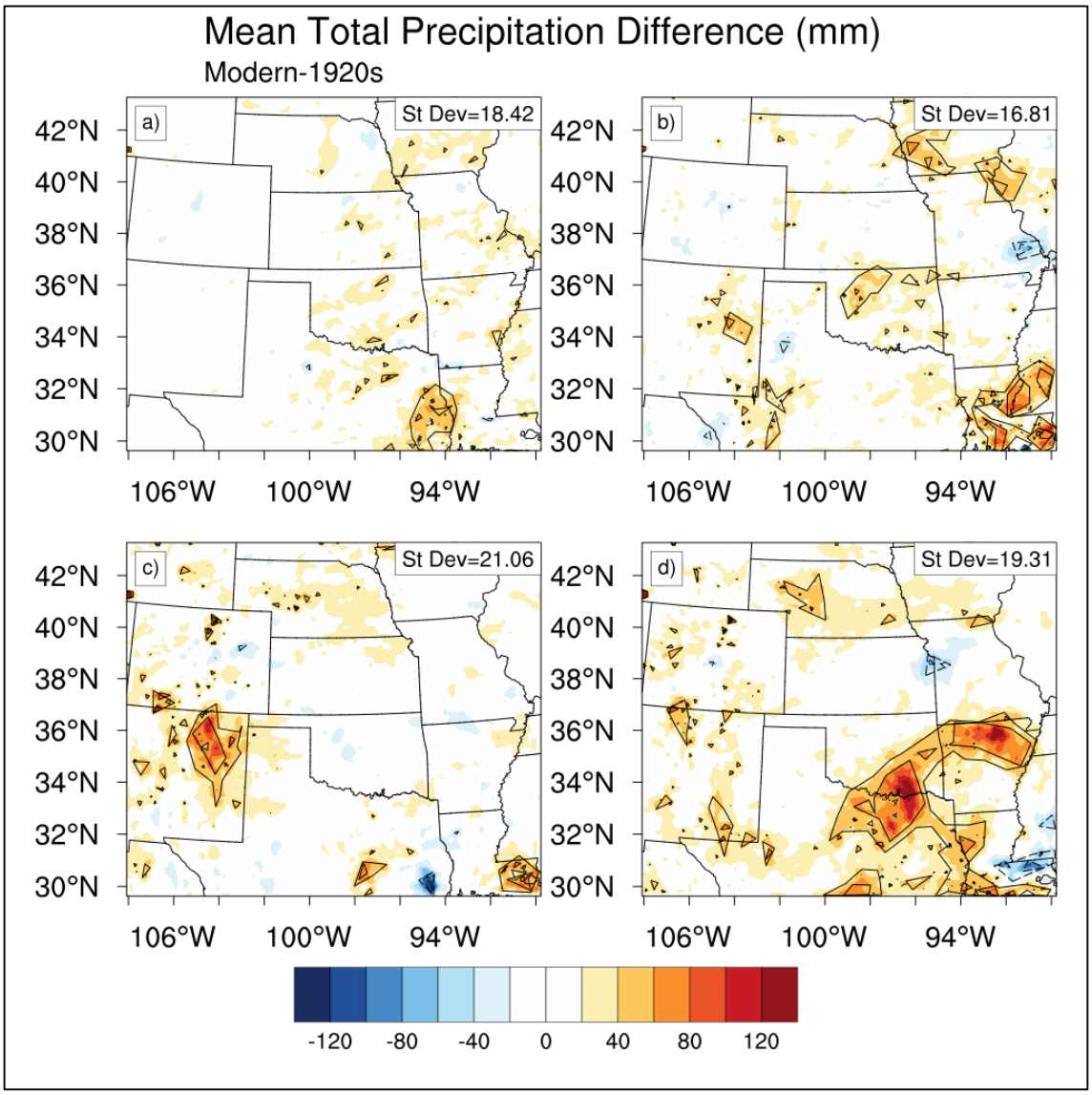

Figure 3.27. Mean May (a), June (b) July (c) and August (d) total precipitation differences (modern day minus 1920s). $\pm 2\sigma$ contoured in black; solid line for $+2\sigma$ and dashed for -2σ.

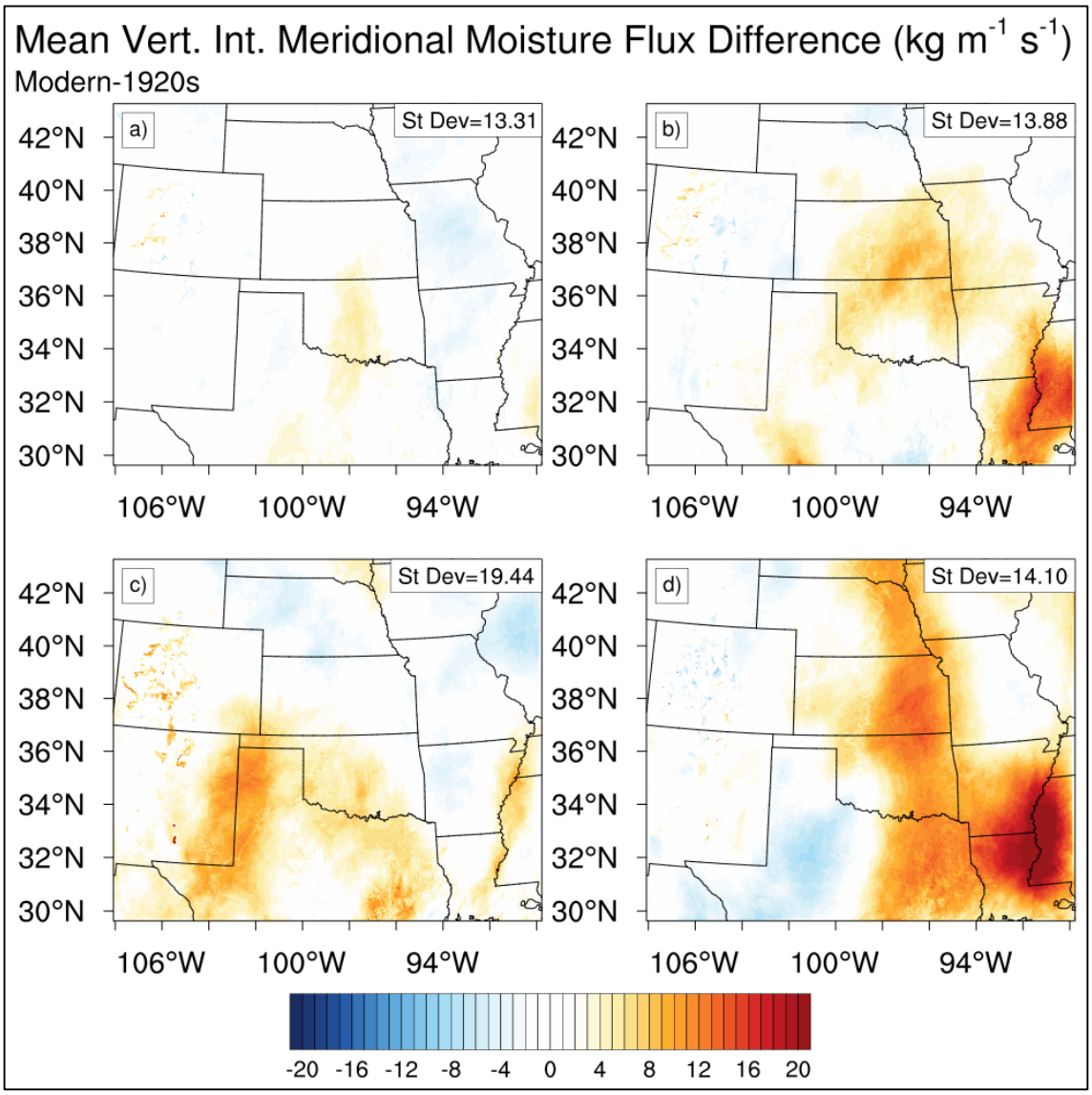

Figure 3.28. Mean May (a), June (b), July (c) and August (d) vertically integrated (1000hPa – 700hPa) meridional moisture flux differences (modern day minus 1920's).

c. Modern Day versus Dust Bowl

i. Surface Energy Budget

The change from the Dust Bowl LULC of barren or sparsely vegetated land to the modern day usage of grassland and cropland did not result in a significant surface albedo difference. The mean surface albedo of the modern day was slightly lower than in the Dust Bowl. However, while the magnitude of the change was small (changes of about 0.02), they occurred on a large spatial scale, as lower albedos occurred over most of the panhandles of the Texas and Oklahoma and the surrounding area in the modern day scenario (Figure 3.29). The small changes in surface albedo also coincided with only slight changes in the sensible heat fluxes (Figure 3.30). However, the LULC change from the Dust Bowl scenario to the modern day scenario did result in differences to the surface latent heat flux and soil moisture. Higher surface latent heat fluxes and soil moisture (in the top soil layer) were found over the region modified due to wind erosion during the Dust Bowl, with the greatest differences over the panhandle of Oklahoma where wind erosion was most severe (Figures 3.31, 3.32). In addition, the evaporative fraction was also higher in the modern day, indicating more evaporation it the modern day than in the Dust Bowl (Figure 3.33). While the higher moisture content in the top soil layer in the modern day were not significant, the differences in surface latent heat flux were significant. This result is probably not realistic, as the soil was extremely dry during the Dust Bowl. Thus, significantly high soil moisture contents were anticipated. Because barren soil and sparsely vegetated land hold minimal moisture, and hold far less than the modern cropland, almost all of the incoming radiation can be utilized as sensible heat (Figure 3.30).

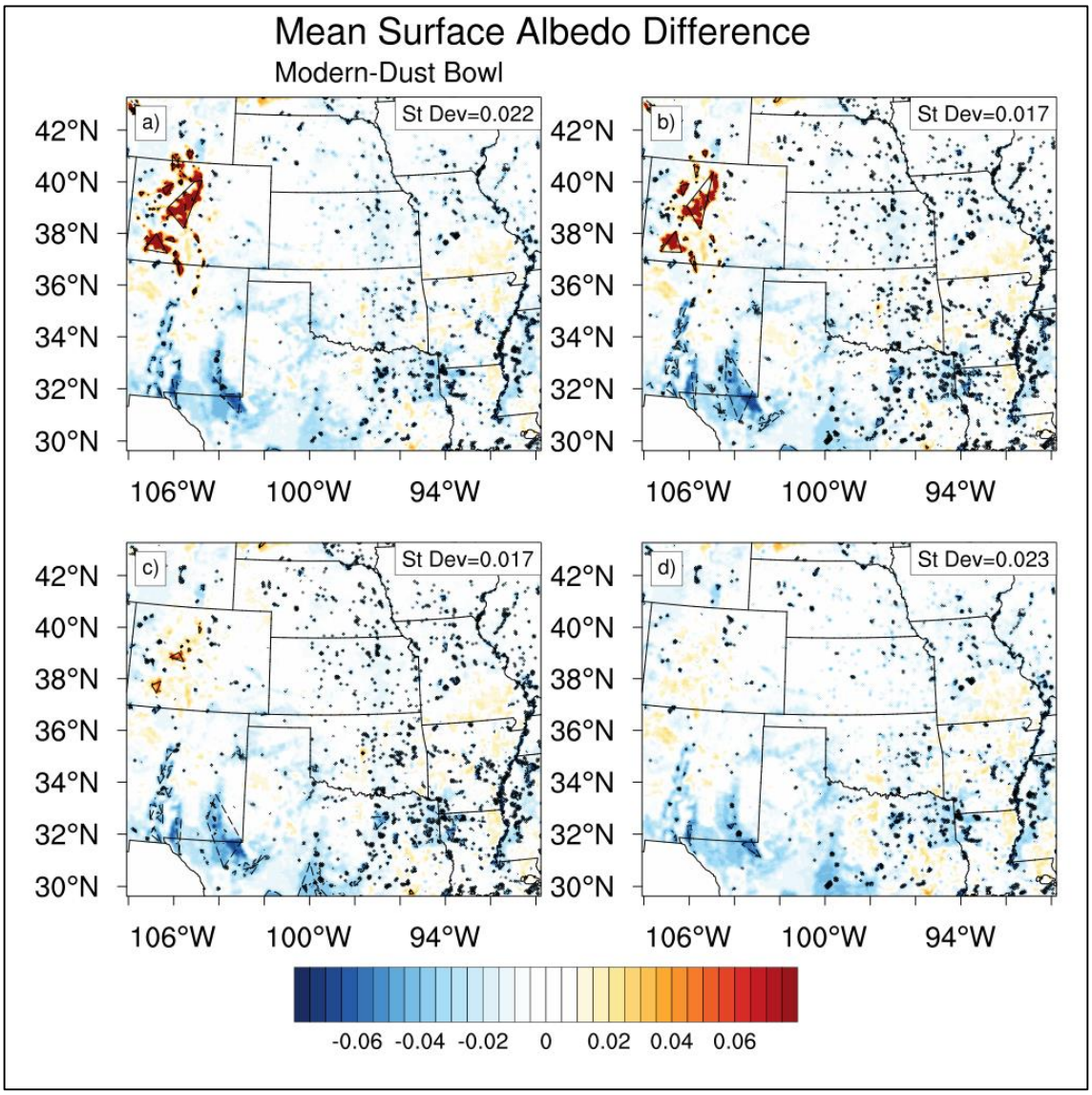

Figure 3.29. Mean May (a), June (b) July (c) and August (d) surface albedo differences (modern day minus Dust Bowl). $\pm 2\sigma$ contoured in black; solid line for $+2\sigma$ and dashed for -2σ.

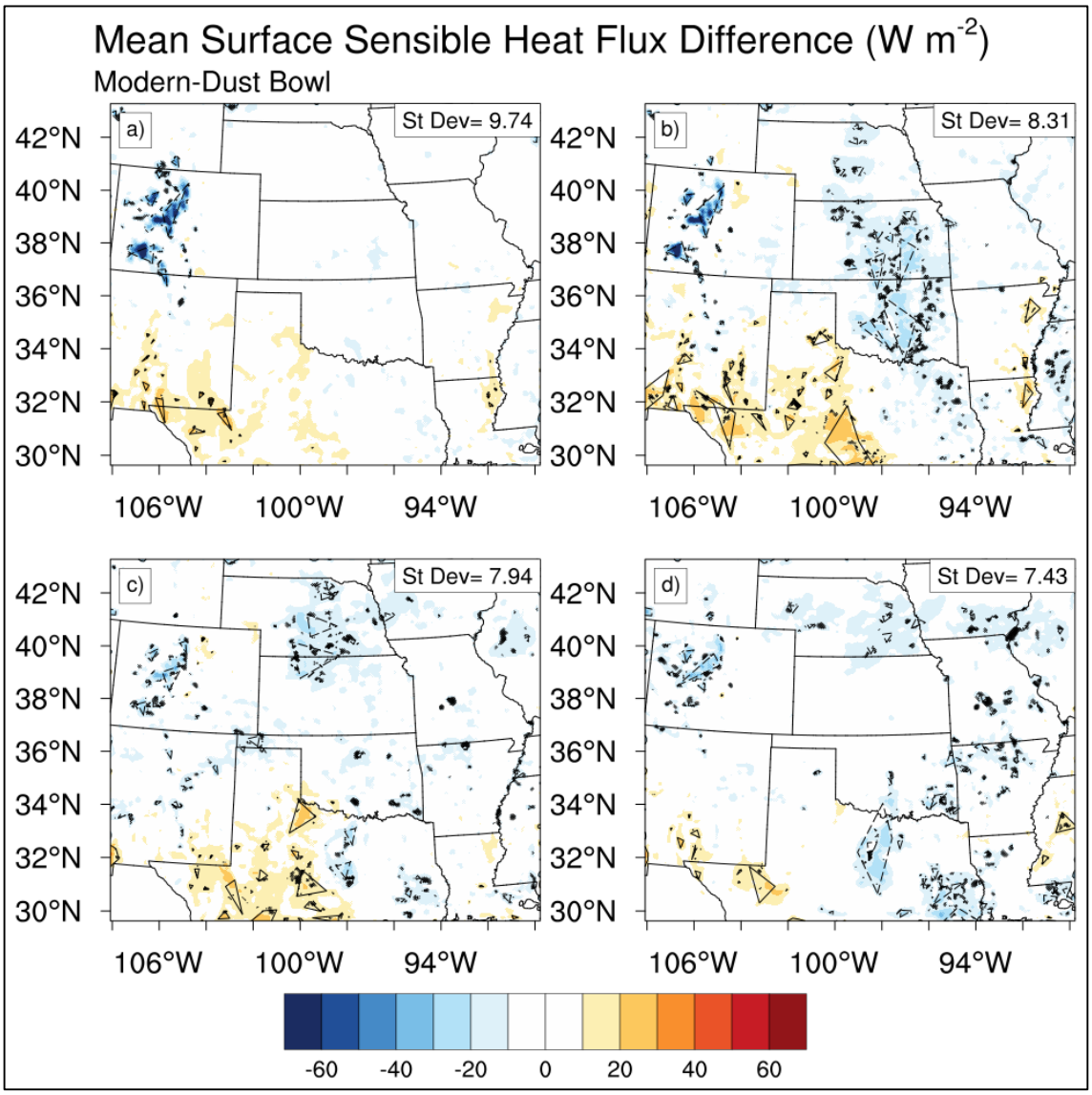

Figure 3.30. Mean May (a), June (b) July (c) and August (d) surface sensible heat flux differences (modern day minus Dust Bowl). $\pm 2\sigma$ contoured in black; solid line for $+2\sigma$ and dashed for -2σ.

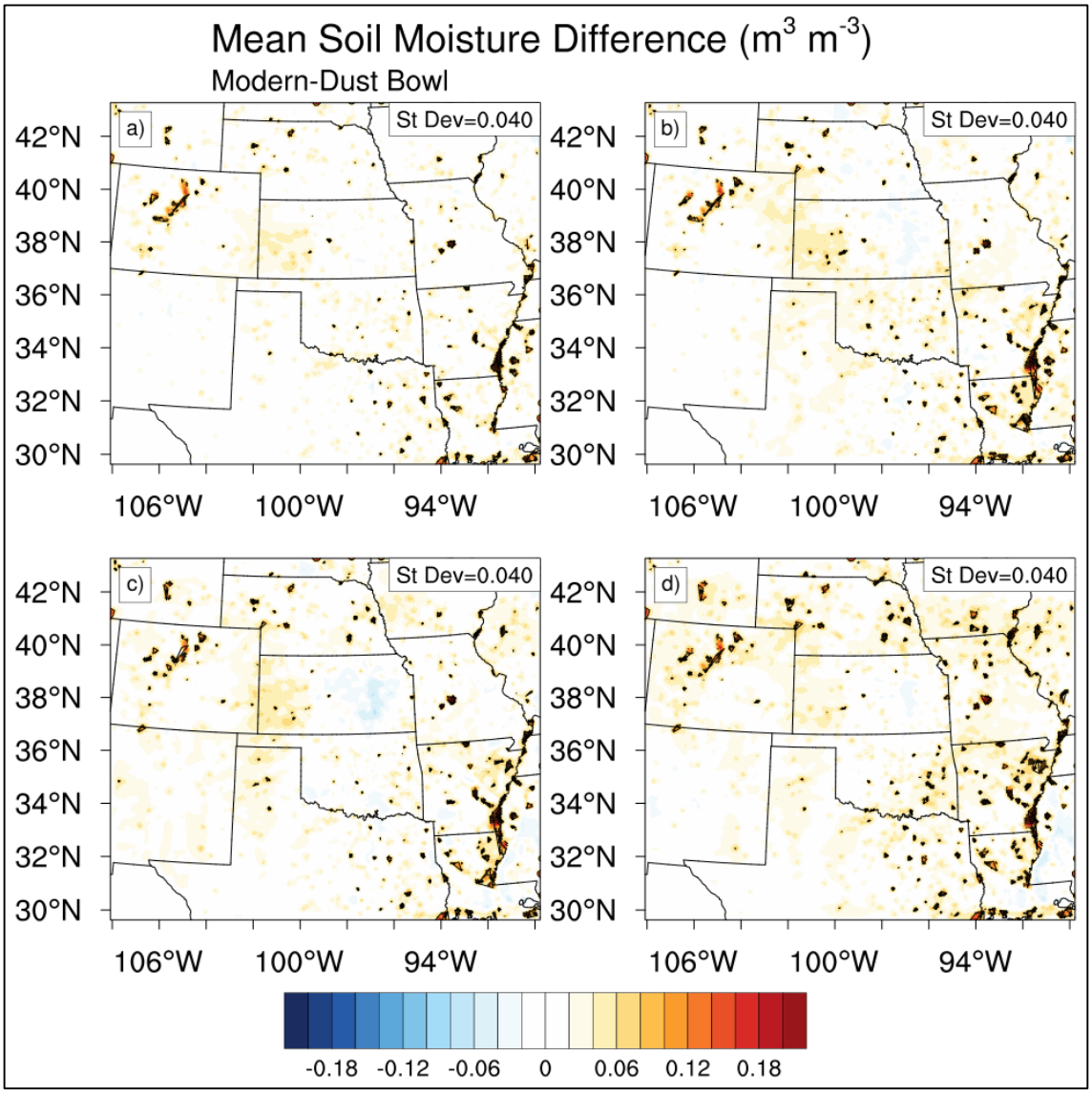

Figure 3.31. Mean May (a), June (b) July (c) and August (d) top soil layer moisture differences, centered at 7 cm (modern day minus Dust Bowl).
$\pm 2\sigma$ contoured in black; solid line for $+2\sigma$ and dashed for -2σ.

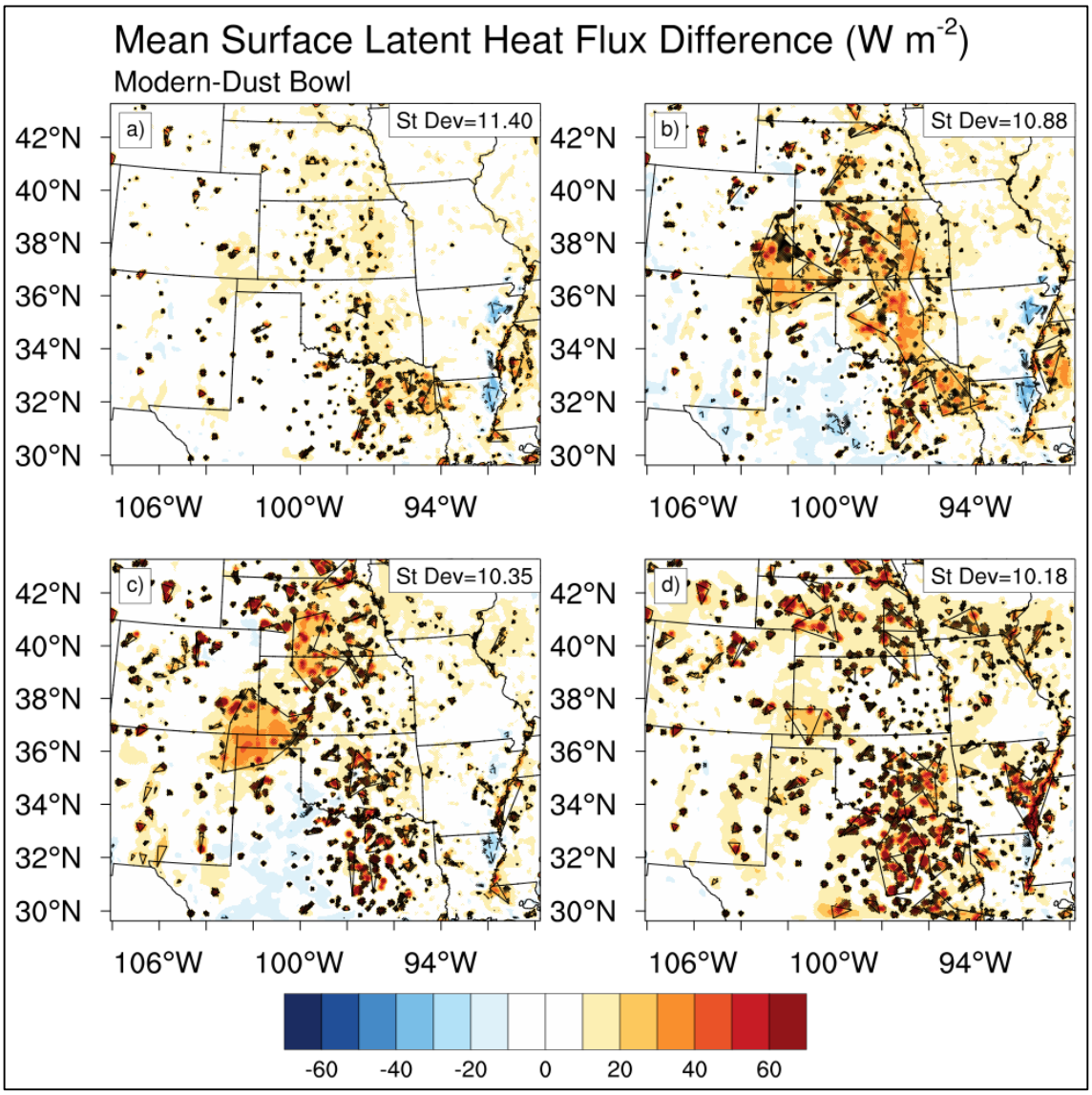

Figure 3.32. As in Figure 3.30 but for surface latent heat flux differences.

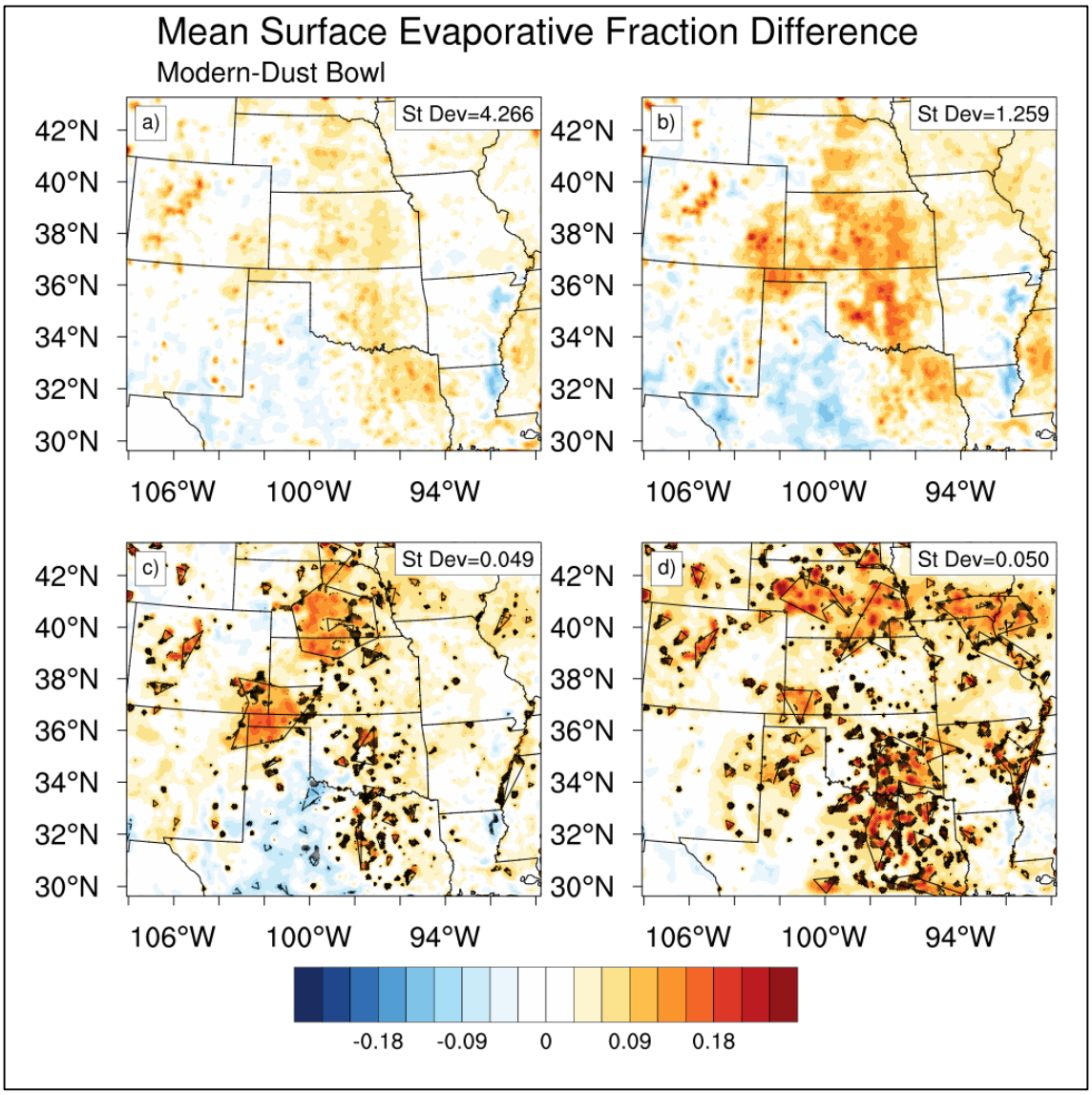

Figure 3.33. Mean May (a), June (b) July (c) and August (d) surface evaporative fraction differences (modern day minus Dust Bowl). $\pm 2\sigma$ contoured in black; solid line for $+2\sigma$ and dashed for -2σ.

ii. Dewpoint and Temperature

Both 2m air temperature and dewpoint were lower in the modern day than in the Dust Bowl scenario over the region impacted by wind erosion, although neither of the results was significant. The largest temperature differences occurred in August, while the

largest dewpoint differences occurred in May, both areas coinciding with the largest concentrated area of barren soil (Figures 3.34, 3.35). It was hypothesized that lower temperature in the modern day would be a result of a decrease in the sensible heat flux in the modern day. However, the sensible heat flux was not different between the two LULC scenarios.

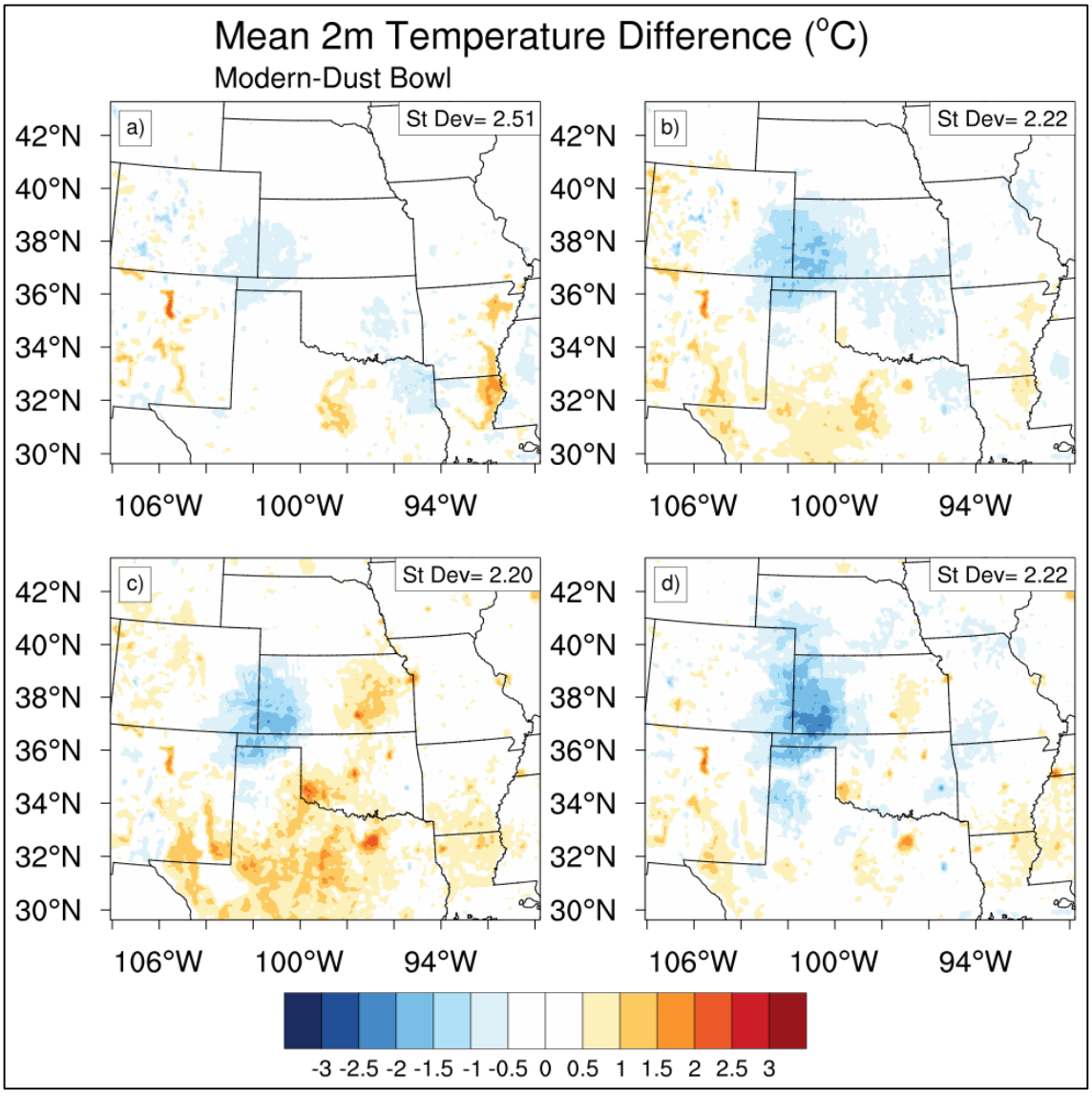

Figure 3.34. Mean May (a), June (b) July (c) and August (d) 2m air temperature differences (modern day minus Dust Bowl).

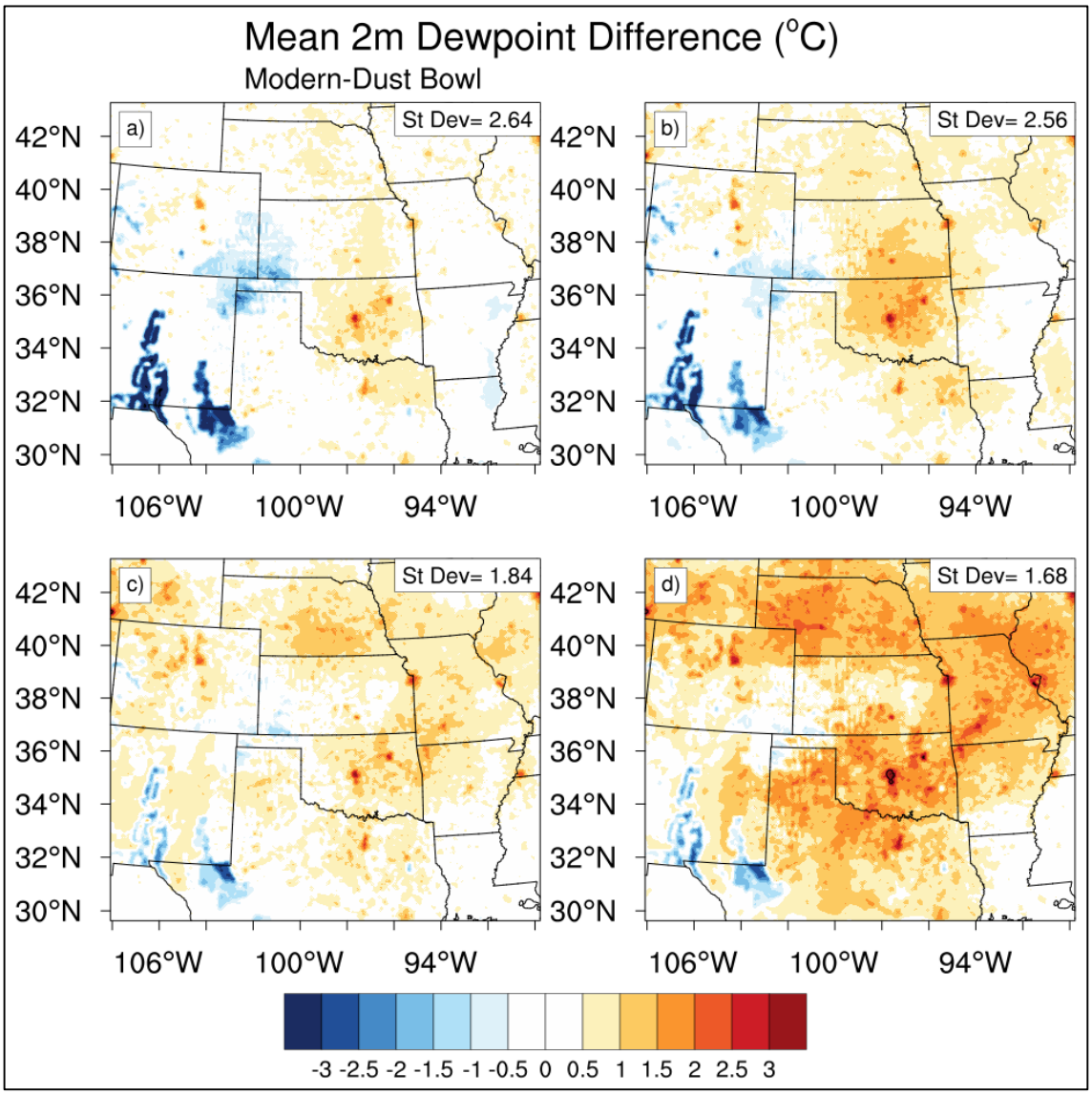

Figure 3.35. As in Figure 3.34, but for 2m dewpoint differences.

iii. Regional Circulation

Although much of the domain was unaltered for the Dust Bowl scenario and thus exhibited the same LULC as the 1920's era, there were differences in the regional circulation that resulted from changing only a small portion of the domain's LULC. However, similar to the previous analyses of the modern day versus the pre-settlement

and the modern day versus the 1920s, the difference in mean sea level pressure were small in magnitude and were not significant. Generally, slightly higher surface pressure was evident over the northeastern and eastern portion of the domain, and slightly lower surface pressure was evident over the southern portion of the domain. There are very few similarities between the altered mean surface pressure differences between the modern day versus 1920's and the modern day versus Dust Bowl (compare Figures 3.24, 3.36).

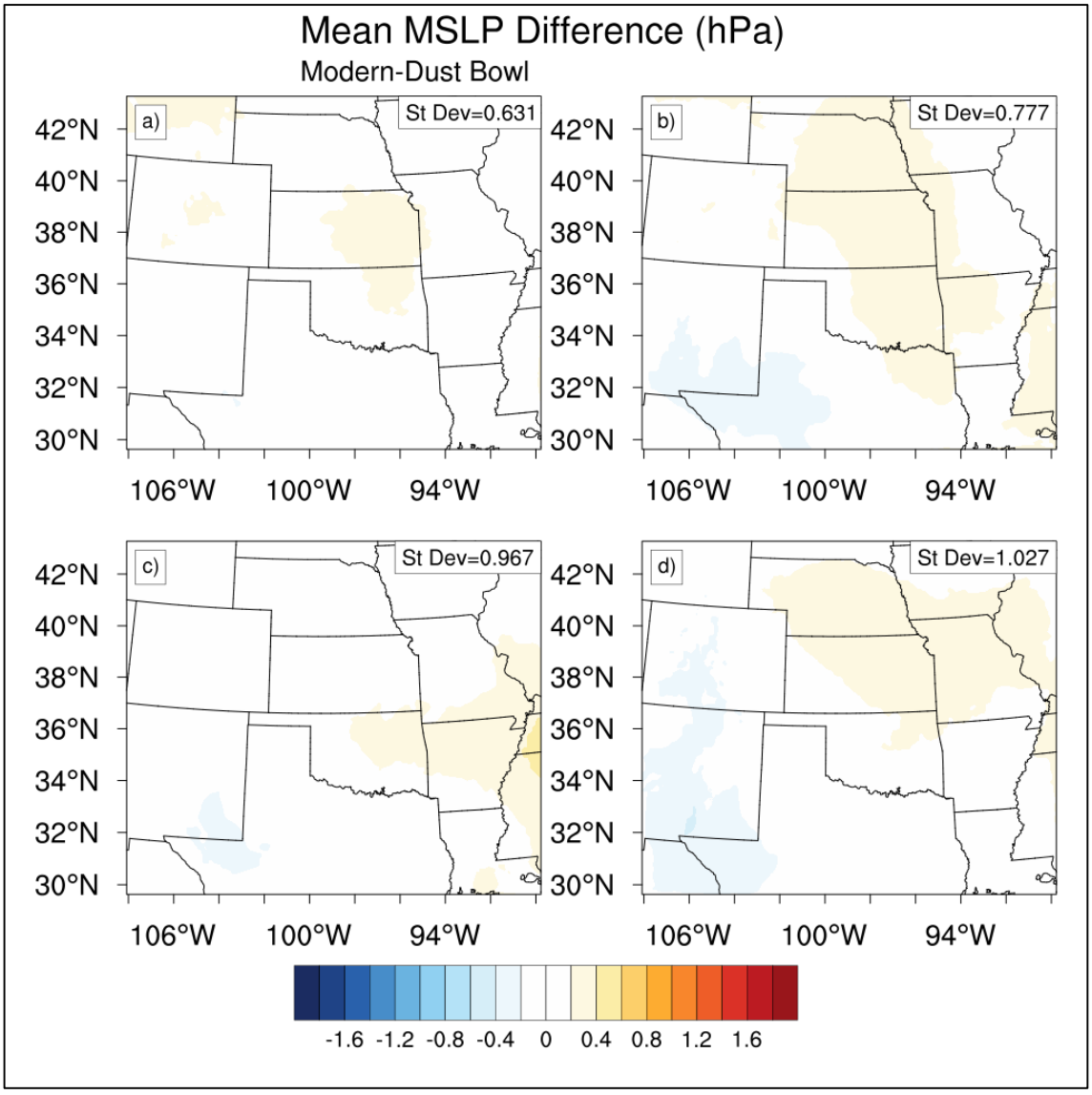

Figure 3.36. Mean May (a), June (b), July (c) and August (d) surface pressure differences (modern day minus Dust Bowl).

The change in the zonal winds during the Dust Bowl scenario were variable. In May, slightly stronger negative U-winds were present and the difference increased in June. In July, there was a couplet of stronger positive U-winds and negative U-winds over the Dust Bowl region. In August, there was an area of stronger negative U-winds in north central Texas, but this area was not impacted by the Dust Bowl (Figure 3.37). The meridional winds over the Dust Bowl region were predominately stronger negative V-winds. As seen in Figure 3.14, the mean V-winds in the modern day scenario were strongly positive, so the negative V-winds differences indicate that the strong positive V-winds were weakened during the Dust Bowl scenario. The greatest differences were present in June and in August, and these differences were significant. This result is notable, as the wind shift suggests a possible positive feedback for the region already experiencing drought conditions: stronger negative V-winds will inhibit the flow of moisture from the Gulf of Mexico and as a result the region will remain drier (Figure 3.38).

Generally, there were only small differences in the moisture flux between the modern day and Dust Bowl scenarios over the region altered by the Dust Bowl, even though the V-winds were different. In both June and July, there was slightly greater moisture flux over the panhandles of Texas and Oklahoma, and there were no differences in May and August (Figure 3.39). Although the overall regional circulation was altered by the Dust Bowl, comparing the results from the previous section (modern day minus the 1920's) and these results, there were only small differences in the moisture flux. This suggests that the impacts of the wind erosion of the Dust Bowl had a very local effect on the moisture flux, as the overall regional moisture flux was not changed.

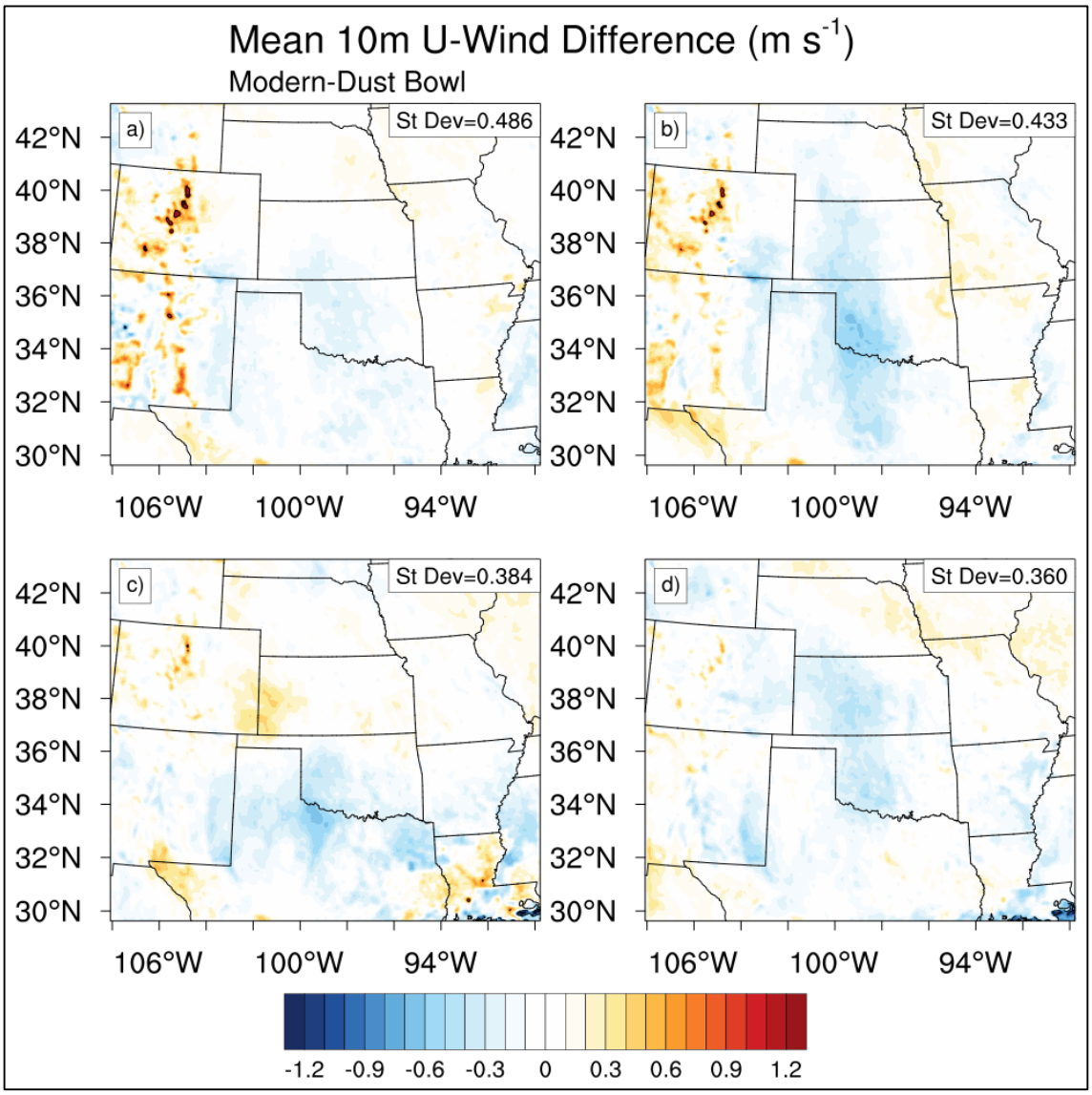

Figure 3.37. Mean May (a), June (b), July (c) and August (d) 10m U-wind differences (modern day minus Dust Bowl). $\pm 2\sigma$ contoured in black; solid line for $+2\sigma$ and dashed for -2σ.

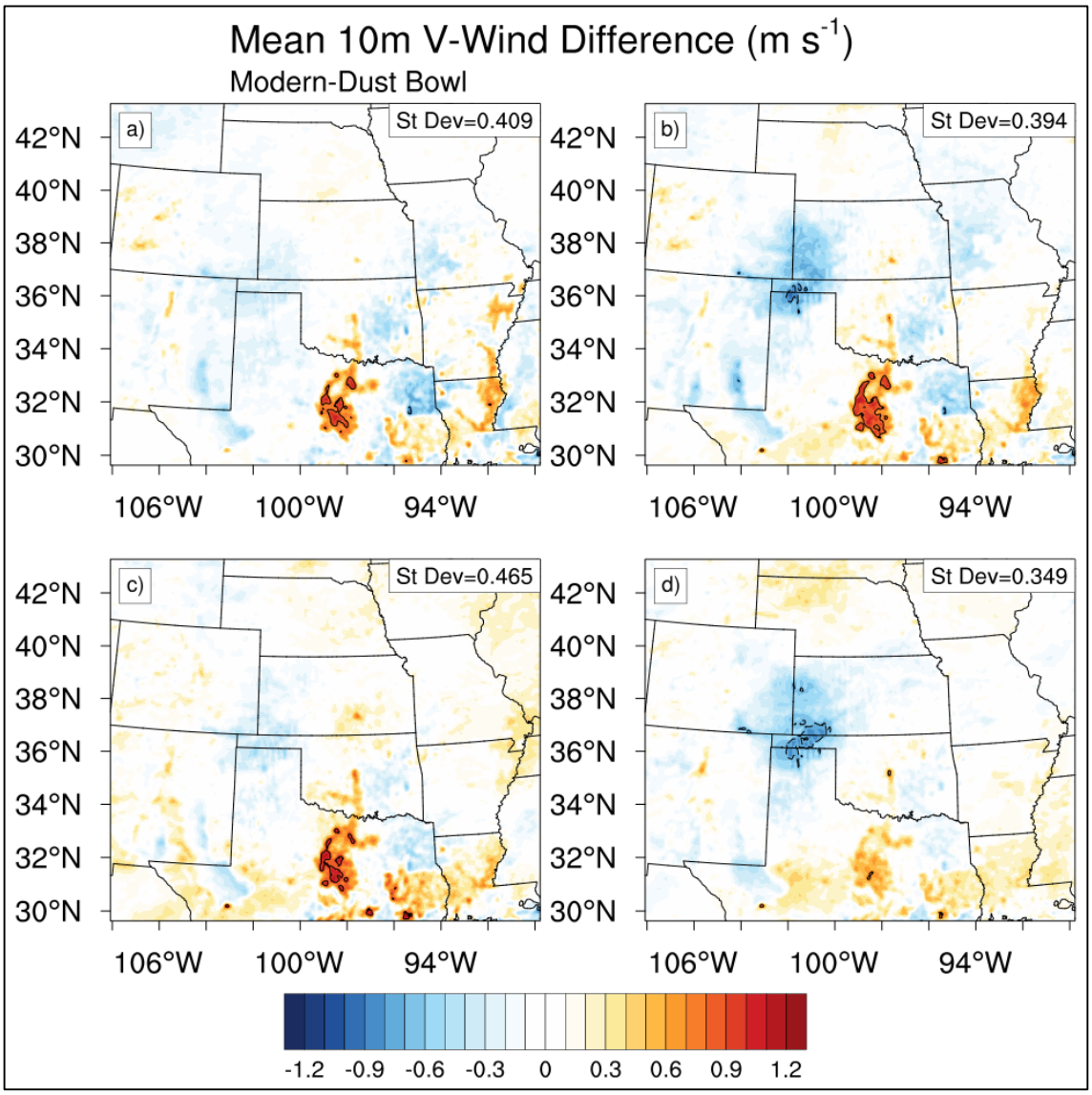

Figure 3.38. As in Figure 3.37, but for 10m V-wind differences.

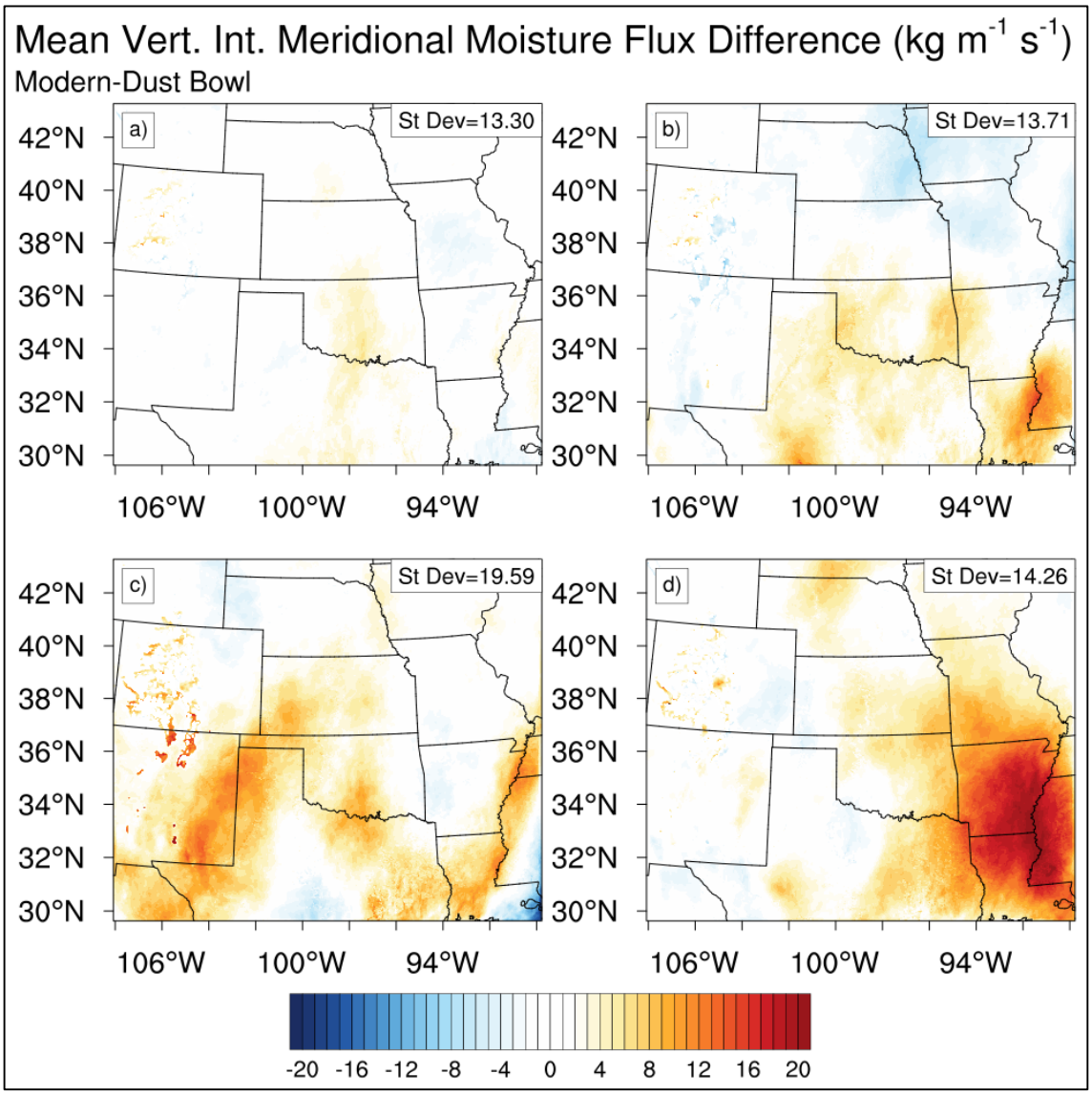

Figure 3.39. Mean May (a), June (b), July (c) and August (d) vertically integrated (1000hPa – 700hPa) meridional moisture flux differences (modern day minus Dust Bowl).

v. Precipitation

In June, July and August, the modern day saw an increase in precipitation in the panhandles of Texas and Oklahoma compared to the Dust Bowl (Figure 3.40b-d). The greatest changes occurred in June, where significant greater precipitation was evident

over the panhandles of Texas and Oklahoma. This region was dominated by barren soil during the Dust Bowl, and is now covered by cropland. The remainder of the precipitation results were described in the previous section (Figure 3.27).

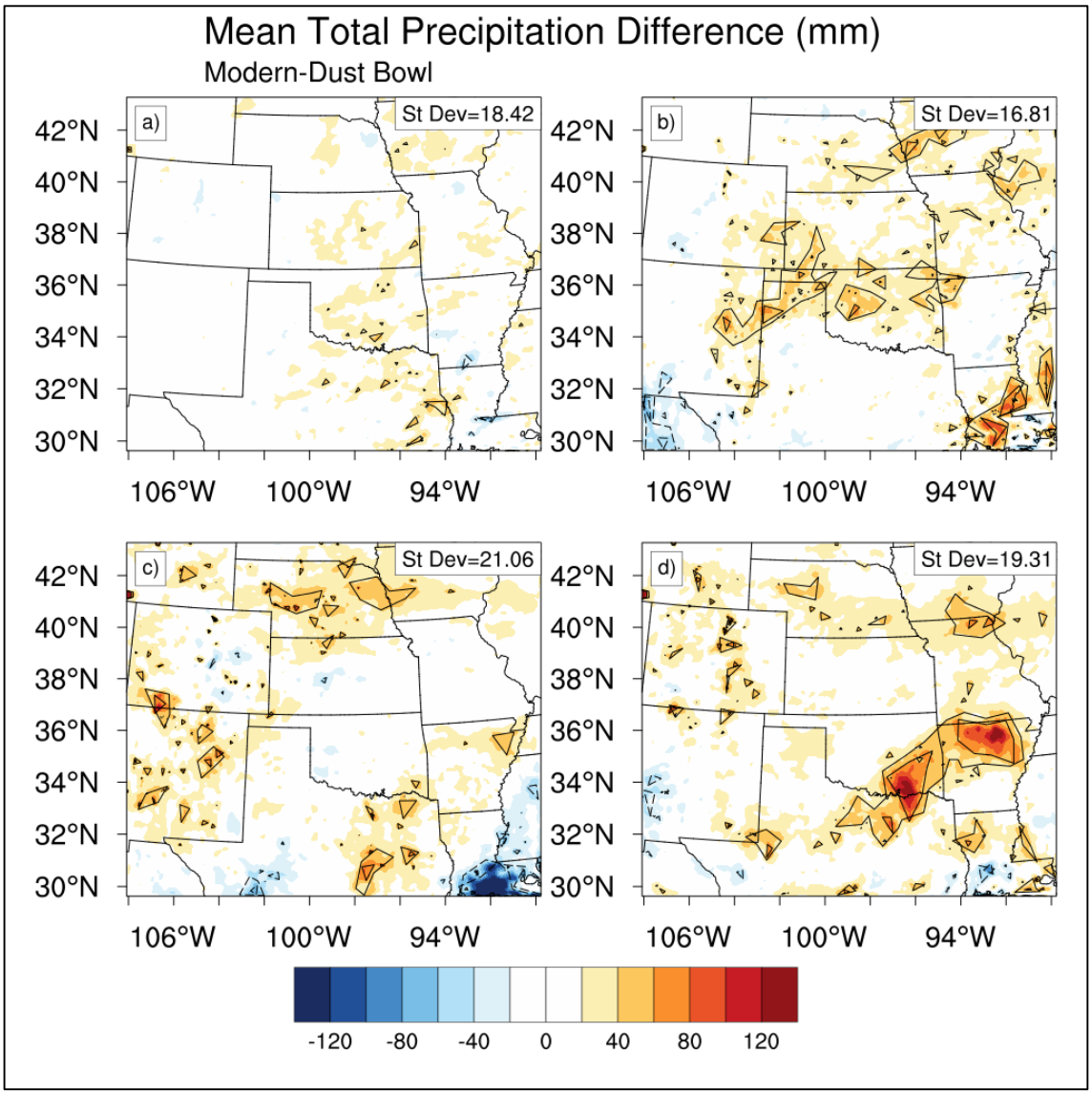

Figure 3.40. Mean May (a), June (b) July (c) and August (d) total precipitation differences (modern day minus Dust Bowl). $\pm 2\sigma$ contoured in black; solid line for $+2\sigma$ and dashed for -2σ.

Chapter 4. Conclusions

The Southern Great Plains have undergone significant land use land cover changes over the last two centuries. The most widespread change has been the expansion of land designated for agriculture at the expense of native vegetation primarily composed of grassland and savanna. Nearly half of the domain was converted to cropland from the pre-settlement era to the 1920's, and the transition has continued to the current day.

The LULC changes altered the surface energy budget through the partitioning of surface sensible and latent heat fluxes. The widespread transition to cropland resulted in higher surface latent heat fluxes in the modern day, compared to the pre-settlement, 1920s and Dust Bowl scenarios. In addition, the moisture content in the top soil layer also increased, as did the evaporative fraction. These results suggest that evaporation was greater with the cropland than the native grassland and savanna. The greater evaporation also resulted in greater surface humidity, evident by the lower 2m air temperatures and higher 2m dewpoints.

The change in the surface energy budget also caused changes to the regional circulation. The increased latent heat flux and associated evaporation resulted in higher mean sea level pressure over parts of Nebraska, Kansas, Iowa, Missouri and Arkansas. The wind field responded to the change in mean sea level pressure, with stronger negative U-winds on the southern extent of the higher pressure, and stronger positive V-winds on the western edge of the higher pressure. The change in the wind field is an important result, due to its implication for moisture transport. The Southern Great Plains relies on southerly flow from the Gulf of Mexico for its moisture source;

these results suggest that this flow has been enhanced as a result of the LULC changes leading up to the current day.

Finally, the results indicate that changes in the surface energy budget driven by changes in the LULC had an impact on precipitation over the Southern Great Plains. Compared to the pre-settlement, 1920s and Dust Bowl scenario, precipitation amounts are greater in the modern day, and these changes are statistically significant in some areas. The largest differences occurred over southern Oklahoma and northern Texas, and this result was found in each comparison between the modern day and three previous scenarios. The cause of the higher precipitation amounts likely regards the altered regional circulation, which changed the vertically integrated meridional moisture flux and resulted in greater moisture flux which was generally well aligned with the regions of greater precipitation. In addition, there was an increase in the moisture content of the air through greater surface evaporation, due to the increased evaporation potential of cropland compared to native vegetation. Results of the comparison between the Dust Bowl and modern day scenario were fairly intuitive. The latent heat flux was greater in the modern day compared to the Dust Bowl scenario, which was anticipated since barren soil and sparsely vegetated land does not hold much moisture. In addition, the results suggest the potential for a positive feedback over the region greatest impacted by wind erosion of the Dust Bowl: negative V-winds were found over this region, which would inhibit the transport of moisture from the Gulf of Mexico, keeping the region dry and the soil barren and sparsely vegetated. The change in the regional circulation due to the wind erosion of the Dust Bowl did not have a noticeable impact on the moisture flux over the region, as the differences in moisture flux were fairly similar compared to the differences

between the modern day and 1920's scenarios. The results suggest a potential positive feedback; with a drought-favoring remote forcing to initiate the drought conditions, the altered regional circulation due to the altered LULC allowed for the drought to continue.

The results of this study have shown that the past 160 years of land use land cover changes in the Southern Great Plains have changed the regional circulation, and resulted in precipitation increases over a large portion of the region. The results suggest that the expansion of agriculture is the main driver for these changes. In addition to an increase in precipitation, mean August temperature has decreased in the current day compared to the pre-settlement scenario, and has not changed dramatically since the 1920's or Dust Bowl time periods. These feedbacks are important to understand as the land use continues to change in this region.

REFERENCES

Bagley, J.E., A.R. Desai, K.J. Harding, P.K. Snyder, and J.A. Foley, 2014: Drought and Deforestation: Has Land Cover Change Influenced Recent Precipitation Extremes in the Amazon?. *J. Climate*, **27**, 345–36

Balling, R.C., Jr., 1989: The impact of summer rainfall on the temperature gradient along the United States–Mexico border. *J. Appl. Meteor.*, **28,** 304–308.

Bonan, Gordon B. (2016) Ecological Climatology: Concepts and Applications, Third Edition, Cambridge: Cambridge University Press.

Charney, J., P.H. Stone, and W.J. Quirk, 1975: Drought in the Sahara: A biogeophysical feedback mechanism. *Science*, **187**, 434-435.

Chen, L. and P. A. Dirmeyer, 2017: Impacts of land use/land cover change on afternoon precipitation over North America. *J. Climate*, **30**, 2121-2140.

Cheng, F., Y. Hsu, P. Lin, and T. Lin, 2013: Investigation of the Effects of Different Land Use and Land Cover Patterns on Mesoscale Meteorological Simulations in the Taiwan Area. *J. Appl. Meteor. Climatol.*, **52**, 570–587

Cosgrove, B. A., et al. (2003), Land surface model spin-up behavior in the North American Land Data Assimilation System (NLDAS), *J. Geophys. Res.*, **108**, 8845.

Davin, E.L. and N. de Noblet-Ducoudré, 2010: Climatic Impact of Global-Scale Deforestation: Radiative versus Nonradiative Processes. *J. Climate*, **23**, 97–112.

Drummond, M.A., and Auch, R.F., 2015: Land-cover trends in the Great Plains of the United States—1973 to 2000. In, Taylor, J.L., Acevedo, W., Auch, R.F., and Drummond, M.A., eds., 2015: Status and trends of land change in the Great Plains of the United States—1973 to 2000. *U.S. Geological Survey Professional Paper* **1794–B**, p. 3-16.

Dudhia, J., 1989: Numerical study of convection observed during the Winter Monsoon Experiment using a mesoscale two–dimensional model. *J. Atmos. Sci.,* **46**, 3077–3107.

Gentine, P., D. Entekhabi, and J. Polcher, 2011: The Diurnal Behavior of Evaporative Fraction in the Soil–Vegetation–Atmospheric Boundary Layer Continuum. *J. Hydrometeor.,* **12**, 1530–1546

Gutmann, M. P., Deane, G. D., Lauster, N., & Peri, A., 2005: Two population-environment regimes in the Great Plains of the United States, 1930–1990. *Population and Environment*, **27**, 191–225.

Homer, C.G., Dewitz, J.A., Yang, L., Jin, S., Danielson, P., Xian, G., Coulston, J., Herold, N.D., Wickham, J.D., and Megown, K., 2015: Completion of the 2011 National Land Cover Database for the conterminous United States-Representing a decade of land cover change information. *Photogrammetric Engineering and Remote Sensing*, **81**, no. 5, p. 345-354

Hong, S.-Y., J. Dudhia, and S.-H. Chen, 2004: A revised approach to ice microphysical processes for the bulk parameterization of clouds and precipitation. *Mon. Wea. Rev*., **132**, 103–120.

Hong, Song–You, Yign Noh, Jimy Dudhia, 2006: A new vertical diffusion package with an explicit treatment of entrainment processes. *Mon. Wea. Rev.*, **134**, 2318–2341.

Hu, Q., and S. Feng, 2012: AMO- and ENSO-driven summertime circulation and precipitation variations in North America. *J. Climate*, **25**, 6477–6495.

Hu, Z.-Z., and B. Huang, 2009: Interferential impact of ENSO and PDO on dry and wet conditions in the U.S. Great Plains. *J. Climate*, **22**, 6047–6065.

Hu, Q., S. Feng, and R. J. Oglesby, 2011: Variations in North American summer precipitation driven by the Atlantic multidecadal oscillation. *J. Climate*, **24**, 5555–5570.

Hurtt, G. C., and Coauthors, 2006: The underpinnings of land-use history: Three centuries of global gridded land-use transitions, wood-harvest activity, and resulting secondary lands. *Global Change Biol*., **12**, 1208–1229.

Kain, J. S., 2004: The Kain-Fritsch convective parameterization: An update. *J. Appl. Meteor.*, **43**, 170-181.

Lawrence, D. M., K. W. Oleson, M. G. Flanner, P. E. Thornton, S. C. Swenson, P. J. Lawrence, X. Zeng, Z. Yang, S. Levis, K. Sakaguchi, G. B. Bonan, and A. G. Slater, 2011: Parameterization improvements and functional and structural advances in version 4 of the Community Land Model. *J. Adv. Model. Earth Syst.*, **3**, M03001.

Lee, S. and E.H. Berbery, 2012: Land Cover Change Effects on the Climate of the La Plata Basin. *J. Hydrometeor.*, **13**, 84–102.

LeMone, M. A., F. Chen, J. G. Alfieri, M. Tewari, B. Geerts, Q. Miao, R. L. Grossman, and R. L. Coulter, 2007: Influence of land cover and soil moisture on horizontal distribution of sensible and latent heat fluxes in southeast Kansas during IHOP_2002 and CASES-97. *J. Hydrometeor.,* **8**, 68–87.

Lu, Y., and L. M. Kueppers (2012), Surface energy partitioning over four dominant vegetation types across the United States in a coupled regional climate model (Weather Research and Forecasting Model 3–Community Land Model 3.5), *J. Geophys. Res.*, **117**, D06111.

Manabe, S., 1969: Climate and the ocean circulation. I: The atmospheric circulation and the hydrology of the earth's surface. *Mon. Wea. Rev.*, **97,** 739–774.

Marshall C. H., Pielke R. A. Sr.. 2004. Has the conversion of natural wetlands to agricultural land increased the incidence of severity of damaging freezes in south Florida? *Mon. Wea. Rev.* **132**: 2243–2258.

Mesinger, F., and Coauthors, 2006: North American regional reanalysis. *Bull. Amer. Meteor. Soc.,* **87**, 343-360.

Mueller, N.D., A. Rhines, E.E. Butler, D.K. Ray, S. Siebert, N.M. Holbrook, and P. Huybers, 2017: Global Relationships between Cropland Intensification and Summer Temperature Extremes over the Last 50 Years. *J. Climate,* **30**, 7505–7528.

Narisma, G. and A. Pitman, 2003: The Impact of 200 Years of Land Cover Change on the Australian Near-Surface Climate. *J. Hydrometeor.*, **4**, 424–436,

Nigam, S., B. Guan, and A. Ruiz-Barradas (2011), Key role of the Atlantic Multidecadal Oscillation in 20th century drought and wet periods over the Great Plains, *Geophys. Res. Lett.,* **38**, L16713.

Niu, G.-Y., Z.-L. Yang, K. E. Mitchell, F. Chen, M. B. Ek, M. Barlage, L. Longuevergne, A. Kumar, K. Manning, D. Niyogi, E. Rosero, M. Tewari, and Y. Xia (2011), The community Noah land surface model with multiparameteization options (Noah-MP): 1. Model description and evaluation with local-scale measurements, *J. Geophys. Res.*, **116**, D12109.

Nobre, C., P. Sellers, and J. Shukla, 1991: Amazonian Deforestation and Regional Change. *J. Climate*, **4**, 957–988.

Oleson, K. W., D. M. Lawrence, G. B. Bonan, M. G. Flanner, E. Kluzek, P. J. Lawrence, S. Levis, S. C. Swenson, and P. E. Thornton, 2010: Technical description of version 4.0 of the Community Land Model (CLM). NCAR, 266 pp. [Available online at http://www.cesm.ucar.edu/models/ccsm4.0/clm/CLM4_Tech_Note.pdf]

Oleson, K.W., Bonan, G.B., Levis, S. et al., 2004. *Climate Dynamics* **23**: 117. https://doi.org/10.1007/s00382-004-0426-9

Omernik, J., & Griffith, G. (2008). Ecoregions of the United States-Level IV (EPA).

PRISM Climate Group, Oregon State University, http://prism.oregonstate.edu, created 4 Feb 2004.

Skamarock, W., J.B. Klemp, J. Dudhia, D.O. Gill, D. Barker, M.G. Duda, X.-Y. Huang, and W. Wang, 2008: A Description of the Advanced Research WRF Version 3. NCAR Technical Note NCAR/TN-475+STR, 88pp.

Smith, A., N. Lott, T. Houston, K. Shein, J. Crouch, and J. Enloe, 2016: U.S. billion-dollar weather & climate disasters 1980–2016. NOAA National Centers for Environmental Information, accessed 15 November 2016. [Available online at https://www.ncdc.noaa.gov/billions/events.pdf.]

Steyaert, L. T., and R. G. Knox (2008), Reconstructed historical land cover and biophysical parameters for studies of land-atmosphere interactions within the eastern United States, *J. Geophys. Res*., **113**, D02101.

Van Den Broeke, Matthew, A. Kalin, J.A.T. Alavez, R. Oblesby, Q. Hu, 2017: A warm-season comparison of WRF coupled to the CLM4.0, Noah-MP, and Bucket hydrology land surface schemes over the central USA. *Theor. Appl. Climatol.*, in press.

Weaver, S. J., S. Schubert, and H. Wang, 2009: Warm season variations in the low-level circulation and precipitation over the central United States in observations, AMIP simulations, and idealized SST experiments. *J. Climate*, **22**, 5401–5420.

Yan, J.W., J.Y. Liu, B.Z. Chen, M. Feng, S.F. Fang, G. Xu, H.F. Zhang, M.L. Che, W. Liang, Y.F. Hu, W.H. Kuang, H.M. Wang, 2014: Changes in the land surface

energy budget in eastern China over the past three decades: contributions of land-cover change and climate change. *J. Clim.*, **27**, pp. 9233–9252.

Zhang, D.–L., and R.A. Anthes, 1982: A high–resolution model of the planetary boundary layer– sensitivity tests and comparisons with SESAME–79 data. *J. Appl. Meteor.*, **21**, 1594–1609.